

---

ANALYSIS OF THE RAINFALL RUNOFF  
PROCESSES OF ANDEAN ECOSYSTEMS IN  
SOUTHERN ECUADOR: USING  
HYDROMETRIC, TRACERS AND MODELING  
APPROACHES

---

PATRICIO JAVIER CRESPO SANCHEZ

A dissertation submitted to the Department of Natural Sciences and prepared at the  
Department of Agricultural Sciences, Nutritional Sciences and Environmental  
Management of the  
Justus-Liebig-Universität Gießen, Germany  
for the degree of Doctor of natural Sciences (Doctor rerum naturalium).

Submitted May 2012

Referees

Prof. Dr. Hans-Georg Frede, Justus-Liebig-Universität Gießen

PD Dr. Lutz Breuer, Justus-Liebig-Universität Gießen

Prof. Dr. Jan Feyen, Universidad de Cuenca

Prof. Dr. Markus Fuchs, Justus-Liebig-Universität Gießen

---

# TABLE OF CONTENTS

<b>1 SYNOPSIS .....</b>	<b>1</b>
1.1 INTRODUCTION .....	1
1.2 GENERAL OBJECTIVE .....	4
1.3 STUDY AREAS DESCRIPTION .....	6
1.4 THESIS OUTLINE.....	10
1.5 SUMMARY OF RESULTS.....	12
1.6 FUTURE RESEARCH.....	16
<b>2 IDENTIFYING CONTROLS OF THE RAINFALL-RUNOFF RESPONSE OF SMALL CATCHMENTS IN THE TROPICAL ANDES (ECUADOR) .....</b>	<b>19</b>
2.1 INTRODUCTION .....	20
2.2 METHODS.....	21
2.3 CASE STUDY CATCHMENT DESCRIPTION .....	26
2.3.1 CLIMATE .....	26
2.3.2 LAND COVER AND USE.....	29
2.3.3 GEOLOGY.....	30
2.3.4 SOILS.....	31
2.4 RESULTS AND DISCUSSION .....	32
2.4.1 STREAMFLOW PATTERN.....	32
2.4.2 WATER YIELD AND ACTUAL EVAPOTRANSPIRATION .....	36
2.4.3 HYDROLOGICAL PROCESSES.....	38
2.5 CONCLUSIONS .....	42
<b>3 PRELIMINARY EVALUATION OF THE RUNOFF PROCESSES IN A REMOTE MONTANE CLOUD FOREST BASIN USING MIXING MODEL ANALYSIS AND MEAN TRANSIT TIME.....</b>	<b>44</b>
3.1 INTRODUCTION .....	45
3.2 MATERIALS AND METHODS.....	47
3.2.1 STUDY AREA .....	47
3.2.2 FIELD SAMPLING AND LABORATORY ANALYSIS.....	50
3.2.3 HYDROMETRIC MEASUREMENTS.....	53
3.2.4 MIXING MODEL ANALYSIS.....	54
3.2.5 MEAN TRANSIT TIME ESTIMATION.....	55
3.3 RESULTS AND DISCUSSION .....	56
3.3.1 RAINFALL-RUNOFF.....	56
3.3.2 HYDROCHEMISTRY .....	58

3.3.3	<i>ISOTOPIC TRACERS AND MEAN TRANSIT TIME</i> .....	61
3.3.4	<i>END-MEMBER IDENTIFICATION</i> .....	65
3.3.5	<i>MIXING MODEL ANALYSIS</i> .....	67
3.4	CONCLUSIONS .....	70
<b>4</b>	<b>DEVELOPMENT OF A CONCEPTUAL MODEL OF THE HYDROLOGIC RESPONSE OF TROPICAL ANDEAN MICRO-CATCHMENTS IN SOUTHERN ECUADOR</b> .....	<b>71</b>
4.1	INTRODUCTION .....	72
4.2	MATERIALS AND METHODS.....	74
4.2.1	<i>CASE STUDY CATCHMENT DESCRIPTION</i> .....	74
4.2.2	<i>MONITORING</i> .....	79
4.2.3	<i>DESCRIPTION OF THE CONCEPTUAL MODEL</i> .....	80
4.2.4	<i>MODEL PERFORMANCE ANALYSIS</i> .....	83
4.3	RESULTS AND DISCUSSION .....	84
4.3.1	<i>RAINFALL-RUNOFF</i> .....	84
4.3.2	<i>MODEL CALIBRATION AND EVALUATION</i> .....	85
4.3.3	<i>EVALUATION OF THE CONCEPTUAL MODEL</i> .....	91
4.4	CONCLUSIONS .....	95
<b>5</b>	<b>REFERENCES</b> .....	<b>97</b>
	<b>ACKNOWLEDGMENTS</b> .....	<b>111</b>

## LIST OF FIGURES

Figure 1–1: Location of the study sites within Ecuador .....	7
Figure 1–2: Views of the landscape of the studied ecosystems: (a) upper montane forest (Ortigas), photo: M. Ramirez; (b) tussock grass (Quimsacocha), photo: P. Crespo; (c) cushion plants (Quimsacocha), photo: P. Borja; (d) upper montane cloud forest (San Francisco), photo: P. Crespo. ....	8
Figure 1–3: Representation of the 1-hourly timeseries of rainfall (mm hr <sup>-1</sup> ) and total streamflow (l s <sup>-1</sup> km <sup>-2</sup> ) characteristic for the main climate regimes encountered in the study areas.....	10
Figure 1–4: Schematic representation of the Andosol and Histosol soil profile under páramo and cloud forest cover (left), and perception of the soil water dynamics by a series of linear reservoirs for a profile consisting of 3 (bottom right) and 4 (top right) horizons, respectively for dry to wet condition .....	14
Figure 2–1: Geographical location of the 13 study micro-catchments (UTM coordinates) .....	27
Figure 2–2a: 1-hour FDCs of the micro-catchments M1, M2 and M3 (Group 1) situated in the Pacific climate zone .....	33
Figure 2–3: Ordination plot of the study micro-catchments according to the principal components 1 and 2 .....	41
Figure 3–1: Location of the study area and nested subcatchments. 1 = PL, Planta (catchment outlet), 2 = SF, Rio San Francisco, 3 = FH, Rio San Francisco headwater, 4 = QR1, Quebrada Ramon 1, 5 = QR2, Quebrada Ramon 2, 6 = QM, Quebrada Milagro, 7 = QZ, Quebrada Zurita, 8 = QN, Quebrada Navidades, 9 = QP, Quebrada Pastos, 10 = QC, Quebrada Cruces, OL = soil water sampled in organic layer, AL = soil water sampled in A horizon layer, W = rock water.....	48
Figure 3–2: Hourly timeseries of rainfall and total streamflow in mm of the San Francisco basin. ....	57
Figure 3–3: Correlation between discharge and streamwater Na and Al concentration at the outlet (PL) of the San Francisco basin.....	60
Figure 3–4: Sine-wave regression models for δ <sup>18</sup> O in precipitation (filled points with dashed regression line derived from Wagner (2020) and Goller et al. (2005) data,	

solid points with solid regression line derived from OICP data) and streamwater for the San Francisco basin (PL) and subbasins (FH, QR1, QR2, QZ, QP).  
 Acronyms for subbasins are provided in Figure 3-1..... 63

Figure 3–5: Scatterplots of MTT versus Mean Absolute Error (MAE) for 2000 Monte Carlo simulations for streamflow  $\delta^{18}\text{O}$  using the EPM. .... 65

Figure 3–6: Mixing diagrams for Na and Al concentration for the San Francisco basin outlet (PL) and subbasins FH, QR1, QR2, QZ and QP. End members (including maximum and minimum) are represented by green circle = precipitation; brown square = OL, soil water in organic layer horizon; blue triangle = AL, soil water in A horizon layer; red cross = rock water..... 68

Figure 4–1: Location of the four study micro-catchments ..... 74

Figure 4–2: Schematic presentation of the concept of the 3-Res (3-reservoir) model (based on Crespo et al., 2011a,b)..... 82

Figure 4–3: Hourly flow duration curves for the observed discharge and the 5 and 95% uncertainty limits of the four micro-catchments applying respectively the 2- and 3-Res model structure ..... 87

Figure 4–4: Observed discharge and the 5 and 95% uncertainty limits on the predicted discharge with application to the four micro-catchments. Left figures correspond to the 2-Res model structure, while right figures to the 3-Res model structure. 2-Res model results for M3 correspond to the best model simulation..... 89

Figure 4–5: Discharge components according to the 3-Res model structure, with application to the four micro-catchments ..... 93

## LIST OF TABLES

Table 1–1: Principal characteristics of the study sites.....	5
Table 2–1: Main catchment characteristics.....	24
Table 2–2: Properties per horizons of the main soils in the studied catchments .....	25
Table 2–3: Average terms of the catchment water balance .....	37
Table 2–4: Eigenvectors of the variables retained in the three first principal components .....	38
Table 3–1: Main characteristics of the San Francisco basin and subbasins. Acronyms for subcatchments are explained in Figure 3-1.....	49
Table 3–2: Soil physical and chemical properties (average value and range) per horizon of the main soils in the studied catchment.....	51
Table 3–3: Chemical characteristics (average and range) of rainfall (volume weighted), rock and streamwater.....	59
Table 3–4: Mean, maximum and minimum $\delta^{18}\text{O}$ values, modeled amplitude and mean residence times of the San Francisco basin and subbasins.....	62
Table 4–1: Main catchment characteristics.....	75
Table 4–2: Horizon properties of the main soils in the catchments.....	78
Table 4–3: Model performance indicators.....	86
Table 4–4: Reservoir flow contribution (%).....	94

# 1 SYNOPSIS

## 1.1 INTRODUCTION

The tropical Andes is one of the world's 25 most species rich and exceptional areas, and the montane forest ecosystems in particular are considered as biodiversity hotspots (Myers et al., 2000). Also the high altitude páramo region, between 3500 and 5000 m a.s.l., is another important Andean ecosystem (Castaño 2002; Hofstede et al., 2003). The low temperatures, high intra-day temperature variability and the tendency to be consistently humid throughout the year creates an environment ideal for wet páramo flora primarily consisting of tussock-grasses or bunch-grasses, and the home of a multitude of endemic species. Ecuador possesses the largest net wet páramo area within South America. According to SENPLADES (2007) the montane forests and páramos are two of the most important natural ecosystems that still exist. Both provide essential services to the society such as the biodiversity in flora and fauna, carbon sequestration, and water regulation and supply. These ecosystems are considered as the major water suppliers for Venezuela, Colombia and Ecuador, providing good water quality to millions of habitants of the main cities in the Andean cordillera and coastal areas (Buytaert et al., 2010; Célleri and Feyen, 2009).

Lamentably both Andean ecosystems are very vulnerable, and during the last decades anthropogenic impacts are increasingly affecting the natural environment and biodiversity. The main stressors being deforestation, reforestation with exotic species, the conversion to grazing land, the construction of road infrastructure, and industrial and artisanal mining. Henderson et al. (1991) estimate that tropical forest is among the most rapid disappearing forest ecosystems on earth. Following Hamilton et al. (1995) between 90 to 95% of the mountain forests in South America disappeared in the 90's. According to the FAO (2006) South America suffered the largest net loss of forests between 2000 and 2005, with an average annual loss rate of 4.3 million hectares, followed by Africa with an annual loss rate of 4.0 million hectares. In South America, Ecuador seems to suffer the highest deforestation rate (Mosandl et al., 2008). Similarly, a study carried out in the Ecuadorian Andes identified that just 22.75% of the remaining vegetation above 1800 m a.s.l., the high montane forest and páramo, is still natural

(Baquero et al., 2004). The last decade the Ecuadorian government is investing heavily in a variety of reforestation and conservation programs to counteract further degradation of both ecosystems, however with low success.

Anthropogenic disturbances are mainly the consequence of the rapidly expanding population, which in Ecuador over the last 50 years increased from 3 to nearly 15 million inhabitants, with annual growth rates ranging between 1.54 to 2.9% being one of the highest in South America (INEC, 2011). The tremendous demographic growth is largely responsible for the increasing pressure on the highland ecosystems, primarily as a consequence of the urban and agricultural expansion in the inter-Andean and low lands, resulting in a significant rise of water consumption for domestic, industrial, agricultural and hydroelectrically power uses.

Notwithstanding the socio-economic and environmental importance of the highland ecosystems, good understanding of their functioning is still scarce hindering their conservation and management (Bruijnzeel, 2001 Feddema et al., 2005). According to Neill et al. (2006) and Boy et al. (2008) the geochemical, biologic and ecologic processes in tropical forest and páramo systems are controlled by the water passing through them. Therefore, most socio-economic and ecological services of these ecosystems are strongly linked to the governing hydrological processes. Logically, disturbance of the hydrology will directly affect all water dependent processes and the services provided by them. In this context, it is important and relevant to research the hydrological functioning of the highlands catchments. Good understanding of the hydrology is essential as to conserve in a more effective way these ecosystems. However, a serious bottle-neck in the race to gain more insight in these ecosystems is the lack of consistent and long-term hydrological and ecological datasets. Data collection is constrained by multiple factors such as financial costs, remoteness of the potential study areas, technological deficiencies, lack in monitoring skills, the absence of a data control and instrument maintenance culture, etc., all resulting in dataseries with data gaps and moderate data quality. In general, data collection is conducted within the frame of doctoral and small funded research projects. So far only a few catchments in the Ecuadorian Andes region have been studied in depth, and unfortunately data collection in most of these projects stopped by discontinuation of funding, seriously hindering the collection of long-term datasets. Despite the above mentioned problems,

several research groups deployed during the last decade considerable efforts in monitoring and the generation of climate, hydrological and other datasets in pristine Andean basins, with main objective the unraveling of the processes controlling runoff generation.

Identification of the hydrological processes governing the conversion of precipitation into runoff is one of the major challenges for hydrologists worldwide. A variety of techniques is used as a function of the objective of the study, the complexity of the study area and the availability of data. Hydrometric analysis is likely the most used technique to discern the main aspects of runoff generation, and the work of Kirkby (1978), McDonnell (1990), Bonell (1993), Pearce (1990) and Romkens et al. (1990) are examples of it. These authors use rainfall, discharge, soil moisture, soil water pressure, piezometric behavior, among other measurements to identify key hydrological processes. The technique is mostly used in micro-catchments and hillslopes and is not well suited for inferring hypotheses about the runoff generating processes in larger basins. Tracer methods, using natural or geochemical tracers, are excellent approaches for examining the runoff generation processes at micro- and macro-scale. For example water isotopes can be used to derive the Mean Transit Time (MTT) (Maloszewski et al., 1983). The MTT permits to classify the main components of streamflow such as base, intermittent, and surface flow. Examples of the use of isotopes in hydrology are given in Dincer et al. (1970), Niemi (1977), Payne and Schroeter (1979), Sklash and Farvolden (1979), Turner et al. (1987), Buttle (1994). Geochemical tracers are traditionally used in hydrograph separation (Pinder and Jones, 1969) and end member mixing analysis (EMMA) (Christophersen and Hooper, 1992). Hydrograph separation is applied to quantifying temporal source components, i.e. separating the hydrograph into pre-event and event water, whereas EMMA targets a separation in geographical source components (Barthold, 2010). Examples of the use of the geochemical tracers approaches are given in Christophersen et al. (1990), Hooper et al. (1990), Robson and Neal (1990), Hensel and Elsenbeer (1997).

As described by Leibundgut (1987) a combination of different methods can be used to unravel the hydrological processes of natural systems, a technique called by this author as convergence approach. To use this approach both the input and output parameters need to be measured. The combination of several techniques ensures that the specific

limitations of a single method do not bias the understanding of the functioning of the studied system. Examples of the approach are given in Pearce (1990), Bonell and Fritsch (1997), Kendall and McDonnell (1998), Wels et al. (1991), and Giusti and Neal (1993). Finally, numerical models are also applied to identify and test the processes governing runoff generation. Models can be black-box, conceptual or physical, and applied in a lumped or partial to fully distributed way. Multi-objective calibration methods using geochemical variables are commonly used to reduce the model uncertainty. An alternative calibration method is a top-down approach combining conceptual modeling with tracers (Klemeš, 1983). Examples on the use of models for the simulation and prediction of runoff are given in Stephenson and Freeze (1974), Beven and Kirkby (1977), Dunne (1983), Beven et al. (1995), and Beven (2001a). The main advantage of combining several methods is that in a relative short period on the basis of a limited amount of data a fairly accurate reconstruction of the water contributing areas and flow paths under variable rainfall conditions and landuses can be made.

## 1.2 GENERAL OBJECTIVE

The main objective of this dissertation was to identify the rainfall runoff processes that control the discharge generation of the study areas. The research uses multi techniques including hydrometric data analysis, tracers (isotopes and chemical constituents) and conceptual modeling. The research questions were (i) in which way streamflow is controlled by micro-climate, precipitation pattern, slope, land cover and soil properties, amongst other catchment properties?, (ii) what are the main sources of water within the study areas?, and how the soil properties are influencing the runoff generation?, and (iii) could the identified conceptual model, using previous knowledge, be applied for the studied areas in the south of Ecuador?

Table 1–1: Principal characteristics of the study sites

Site code	Area name	Basin	Ecosystem	N° monitored micro-catchments	Altitude (m a.s.l)	Vegetation cover	Land use	Climate regime	Analyzed in chapter			
									2	3	4	
I	Ortigas	Chanchán	Upper montane forest	2	2230-3280	Upper montane forest, shrubs, pasture, cropland	N, EG, PT	Pacific coastal	X			X
II	Panama	Bulu Bulu	Upper montane forest	1	2050-3080	Upper montane forest, pasture, cropland	EG, N, M	Pacific coastal	X			
III	Marianza	Paute	Tussock grass	2	2980-3740	Upper montane forest, tussock grass, Pine forest	N, PF	Pacific-Amazonian		X		
IV	Huagrahuma	Paute	Tussock grass	2	3520-4100	Tussock grass, cropland	N, PT, IG	Pacific-Amazonian		X		X
V	Quimsacocha	Paute/Jubones	Tussock grass, cushion plants	4	3590-3960	Tussock grass, cushion plants, shrubs	N, EG	Pacific-Amazonian		X		X
VI	San Francisco	Zamora	Upper montane cloud forest	10	1742-3250	Upper montane cloud forest, sub-páramo, shrubs, pasture	N, W, EG	Amazonian	X	X		X

Legend: PT, potatoes; M, maize PF, pine forest. IG, intensive grazed; EG, extensive grazed; N, natural. W, Wood

### 1.3 STUDY AREAS DESCRIPTION

The research was conducted on six sites (site codes I to VI, Figure 1-1), varying in climate, topography, soil and geology, land cover and use and location (see Table 1-1). The study sites are located in the south of Ecuador, between latitude 2°24' and 3°58', the altitude range between 1742 to 4100 m a.s.l.. The study sites I and II drain to the Pacific Ocean and have two paired monitored micro-catchments each one. Sites III, IV, and VI are tributary of Amazonian River Basin, the first two have two paired monitored micro-catchments each one, while site VI has ten monitored micro-catchments. On the site V five paired catchments were monitored; four of the monitored micro-catchments belong to the Amazonian basin and one micro-catchment drain to the Pacific Ocean. The sites I and II are representative for the upper montane forest ecosystems situated on the west flank of the western cordillera in the Chanchán and Bulu Bulu River Basins; sites III, IV and V comprises the wet páramo ecosystems (tussock grass and cushion plants) of southern Ecuador located in the Paute and Jubones River Basin near Cuenca city (the third largest city of Ecuador); and site VI represents the montane cloud forest ecosystems in the south of Ecuador, the micro-catchments drain to the San Francisco River Basin, tributary of the Zamora river basin. The landscape of the study sites is depicted in Figure 1-2. Although a complete description of the location, vegetation, land use, soils, geology and climate for the study micro-catchments is given in Chapter 2 and 3, a brief description of the most important characteristics of the study sites is given below.

Within each study site, micro-catchments with pristine and anthropogenic degraded conditions were monitored. The pristine vegetation on the sites I and II is mainly composed by upper montane forest (Asteraceae, Boraginaceae, Coriaceae, Euphorbiaceae, Juglandaceae, Fabaceae, Melastomataceae, Scrophulariaceae, Solanaceae, Verbenaceae) (Bruijnzeel, 2001; Crespo et al., 2008). The farmers commonly cut and burn the forest and replace it by pasture for grazing or cultivation (annual rotation of potatoes, corn and vegetables), representing the most degraded conditions in the study sites I and II. When the land is exhausted land is abandoned and natural regeneration of the vegetation occurs, consisting of small shrubs and patches of forest.

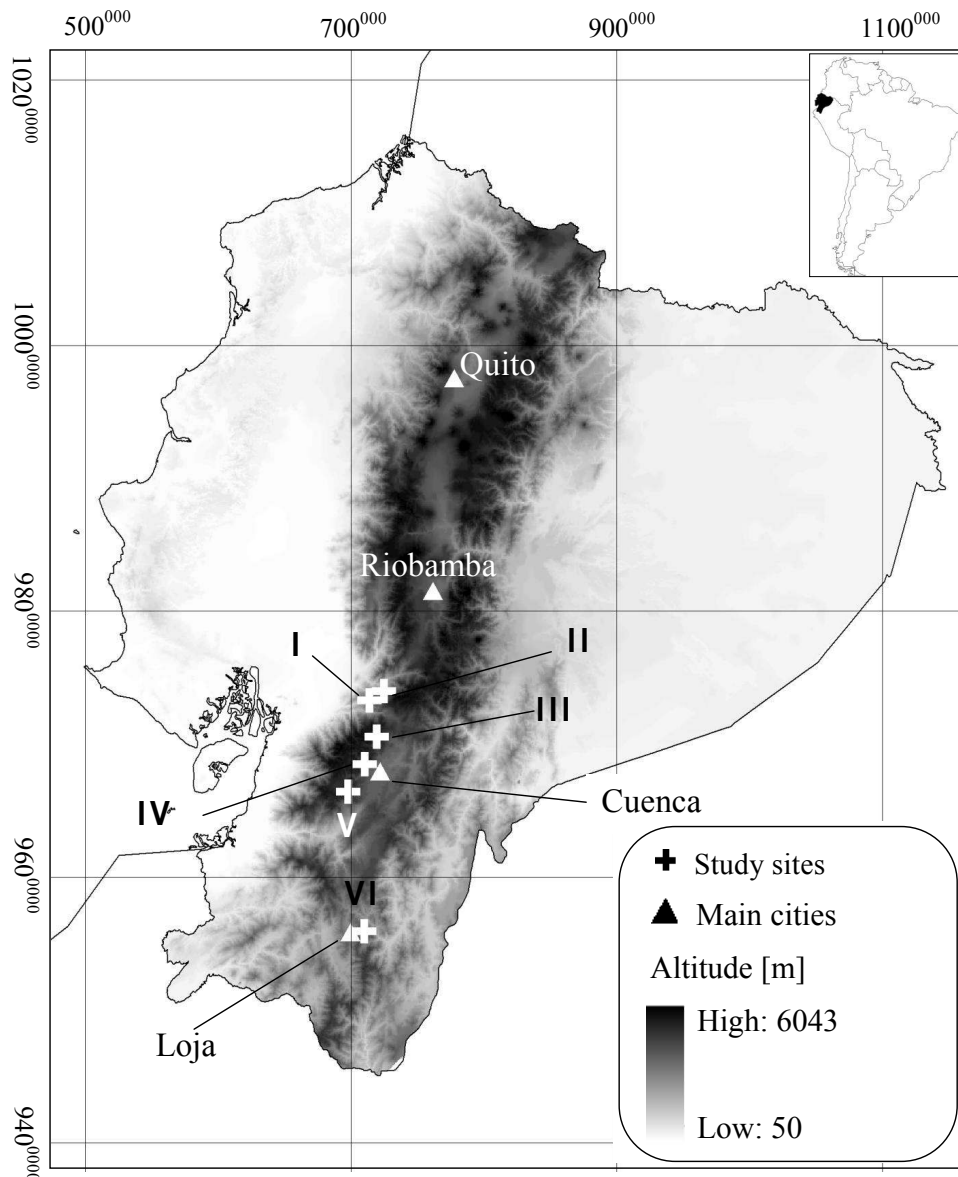


Figure 1–1: Location of the study sites within Ecuador

The study sites III to V belong to the wet páramo ecosystems (neotropical alpine grassland) and are located above the tree line, approximately at 3500 m a.s.l. (Luteyn, 1992; Hofstede, 1995; Medina and Vásquez, 2001). During pristine conditions the vegetation is mainly composed by tussock grass and cushion plants (Figure 2 b,c), nevertheless low shrubs and upper montane forest are also present especially along rivers. During the last decades páramos are being used for the cultivation of potatoes and extensive and intensive grazing by cattle altering the natural conditions (Buytaert, 2004). Normally during intensive grazing the tussock grass is replaced by more nutritious pastures. Planting *Pinus* is also a common practice in the páramos during the

last 30 years (Buytaert et al., 2007), some projects are taking place for wood production and within the frame of the international market on carbon sequestration.

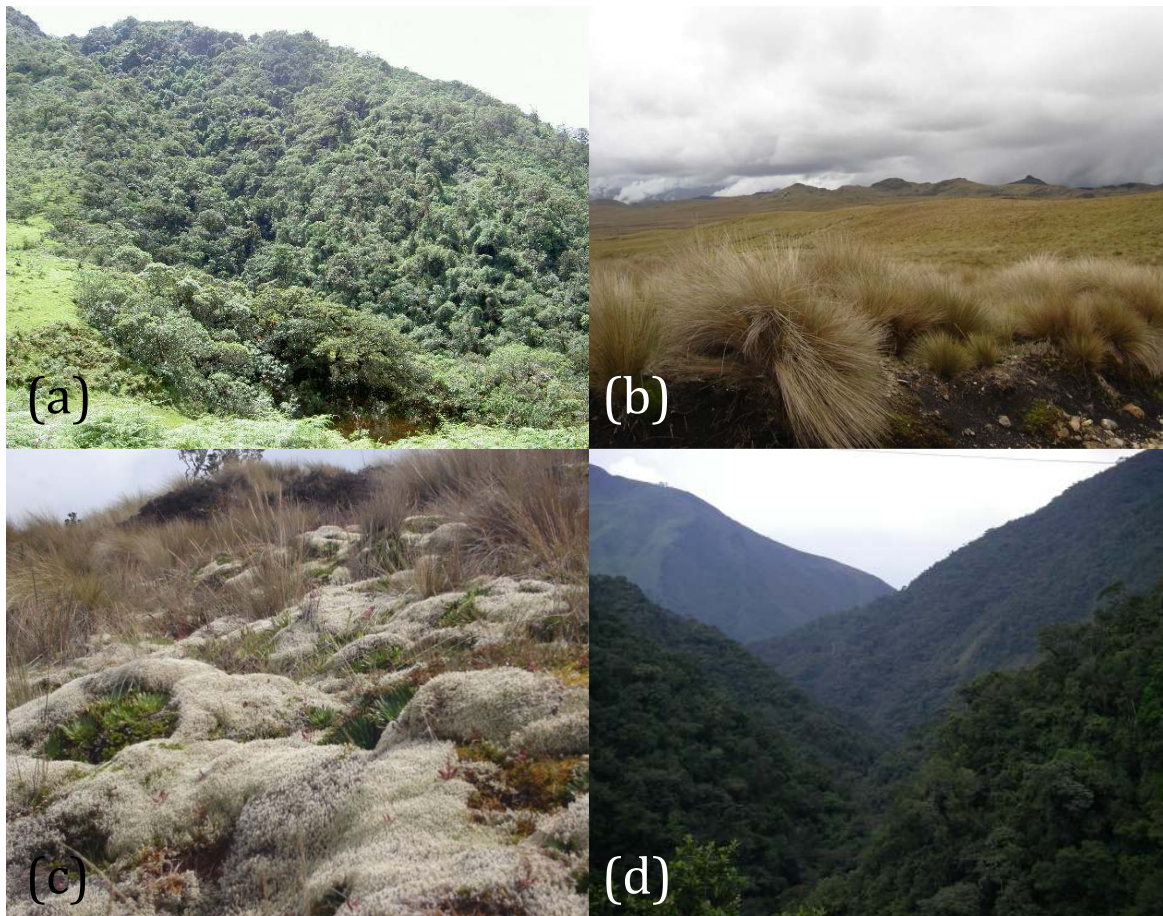


Figure 1–2: Views of the landscape of the studied ecosystems: (a) upper montane forest (Ortigas), photo: M. Ramirez; (b) tussock grass (Quimsacocha), photo: P. Crespo; (c) cushion plants (Quimsacocha), photo: P. Borja; (d) upper montane cloud forest (San Francisco), photo: P. Crespo.

The last group of study catchments corresponds to the site VI, where during pristine conditions the vegetation is mainly composed by upper montane cloud forest with dominant plants of the families Lauraceae, Euphorbiaceae, Melastomataceae and Rubiaceae (Homeier et al., 2002), while above 3250 m a.s.l. the vegetation consists of elfin forest and small shrubs (sub-páramo) (Beck et al., 2008). Pristine conditions mainly exist at the south of the San Francisco basin because this area is protected, while in the north the basin is characterized by different land uses. Here forest is mainly replaced by pastures for extensive grazing (Werner et al., 2005). Similarly as in the sites I and II, when the land is exhausted the farmers abandon it, natural regeneration occurs and the pastures are replaced by ferns. Anthropogenic impacts at the north further

consists of extensive wood cutting, gravel mining in the river bed, a draining gravel road, and hydropower station.

Climate in the Andes mountain range of Ecuador is influenced by the air masses coming from the Pacific and Amazon basin. The climate of the western slopes is strongly influenced by the Pacific coastal climate, while the climate in the eastern slopes is dominated by the Amazonian climate regime (Vuille et al., 2000). The climate in the inter-Andean region is additionally controlled by the Inter-Andean depression that separates the Western and Real cordillera of the Andes. According to Beck et al. (2008) the geographic location, namely the distance to the coast or the Amazonian basin and the altitude, are responsible for the high spatial and temporal variability of the climate. This variety is responsible of the high variability in runoff throughout the country. Additionally, the lack of a snow reservoir to buffer the water delivery during dry spell periods, common for most of the Andean basins in the center and south of the country, implies that the discharge is strongly controlled by the rainfall variability as is shown in the Figure 1-3 (Célleri, 2007).

More in particular, in the study sites I and II, with a mean annual precipitation ranging between 500 and 1900 mm, the climate is mainly influenced by the Pacific coastal regime (Figure 1-3), with a well-marked inter-annual seasonality. The wet season is from December to May with a precipitation varying between 60 and 80% of the annual rainfall, and the dry season from June to November. The annual rainfall in the study areas III to V, belonging to the wet páramo, ranges between 900 to 1600 mm, which during the rainy periods is fairly uniformly distributed. However, the annual precipitation pattern is bimodal as a consequence of the influence of both the Pacific coastal and Amazonian climate regimes (Figure 1-3), resulting in a major dry season from August to September and a less intensive dry season from December to February. Finally, the climate in the study site VI, with an annual precipitation ranging from 900 to 4700 mm, is mainly influenced by the Amazonian climate regime (Figure 1-3) with a moderate to low inter-annual rainfall variability. The main wet season is from April to September. A complete description of the climate of each study site is given in Buytaert et al. (2006a), Célleri et al. (2007), Bendix et al. (2008), and Crespo et al. (2011a).

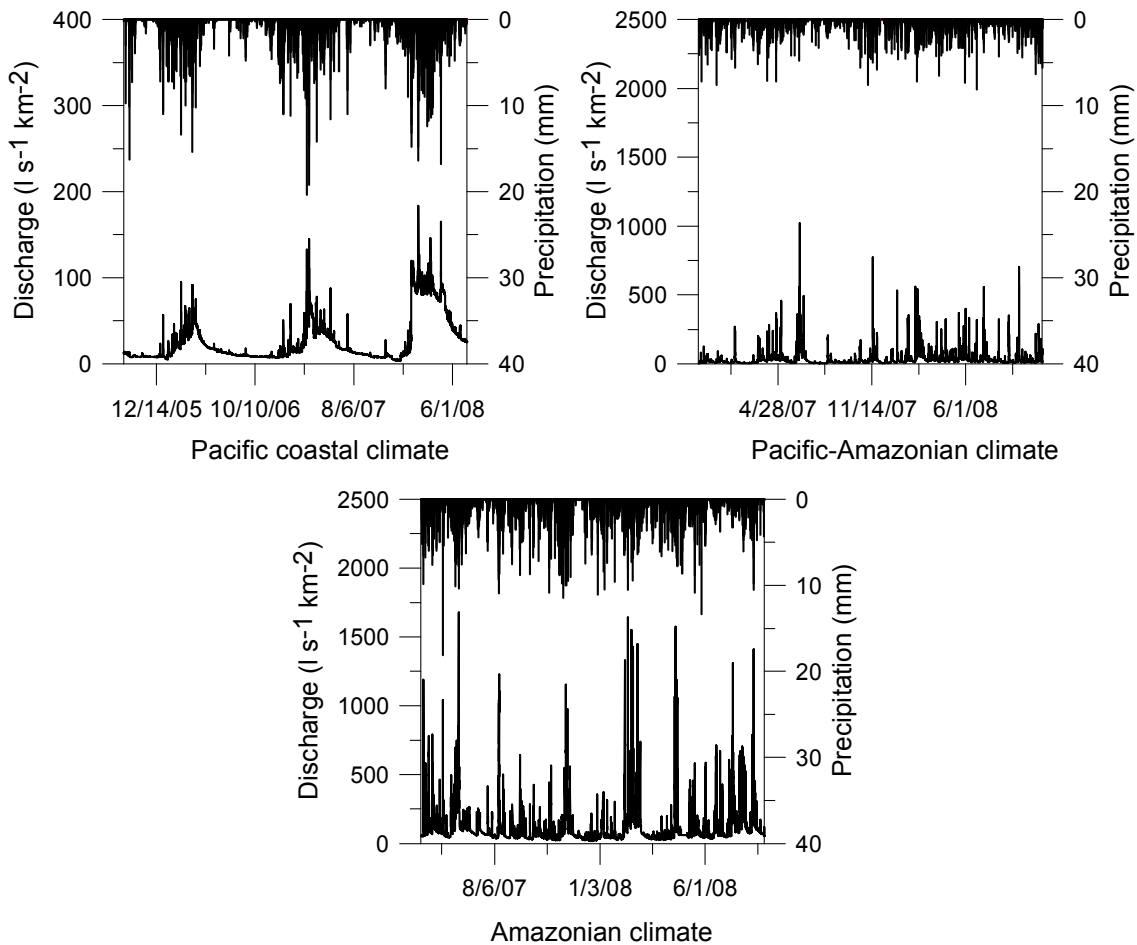


Figure 1–3: Representation of the 1-hourly timeseries of rainfall ( $\text{mm hr}^{-1}$ ) and total streamflow ( $\text{l s}^{-1} \text{km}^{-2}$ ) characteristic for the main climate regimes encountered in the study areas

## 1.4 THESIS OUTLINE

The dissertation is a composition of three interlinked papers describing the main processes controlling rainfall-runoff using multiples techniques, such as hydrometric data analysis, the use of environmental (geochemicals and isotopes) tracers, and modeling. Chapter 2 addresses the hydrometric analysis of precipitation and streamflow data of 13 micro-catchments, different in climate, precipitation pattern, topography, land cover and soil properties, and other characteristics. The chapter sketches the way streamflow is controlled by catchment properties. A challenge that controlled the selection of the study micro-catchments was the availability of sufficient long timeseries of precipitation and streamflow. General characteristics of the analyzed study sites are presented in the Table 1-1.

As mentioned before, the use of environmental tracers can strongly help with the identification of the main hydrological processes and the main water contributing areas. A combination of hydrometric, hydrochemistry and isotopic measurements was used to derive for the study site VI, using a nested approach for monitoring, a preliminary impression of the main rainfall-runoff processes. This site was selected because of the availability of tracer data, which is very scarce or inexistent in Ecuador. The research, as outlined in Chapter 3, offered an unique possibility to test the capability of the combination of different methods for identifying the water contributing areas in micro- to meso-scale basins in the southern Andean region of Ecuador. In Chapter 3 estimates of the mean transit time of streamflow for the different sub-catchments of the San Francisco basin are given, using an exponential piston-flow model (EPM) with a simple sine-wave approach as described by Maloszewski *et al.* (1983) and DeWalle *et al.* (1997). Additionally, the chapter describes the results of the Mixing Model Analysis (MMA) as outlined by Hooper *et al.* (1990) for the characterization of the contribution of rainfall, soil water and rock water to streamflow. The applied MMA is based on the three End-members combination.

Chapter 4 presents a hydrologic modeling approach using a conceptual model for simulating the rainfall-runoff response of four micro-catchments with natural vegetation, belonging respectively to the sites I, IV, V and VI (Table 1-1). Based on the knowledge acquired from the hydrometric analysis of medium to long-term datasets (Chapter 2) and the hydrologic investigation using different techniques (Chapter 3) a conceptual model was derived with the ambition mimicking the runoff response. The structure of the model is heavily based on the soil profile, which as identified in previous chapters strongly controls the conversion of rainfall into runoff. The presented conceptual model mimics the soil hydrology by a set of three reservoirs in series, representing the succession of discharge contributing horizons. The model performance was assessed using the Generalized Likelihood Uncertainty Estimation method (GLUE) of Beven and Binley (1992). The most relevant contribution of the chapter is the evaluation of the applicability of the conceptual model to basins with distinct climate, vegetation and soil composition and to test the level of model complexity, i.e. a 2- or 3-reservoir model, that best describes the runoff process of micro-catchments situated in the high mountain range of the Andes in South Ecuador.

## 1.5 SUMMARY OF RESULTS

The main emphasis of the doctoral research was analyzing in debt the processes controlling the conversion of rainfall into runoff of high mountain micro-catchments of the Andes region in South Ecuador. Results obtained using a variety of techniques and the detailed analysis of existing datasets and the collection of new datasets revealed that the hydrology of the study catchments is strongly controlled by the soil. This knowledge is very useful in deriving policies and regulations that best manage and protect the gamma of ecological services offered by these fragile ecosystems. For the generic use of the acquired knowledge findings were translated into a conceptual model mimicking the rainfall-runoff process, primarily based on mimicking the soil hydrology. With the tested model it will be possible to predict the impact on the runoff of future changes in climate and land use, and to test the effect of mitigation and management policies with respect to the sustainability in water delivery by this catchments for the multiple water uses in the region. The findings are representative for the area in which the study sites, as listed in Table 1-1, are located. Given the similarity in properties of the micro-basins in the Ecuadorian Andes cordillera above 2500 m a.s.l., stretching from Riobamba to the border with Peru, a bird-flight distance of 600 km, it is very likely that the modeling concept can be used for the prediction of the runoff in most, if not all, of the micro-catchments in this region.

Chapter 2 explores hydrometric data and catchment characteristics to explain the hydrology of the study micro-catchments. The objective of the study was to search in which way streamflow is conditioned by micro-climate, precipitation pattern, slope, land cover and soil properties, amongst other catchment properties. The specific objectives of the paper are: (i) how the streamflow pattern is controlled by the climate and other catchment characteristics, (ii) quantification of the water yield and actual evapotranspiration and which properties are controlling them, and (iii) identification of the main hydrological processes driving the runoff generation. Results clearly show that the streamflow of the 13-studied micro-catchments is mainly controlled by the annual rainfall depth and regime. During the land phase the temporal distribution of the discharge is managed by the horizon sequence, the physical soil properties such as the

lateral saturated hydraulic conductivity and the soil water retention, and the antecedent soil moisture content of each horizon. The results also indicate the likely influence of the slope on runoff. Streamflow data were processed to flow duration curves and grouped according to the dominant climate. This already revealed the difference in water yield between the Amazonian influenced micro-catchments, the catchments situated in the inter-valley, on the east flank of the Andes mountain range and the west flank of which the micro-climate is affected by the Pacific Ocean. The evapotranspiration is highest for catchments covered with forest, given the evaporation of intercepted rainfall and fog. The evapotranspiration is lower for páramo catchments. On the other hand, the similarity observed in the shape of the flow duration curves suggests that the same processes control the runoff generation notwithstanding differences in climate and catchments properties. According to the results of the hydrometric study streamflow primarily consists of subsurface flow, the slow flow component is the main contributing fraction to runoff, and the antecedent soil water content controls which soil layers are contributing. During dry-tropic conditions the slow flow component consist of lateral flow in the C-horizon and contributions of the top layer in the bedrock. Under wet conditions the slow flow component represents the lateral flow through the organic horizons and litter layer. Hortonian overland flow is low to inexistent, and primarily occurs by saturation excess. The anthropogenic effects seem to have a minimal effect on the processes controlling the runoff generation, but a considerable impact on the annual discharge and its temporal distribution. Vegetation does not seem to have an effect on the rainfall-runoff process, except on the evapotranspiration when interception of rainfall and fog are important.

Based on the findings presented in Chapter 2 the hydrology of the studied micro-catchments can be mimicked by a series of linear reservoirs of which the size of the bottom orifice and lateral orifices or side-ways overflow decreases with depth. The reservoirs are active depending on the antecedent soil water content and the storage capacity is function of the soil properties. Figure 1-4 gives a schematic of the hydrometric based perception how runoff is generated for two characteristic soils, respectively under páramo and cloud forest.

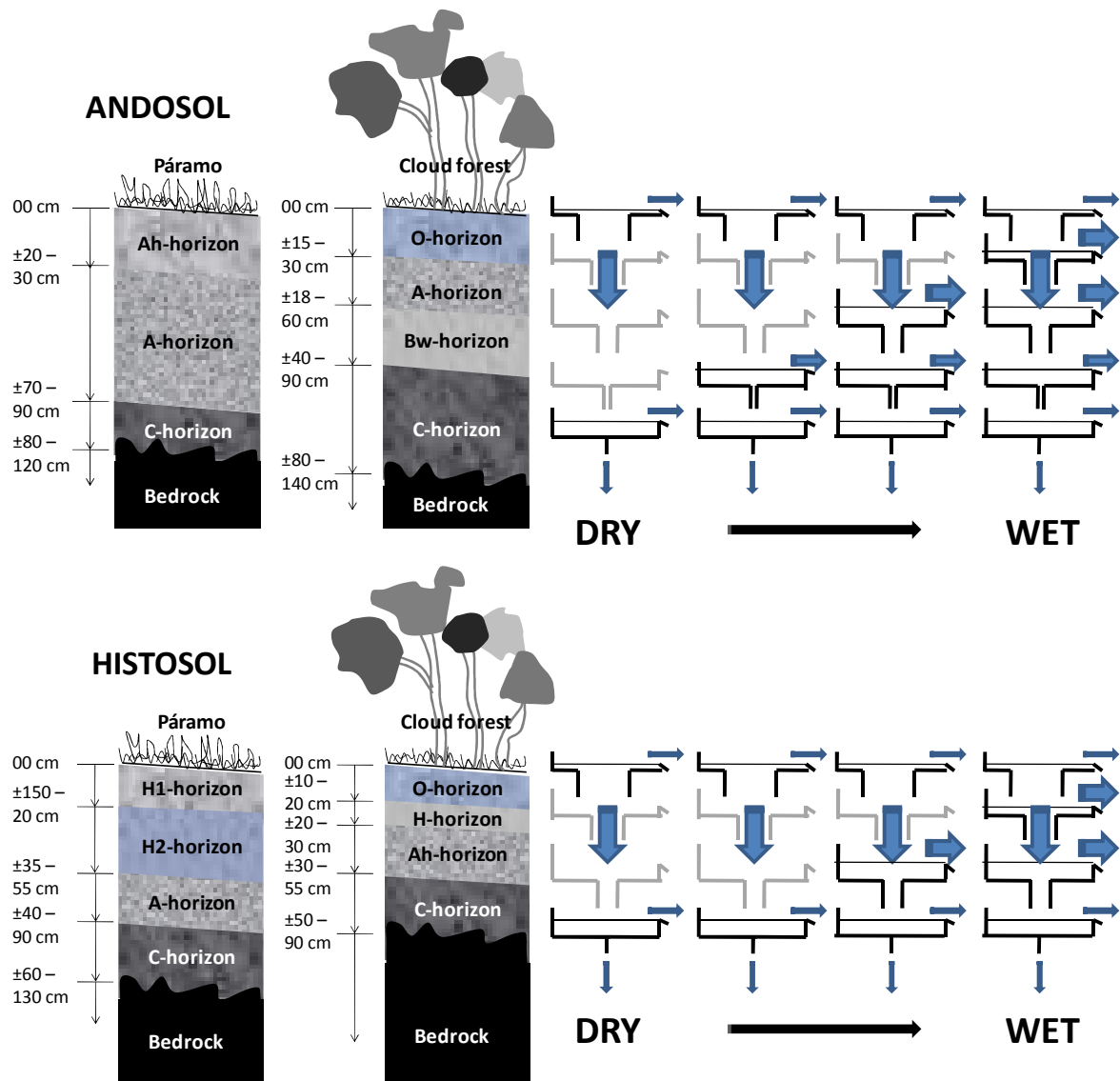


Figure 1–4: Schematic representation of the Andosol and Histosol soil profile under páramo and cloud forest cover (left), and perception of the soil water dynamics by a series of linear reservoirs for a profile consisting of 3 (bottom right) and 4 (top right) horizons, respectively for dry to wet condition

The research described in Chapter 3 aimed at identifying the dominant runoff contributing water sources and hydrologic processes in a medium sized basin in the southern Andes of Ecuador. The work consisted in deriving a picture of the streamflow generating processes, with application to the San Francisco River basin (South Ecuador) using respectively hydrometric, hydrochemistry and isotopic measurements. Based on the knowledge generated by Chapter 2 and literature findings the following hypotheses were postulated at the onset of the research activities of which the results are presented in Chapter 3: (i) use of multi-approach techniques allows identification of the principal hydrological processes and the main runoff water contributing areas, (ii) the mean

transit time (MTT) of the streamwater in the San Francisco basin is short and not influenced by deep water contribution, (iii) the subsurface lateral flow through the organic horizon dominates the runoff generation during wet conditions, and (iv) monitoring of the isotope and geochemical composition of water samples in different parts of the basin yields in a relative quick and inexpensive way key features on the hydrology of ungauged or poorly gauged basins.

Results confirm that the combination of hydrometric data, chemical signatures of water samples and isotopic tracers allow the identification of the dominant rainfall-runoff processes and runoff contributing water source areas. The multi-technique approach is a rather fast and low cost technique facilitating the understanding of the hydrology of ungauged to poor gauged catchments, of particular interest for the analysis of the multitude of micro- to meso-catchments in the Andes. Monitoring and analysis of environmental tracers, in contrast with hydrometric data analysis, permits to understand the runoff response on the basis of relative short-term data sets. In concrete, the chapter presents an estimation of the MTT values for the studied subcatchments. The three main water contributing areas to the total discharge were defined constructing the mixing diagrams of two dissolved chemical elements. The inclusion of spring water samples in the mixing analysis allowed quantifying the contribution of deep water to discharge. Results of the Mixing Model Analysis and MTT suggest a significant contribution of deep water to discharge during dry conditions, and that this contribution is unaffected by land use and topography. Under dry conditions runoff is mainly generated by the lateral flow through the C-horizon and cracks in the weathered top layer of the bedrock. During moderate conditions streamflow is dominated by the lateral flow through the organic horizons, and during wet conditions it is the lateral flow through the top rooted organic layer and litter layer that mostly contribute to runoff. Although Hortonian overland flow is not excluded during storms, saturation excess overland flow only exceptionally occurs in pastures near the riverbed.

The runoff prediction during model calibration and validation confirmed that the selected soil-based structure is a valid tool for simulating the runoff response to rainfall in the studied micro-catchments. In general, although the differences in climate and catchment properties, the runoff in the studied sites is controlled by similar processes, which are strongly controlled by the soil type. As shown, the antecedent wetness of the

subsequent soil horizons defines which of the horizons mostly contributes to the lateral flow. A three reservoir model predicts in general best the runoff, however the two reservoir model structure well captures the hydrological response under páramo. The linear reservoir based model correctly mimics the runoff from low to peak flows following a transition from a dry spell to a rainy period, confirming that the reservoir storage concept correctly models the hydrology of the micro-catchments. The results also revealed a major contribution of the lateral flow through the organic horizons to the total discharge under normal to wet conditions. Under dry conditions the lateral flow through the C-horizon and in some cases the top layer of the bedrock are mainly contributing to the discharge. The highly rooted organic horizon and the litter layer are mostly contributing to discharge during storm events. Overland flow is in general considered negligible, and occurs very locally. The research findings with respect to the sources of water contributing to runoff and the controlling processes obtained with the modeling approach are consistent with the knowledge derived in previous chapters.

## 1.6 FUTURE RESEARCH

The research work, as described in this doctoral dissertation, contributes towards a better understanding of the processes controlling the runoff generation in high Andean mountain micro-catchments by using a combination of techniques. Notwithstanding the gain in knowledge future research is still needed (i) to test the applicability of the soil based multiple linear reservoir model at regional scale and if needed to improve the model description; (ii) to relate the model parameters with catchment properties as to make the model suitable for ungauged and poorly monitored micro-catchments; and (iii) to analyze if the conceptual model applied at the scale of the hydrologic response units in which basins can be divided will enable to predict the outflow of large-scale basins.

As shown the combination of several techniques is very useful in the understanding of the hydrological processes controlling the rainfall conversion into runoff. Additionally it reduces the time of monitoring and the uncertainty in comparison to using just one method. This will enable to test the modeling concept to a wider scale of micro-catchments in the Andes region above 2500 m a.s.l. at an acceptable cost and within a limited timeframe. Isotopic and geochemical tracers in combination with hydrometric

data can be used to further examine the applicability and explore the hydrology of many more montane ecosystems (Sklash and Farvolden, 1979; Wels et al., 1991) as shown in Chapter 3 for the study case of the cloud forest. The transit time for the main sources of water, such as soil water of the organic and mineral horizons, spring water among others, can be used to understand the internal catchment processes controlling the water and solutes retention and release (Stewart and McDonnell, 1991). The use of the convolution integral with different transit time distributions as described by McGuire and McDonnell (2006) can be set up, in addition to the simple sine-wave approach that was used in this research, which provided an estimation of the MTT for streamflow. End Member Mixing Analysis (EMMA) as described by Christophersen and Hooper (1992) for EMMA-based hydrograph separation including uncertainty analysis (Genereux, 1998) can be used to quantify the contribution of the different components of the hydrologic cycle to streamflow. Once the mechanisms controlling the conversion of rainfall into streamflow for this type of catchments is better understood, time and effort can be devoted to refine the conceptual model as to reduce the uncertainty range on the runoff predictions.

Streamflow prediction in ungauged basins (PUB) is a mayor hydrologic challenge (Sivapalan et al., 2006; Franks et al., 2006). Using a hydrological model is a very common approach, however the use of models in poor gauged to ungauged basins suffers structural arbitrariness and over-parameterization (Klemeš, 1983), resulting in a problem of equifinality (Beven and Freer, 2001; Beven, 2002). Hydrometric analysis of any available data and field knowledge will help in selecting a model from the existing number of hydrologic models that best mimics the basin hydrology. However, due to the large spatial variability in the Andean mountain region, assessment of the value of the model parameters is and remains a big challenge. Extrapolation of model parameter values from calibrated catchments derived on gauged basins to ungauged catchments, also called regionalization of a hydrologic model, might resolve the application of tested models to ungauged basins. As mentioned by Buytaert and Beven (2009) regionalization is receiving considerable attention and considered as a major future research challenge. During this dissertation, a big effort was devoted to collect important information of a limited number of gauged basins in the Andes region of South Ecuador. In total the timeseries and basin information of 13 catchments were used as basis for the hydrometric analysis presented in Chapter 2, and which served as

basis for the developed and tested multi linear reservoir model. Several methods exist to relate parameter values to catchment properties including nearest neighbor, transfer functions and statistical techniques. Some examples are given in Seibert (1999), Parajka et al. (2005), Buytaert and Beven (2009), Young (2006), Sefton and Howarth (1998), Merz and Blöschl (2004), which might inspire regionalization of the conceptual model presented in the Chapter 4.

Many conceptual models are been used to simulate rainfall runoff response during the last decades (Singh and Frevert, 2002). Such models normally do not capture the physics of the processes that control the runoff generation, hindering for example the accurate prediction of the hydrological effect of global stressors, such as climate and land use change, among other anthropogenic impacts. In this context, additional information than rainfall and discharge might help in making conceptual models suitable. In a first step, as is suggested in Chapter 4 and described by Seibert and McDonnell (2002), “soft data” as tracers could be beneficial in guiding future model development, and testing and improving existing models, given more realism to the model structure. Additionally, tracers could be used as basis for a posteriori model calibration criteria, as stated by Vaché and McDonnell (2006). The use of additional soft data during model evaluation would facilitate the state-of-the-art philosophy of cooperative researchers by experimentalists and modelers (Seibert and McDonnell, 2002). The use of soft data is also recommended by the Prediction in Ungauged Basins (PUB) community (Sivapalan et al., 2006). Finally, for the proper addressing of the geographically contribution of the different water components and the interaction between non and saturated areas within the catchments use of physical-based distributed models, such as the Catchment Modeling Framework (CMF), presented by Kraft et al. (2008), might be a way to further explore.

## 2 IDENTIFYING CONTROLS OF THE RAINFALL-RUNOFF RESPONSE OF SMALL CATCHMENTS IN THE TROPICAL ANDES (ECUADOR)

### Abstract

Tropical mountain regions are characterized by strong spatial climate gradients which together with the limited amount of data and knowledge of the underlying processes hinder the management of the water resources. Especially for regional-scale prediction it is important to identify the dominant factors controlling the rainfall-runoff response and link those to known spatial patterns of climate, soils, and vegetation. This study analyses the rainfall-runoff relation of 13 intensively monitored micro-catchments in the Andes of southern Ecuador. The results of this study show that streamflow in the southern cordillera of the Ecuadorian Andes, above 2500 m a.s.l., primarily consists of subsurface flow. The yearly amount of streamflow is controlled by the annual rainfall depth, whereas the temporal distribution is mainly governed by the lateral saturated hydraulic conductivity, the soil water retention and the antecedent soil moisture content. Anthropogenic effects were found insignificant, with the exception in one of the studied micro-catchment. Effect of land use changes in most of the micro-catchments did not reflect in the shape of the flow duration curve because either the spatial extent of human impact was small and/or the overall basin slope was less than 20%.

### Published as

Crespo, P., J. Feyen, W. Buytaert, A. Bücke, L. Breuer, H-G. Frede, M. Ramírez, 2011. Identifying controls of the hydrological response of small catchments in the tropical Andes (Ecuador). *Journal of Hydrology*, 407, 164-174.

## 2.1 INTRODUCTION

The tropical Andes is hydrologically one of the most diverse regions in the world. The convergence of several climate systems, combined with steep topography, results in extreme hydro-climatic gradients. Precipitation easily surpasses 5000 mm on the slopes of the Amazon basin and the Colombian Chocó region, while many regions in the interandean valley have a semi-arid and arid climate (Vuille et al., 2000; Buytaert et al., 2011). Similarly, gradients of soil types and vegetation are driven by temperature and precipitation gradients, as well as geological variability, volcanic activity and human interference (Buytaert et al., 2006b). These gradients give rise to a rich variety of hydrological systems with a very different behavior, ranging from perennially wet cloud forest and tropical mountain wetlands to intensive farming systems.

Many of the natural Andean ecosystems, particularly neotropical alpine wet páramo, grassland and montane cloud forest, provide essential environmental services, of which biodiversity conservation, carbon storage and water supply are the most important. (Buytaert et al., 2011). Strong urban growth, the concentration of agriculture in the dry interandean valley, and the mountainous topography all contribute to the steadily increasing demand of water for domestic and industrial uses, irrigated agriculture and the generation of hydropower. Notwithstanding their socio-economic and environmental importance, catchments in South America are in general ungauged or poorly gauged, which explains why the hydrology of the high Andean mountain range is still not satisfactorily understood.

Additionally, the length and quality of available timeseries are short and of poor quality, containing many gaps. Monitoring for research purposes is limited to doctoral and small funded research projects. Only a few catchments in the Ecuadorian Andes region have been studied in depth, and unfortunately data collection mostly stopped when the project finished or funding dried up. Combined with the extreme variability and gradients of Andean hydrology, data-scarcity hinders extrapolation of hydrological understanding from gauged to ungauged catchments (Buytaert and Beven, 2009).

This study only focuses on micro-catchments, to avoid in the data analysis and interpretation the effect of spatial variability, typical for the medium-sized and large basins in the Andean mountain range. In addition data records of larger basins are very few or limited to timeseries of rainfall and discharge. After pre-processing of the available datasets the timeseries of precipitation and streamflow of the 13 selected micro-catchments were found consistent and sufficiently long for analysis. The objective of the study was to search in which way streamflow is conditioned by micro-climate, precipitation pattern, slope, land cover and soil properties, amongst other catchment properties. Only the selected date period of the data series are presented.

## 2.2 METHODS

Detailed information of the characteristics of the 13 analyzed micro-catchments is summarized in the Tables 2-1 to 2-3. In the following a brief description is given of the methods and equipments uses for data collection and processing.

To account for the spatial rainfall variability as a function of altitude and extent of the micro-catchments two rainfall gauges were installed, respectively in the upper and lower part of each of the micro-catchments M1 to M11 with exception of the catchment M3 where four rain gauges were installed. Rainfall data of the micro-catchments M1-M11 were recorded with HOBO RG3 tipping buckets with a resolution of 0.2 mm. In the study basins M12 and M13, precipitation and fog data from four precipitation stations were provided by the Bendix research group from January 2005 to October 2008. Details on equipment and protocol of rainfall and fog collection and data processing are given in Bendix et al. (2008). The data for all catchments were aggregated to 1-hourly rainfall and used for the calculation of the monthly and annual rainfall and extreme value analysis. Due to the small differences in precipitation depth between the rain gauges in the micro-catchments M1-M11 it was decided to apply the Thiessen polygon method for calculating the basin precipitation. For reason of elevation differences in the M12 and M13 catchments, basin precipitation was calculated using the area weighted elevation approach.

Streamflow in the micro-catchments M1-M11 was recorded with a Thompson (V-notch) weir, and in the catchments M12-M13 the water level was measured in a natural stable cross section. Each gauging site was equipped with pressure transducers or capacitance probe sensors, recording the water level with a 5 min interval and an accuracy of  $\pm 1$  mm; frequent control measurements were made at different flood stages. The Kindsvater-Shen relation (US Bureau of Reclamation, 2001) was used for conversion of the water level to discharge for M1 to M11. Potential and polynomial empirical stage-discharge relationships were developed using discharge measurements to estimate continuous discharge series for M12 and M13. The lowest measurable flow in the gauging stations is 0.0138, 3.3 and 21 l/s for M1 to M11, M12 and M13 respectively. Due to gaps in the data only shorter datasets could be used than the available timeseries which varied from 2.5 years (M12-M13) to 10 years (M6-M7). The window of rainfall and streamflow data used is listed in Table 2-3, second column. Timeseries were selected for periods with comparable rainfall record.

To verify if the rainfall and streamflow data of the micro-catchments collected in different periods are comparable, the selected window of rainfall data of each catchment were verified with the available long term daily rainfall data base (1964-2008) provided by the national hydro-meteorological institute of Ecuador (INAMHI). The extreme value analysis of the short data window and long data series did not show significant differences. Based here on, the authors concluded that the streamflow patterns of the 13 micro-catchments are not affected by the fact that data were collected in different times windows in the period 2001-2010.

A Chapman (1991) recursive digital filter for exponential recessions was used to separate the hydrograph into its components. The method is based on the analysis of the observed hydrograph shape and the magnitude of the recession constant of the flow-components (Vázquez and Feyen, 2003). The flow separation was implemented using the Water Engineering Time Series PROcessing tool (WETSPRO) developed by Willems (2009). Herein a generalization of the Chapman filter is applied consisting in a time variant fraction of the total flow related to the filtered flow component (Willems, 2000). In this study the intermittent flow (also called the subsurface flow) and baseflow component were aggregated and called *slow flow* because the duration of the recession

periods were in general too short to accurately separate intermittent flow from baseflow (Vázquez and Feyen, 2007).

Because soil properties are very similar for all studied catchments, they are not presented as punctual data or grouped by catchments. Instead, Table 2-2 depicts value ranges for the presented soil properties, providing primarily information of the organic horizon. Data on the C horizon, due to incompleteness of data and because this horizon in general is a thin, weathered layer on top of the bedrock, are not listed. However, data of the hydraulic conductivity of the C horizon, whenever available, are mentioned in the text. The saturated hydraulic conductivity listed in Table 2-2 is the horizontal saturated conductivity ( $K_s$ ) measured with the inversed auger-hole method (Kessler and Oosterbaan, 1974). The  $K_s$  data of M5 were derived from literature.

To identify patterns in the multitude of soil and hydrological data, and to express the data in such a way as to highlight their similarities and differences the principal component analysis (PCA) was applied. The objective of PCA is reducing the possibly correlated variables into a smaller number of uncorrelated variables and to transform the data to a new coordinate system such that the greatest variance by any project of the data comes to lie on the first coordinate, called the first principal component. Analogue the second greatest variance is placed on the second coordinate, and so on. Reducing the number of dimensions to three main principal components enabled to group the micro-catchments into distinct clusters, characterized by clear differences in the dominant processes controlling the conversion of rainfall into streamflow. The analysis was conducted using the correlation matrix of 17 variables including precipitation, discharge and various soil parameters. After reduction of the correlated variables a threshold value for the eigenvectors of  $\pm 0.2$  was used as to define the main contributing variables within each of the principal components.

Table 2-1: Main catchment characteristics

Catchment	Area (km <sup>2</sup> )	Altitude (m a.s.l)	Slope (%)	Shape	Geology	Soil distribution (%)	Vegetation cover (%)	Landuse
Ortigas (M1)	0.99	2305-2880	43	SO	Saraguro Fm.: lavas and andesitic	Andosol (74), Leptosol (26)	Upper montane forest (76), pasture (20), cropland (4)	N, EG, PT
Rio Grande (M2)	5.49	2230-3280	48	SO	volcanoclastic deposits	Andosol (58), Leptosol (42)	Upper montane forest (28), shrubs (39), pasture (33)	EG, N
Panama (M3)	10.01	2050-3080	44	SO	Pisayambo Fm.: pyroclastic deposits	Andosol (12), Cambisol (46), Leptosol (42)	Upper montane forest (29), pasture (57), cropland (14)	EG, N, M
Marianza pajonal (M4)	1.00	2980-3740	42	SO		Andosol (>85), Histosol (<15)	Upper montane forest (14), tussock grass (86)	N
Marianza pinos (M5)	0.59	3240-3700	37	CO	Saraguro Fm.: lavas and andesitic	Andosol (>85), Histosol (<15)	Pine forest (>90), tussock grass (<10)	PF
Huagrahuma (M6)	2.58	3690-4100	45	SO	volcanoclastic deposits	Andosol (100)	Tussock grass (100)	N
Soroche (M7)	1.59	3520-3720	20	SO		Andosol (100)	Tussock grass (70), cropland (30)	PT, IG
Quinuahuaycu (M8)	5.01	3590-3880	19	EOR		Andosol (81), Histosol (19)	Tussock grass (78), cushion plants (20), shrubs (2)	N
Calluancay (M9)	4.39	3590-3870	18	CO	Quimsacocho Fm.: volcanic and	Andosol (88), Histosol (12)	Tussock grass (69), shrubs (20), cushion plants (11)	EG
Zhurucay (M10)	1.34	3680-3900	18	EOR	volcanoclastic rocks	Andosol (85), Histosol (15)	Tussock grass (71), shrubs (2), cushion plants (26)	EG
Bermejós (M11)	21.64	3708-3960	19	EOR		Histosol (70), Andosol (30)	Tussock grass (30), cushion plants (70)	N
San Ramon (M12)	4.62	1743-3150	61	CO	Chiguinda unit: palaeozoic	Histosol (60), Cambisol (30), Regosol (10)	Upper montane cloud forest (80), sub-páramo (18), shrubs (2)	N
Zurita (M13)	11.38	2025-3075	55	SO	metamorphic rocks	Histosol (50), Regosol (30), Cambisol (20)	Upper montane cloud forest (73), sub-páramo (15), pasture (12)	W, EG

Legend: TG, tussock grasses; S, shrubs; CP, cushion plants; PT, potatoes; M, maize PF, pine forest. IG, intensive grazed; EG, extensive grazed; N, natural. W, wood; SO, stretched oval; CO, circular to oval; EOR, elongated oval to rectangular; M1-M3: Pacific coastal climate; M4-M11: inter-valley climate zone; M12-M13: Amazonian climate

Table 2-2: Properties per horizons of the main soils in the studied catchments

Soil type	Horizon thickness (cm)	Bulk density (g cm <sup>-3</sup> )	pH	SOM (%)	Ks (mm h <sup>-1</sup> )	pF=0 (cm <sup>3</sup> cm <sup>-3</sup> )	pF=2 (cm <sup>3</sup> cm <sup>-3</sup> )	pF=4.2 (cm <sup>3</sup> cm <sup>-3</sup> )	Sand (%)	Silt (%)	Clay (%)
ANDOSOL (páramo cover)											
Ah1	18-40	0.2-0.5	4.3-4.8	15-35	12-38	0.66-0.90	0.64-0.82	0.39-0.64	37-80	8-62	12-27
Ah2	20-31	0.2-0.8	4.4-4.8	13-36	10-28	0.70-0.86	0.61-0.84	0.36-0.57	21-63	17-50	20-29
A	16-53	0.2-0.9	4.5-5.7	7-31	5-36	0.74-0.81	0.72-0.78	0.30-0.43	24-33	34-55	21-41
ANDOSOL (forest cover)											
O	15-30	0.2	5.6	19	105	0.77	0.71	0.58	50		35-15
A	13-30	0.4-0.6	4.0-6.0	16-29	22-60	0.71-0.93	0.65-0.89	0.48-0.49	28-42	45-47	11-27
Bw	40-50	0.3	5.6-6.0	1-8	23-60	0.64-0.76	0.59-0.76	0.33-0.59	41-68	27-37	5-22
LEPTOSOL											
O	20-25	0.5-0.6	5.6-6.0	11-18	28-32	0.66-0.72	0.59-0.68	0.18-0.47	38-42	43-50	12-15
Ah	15-20	1.0	5.8	6-20	32	0.64	0.59	0.33	38	50	12
HISTOSOL (páramo cover)											
H1	15-20	0.1-0.2	4.6-5.1	23-60	8-15	0.85-0.90	0.84-0.90	0.13-0.39	56-84	6-30	10-34
H2	30-35	0.1-0.3	4.4-5.0	21-66	5-9	0.81-0.88	0.79-0.87	0.12-0.33	64	6-20	4-16
A	14-55	0.1-1.0	4.8-5.1	24-57	3-91	0.56-0.86	0.50-0.83	0.15-0.74	38	2-42	7-20
HISTOSOL (forest cover)											
O	10-20	0.1-0.2	4.2-4.4	33-44	160-167				42	38	20
H	10-20	0.1-0.3	4.8	28	83-91	0.76	0.5	0.23	37	42	21
Ah	10-15	0.2-0.8	5.1	13	11	0.68	0.46	0.20	30	49	21
CAMBISOL											
O	10-16	0.1-0.2	4.2-4.4	33-44	160-167				42	38	20
A	14-40	1-1.1	4.8-5.4	4-28	54-91	0.55-0.76	0.50-0.52	0.23-0.26	29-38	42	20-28
Bw	15-80	1.0-1.3	5.1-5.7	0.3-13	11-23	0.68-0.70	0.46-0.63	0.19-0.36	19-30	42-49	21-38
REGOSOL											
O	10-16	0.1-0.2	4.2-4.4	33-44	160-167				42	38	20
Ah	14-20	1-1.1	4.8-5.4	3.7-28	54-91	0.55-0.76	0.50-0.52	0.23-0.26	29-38	40-42	20-28

Legend: pH, soil acidity expressed as amount of H<sup>+</sup> cations in soil solution; SOM, soil organic matter in %; Ks, saturated hydraulic conductivity; pF, soil matric potential expressed as the log<sub>10</sub>(cm water column) respectively at saturation, field capacity and wilting point; Sand, Silt and Clay, main particle size classes in percent

## 2.3 CASE STUDY CATCHMENT DESCRIPTION

The area of the 13 studied micro-catchments varies between 0.59 and 22 km<sup>2</sup>. They are located in Ecuador between 2°24' and 3°58' south latitude and in the altitude range of 1743 to 4100 m above sea level (see Figure 2-1 and Table 2-1). The micro-catchments M1, M2, M3 and M10 drain to the Pacific Ocean while the other micro-catchments M4 to M13 with exception of M10 are tributaries of the Amazonian River Basin. The shape of the micro-catchments M1 (0.99 km<sup>2</sup>), M2 (5.49 km<sup>2</sup>) and M3 (10.01 km<sup>2</sup>) (Group 1: Pacific climate zone) is stretched oval. The altitude range and average surface slope of those three catchments are very similar, ranging between 2050 to 3280 m a.s.l. and 43 to 48%, respectively (see Table 2-1). The basin area of the micro-catchments M4 to M11 (Group 2: Inter-valley climate zone) varies between 0.59 to 21.64 km<sup>2</sup>. The catchment shape is stretched oval for the micro-catchments M4, M6 and M7; circular oval for the basins M5 and M9; and elongated oval to rectangular for M8, M10 and M11. Based on the topographic characteristics the micro-catchments in this group can be split into two subgroups. The micro-catchments in the first subgroup, M4 to M6, are steep with surface slopes varying between 37 and 45% and altitude range from 2980 to 4100 m a.s.l. The largest difference in elevation (760 m) within a micro-catchment is found in M4. The micro-catchments in the second subgroup consist of the catchments M7 to M11 with an altitudinal range between 3520 to 3960 m a.s.l. and average surface slope of 18 to 20%. The catchment shape is circular to oval for M12 (4.6 km<sup>2</sup>) and stretched oval for M13 (11.3 km<sup>2</sup>) (Group 3: Amazon climate zone), the altitude ranging between 1743 and 3150 m a.s.l. with an average surface slope of 61 and 55% for M12 and M13, respectively.

### 2.3.1 CLIMATE

In the micro-catchments M1 to M3 (Group 1) mean annual precipitation varies between 500 and 1900 mm, based on long-term rainfall record (1970-2008). The inter-annual seasonality is unimodal, influenced by the Pacific coastal regime. The wet season stretches from December to May, comprising 60 to 80% of the annual precipitation and a dry season from June to November, commonly with months without rain and a maximum observed continuous dry period of 78 days. Ninety percent of all monitored

precipitation rates are less than  $15 \text{ mm h}^{-1}$ . The temperature ranges from  $9$  to  $22^\circ\text{C}$  at  $2254 \text{ m a.s.l.}$ , with December being the coldest and October the warmest month. According to Bacuilima et al. (1999) the temperature lapse rate in the region varies between  $0.5$  and  $0.7$ . Air humidity is relatively high with values between  $40$  and  $100\%$ . More details are given in Crespo et al. (2008).

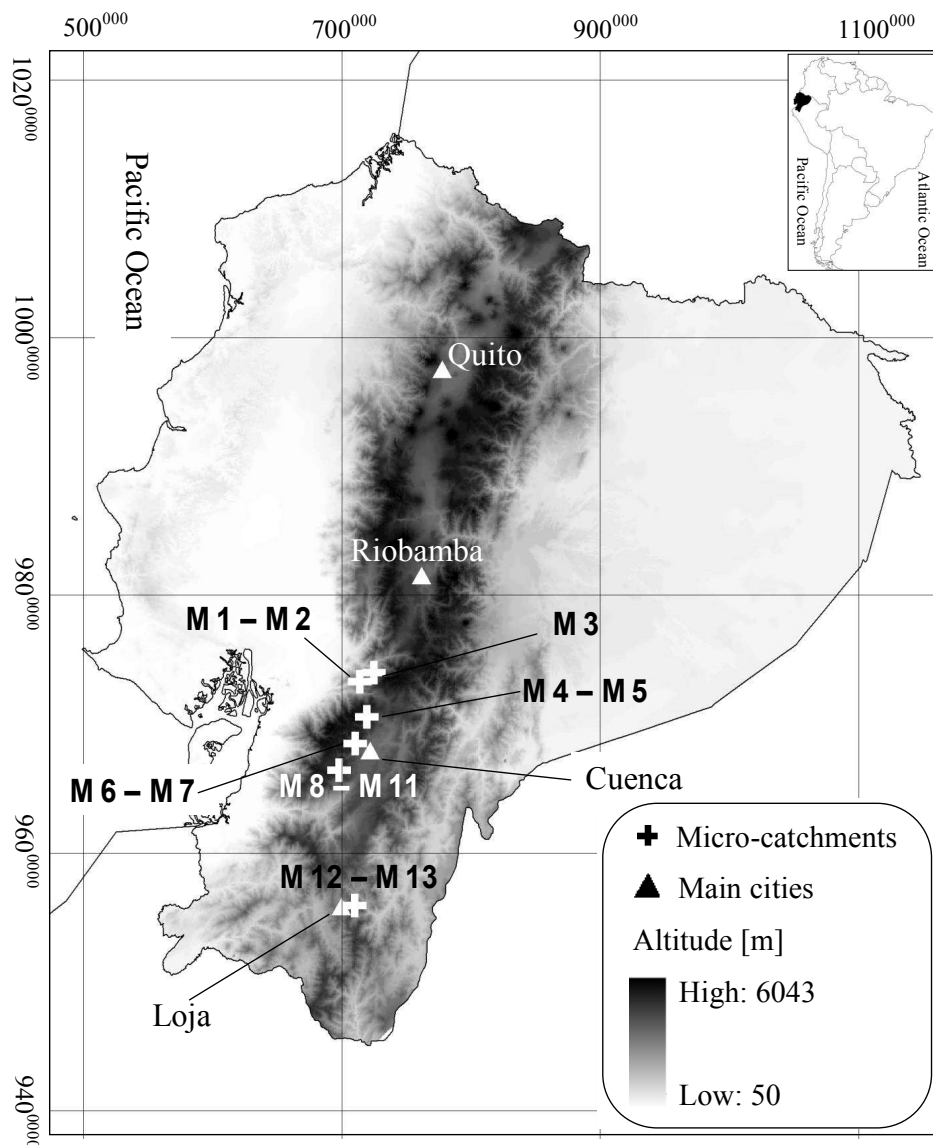


Figure 2–1: Geographical location of the 13 study micro-catchments (UTM coordinates)

The climate of the micro-catchments M4 to M11 (Group 2), located on the east slope of the western cordillera in the altitude range of  $2980$  to  $4100 \text{ m a.s.l.}$ , is influenced by the Pacific coastal regime from the west and the continental and tropical Atlantic air masses from the east (Vuille et al., 2000). The resulting precipitation pattern is bimodal, with a

major wet season in December to February and a less pronounced wet season from August to September (Buytaert et al., 2006), interrupted by short dry spell periods having a maximum length of 16 days. The mean annual precipitation, based on the long-term record of 1964-2008 (INAMHI), varies between 900 and 1600 mm, with 10% of the rains having an intensity larger than  $10 \text{ mm h}^{-1}$  (Buytaert et al., 2006a). The temperature decreases at an average rate of 0.5 to  $0.7^{\circ}\text{C}$  per 100 m (Bacuilima et al., 1999; van der Hammen and Hooghiemstra, 2000; Castaño, 2002), with the mean temperature being around  $7^{\circ}\text{C}$  at 3500 m a.s.l. (Buytaert, 2004). Daily solar radiation and temperature are almost constant throughout the year, while the interday variability is quite marked. Intraday temperature variations can be as large as  $20^{\circ}\text{C}$ . A more detailed description of the climate is available in Buytaert et al. (2006a), Buytaert et al. (2007) and PROMAS/IAMGOLD (2009). Fog interception is negligible as reported by Buytaert et al. (2007), on the basis of which it is assumed that fog captured by the páramo ecosystem not really contributes to the soil water reservoir.

The climate in the micro-catchments M12 and M13 (Group 3) is influenced by the air masses from the east, the Amazonian basin (Beck et al., 2008). The precipitation pattern is unimodal with relative constant seasonality and moderate to low inter-annual variability. The main wet season is from April to September with a maximum of 10 days without rain (Fleischbein et al., 2005). According to Rollenbeck (2006) precipitation is strongly correlated with altitude, and intensities are low with 90% of all monitored rain rates below  $10 \text{ mm h}^{-1}$ . Precipitation is primarily caused by advective orographical clouds. In the period 1964-2008 annual precipitation varied from 900 to 4300 mm (INAMHI) with an average of 2200 mm at an altitude of 1960 m; wind speeds being low and cloud cover less dense at this elevation. Average rainfall increases to 4700 mm (monitoring period 1994-2004) at the Cerro del Consuelo station located at the border of the catchment (3200 m a.s.l.) (Rollenbeck, 2006; Bendix et al., 2008). Horizontal rain and cloud/fog water deposition contributes considerably to the total ecological water input representing up to 41.2% of the basin water yield (Bendix et al., 2008). The mean annual temperature at 1952 m a.s.l. is  $15.2^{\circ}\text{C}$ . The coldest months are June and July, with a mean temperature of  $14.4^{\circ}\text{C}$ ; the warmest month is November with a mean temperature of  $16.1^{\circ}\text{C}$ . The average temperature gradient between the station at 1952 m and 2927 m a.s.l. is  $0.66^{\circ}\text{C}$  per 100 m, and the mean humidity is 86% (period 1998 to 2004) (Fleischbein et al., 2006).

### 2.3.2 LAND COVER AND USE

Micro-catchment M1 represents the pristine condition in Group 1 with 74% of the basin covered by upper montane forest (*Asteraceae*, *Boraginaceae*, *Coriaceae*, *Euphorbiaceae*, *Junglandaceae*, *Fabaceae*, *Melastomataceae*, *Scrophulariaceae*, *Solanaceae*, *Verbenaceae*) (Bruijnzeel, 2001; Crespo et al., 2008). Canopy height is in general 5 to 10 m, occasionally exceeding 15 m (Bussmann, 2005), amply covered by lichens and epiphytes (Balslev and Øllgard, 2002). According to Bendix et al. (2008) fog interception is negligible at this altitude. The micro-catchment M2 is very representative for the anthropogenic degraded condition; forest is cut, and burned, and farmers use the land for cultivation and grazing. When pasture and cropland are exhausted the land is abandoned and left to natural regeneration. Catchments are mainly covered by small shrubs (*Melastomataceae*, *Asteraceae*) (39%); some patches of upper montane forest (28%) and pasture (*Penicetum clandestinum*) (33%). The micro-catchment M3 represents the most human affected condition with 57% of its area covered with pasture (*Penicetum clandestinum*) and 14% cropland (annual rotation of potatoes, corn and vegetables). Montane forest occupies the remaining 29% of the area, primarily in steep and inaccessible zones and near the river bed.

The micro-catchments in Group 2 belong to the páramo ecosystem (neotropical alpine grassland) covering the Andes region above 3500 m a.s.l. (Luteyn, 1992; Hofstede, 1995; Medina and Vásquez, 2001). The landscape above 3500 m a.s.l. is typically composed of relatively flat to concave valleys. Below 3500 m the land is steeper covered by cloud forests. The micro-catchments M4, M6 and M8 have low human impact limited to free roaming cattle. Those catchments are covered with páramo vegetation consisting of tussock grass, low shrubs and upper montane forest (Table 2-1) (Buytaert et al., 2006b). The M11 catchment is a wetland covered by cushion plants and the M8 and M9 micro-catchments are covered by tussock grass, with an animal density of 0.5 to 2 heads per hectare. These catchments are annually burned and grazed. In the micro-catchment M7 grazing with an animal density of 2 to 3 heads per hectare, artificial drainage and cultivation of potatoes take place. Cultivation is continuous throughout the year, without a specific growing season, covering 30% of the catchment. In the rest of the catchment, original grass vegetation has been replaced by more

nutritious species which are intensively grazed by cattle. Micro-catchment M5 is planted with *Pinus patula*. The forest is about 20 years old with a tree density of 1000 stems ha<sup>-1</sup> and covering over 90% of the catchment. A more detailed description of the catchments can be found in Buytaert et al. (2006b), Buytaert et al. (2007) and PROMAS/IAMGOLD (2009).

Micro-catchment M12 (Group 3) is for 80% covered with pristine montane cloud forest, with trees up to 20 m high. Dominant plant species are of the families *Lauraceae*, *Euphorbiaceae*, *Melastomataceae* and *Rubiaceae* (Homeier et al., 2002). In the upland area of the micro-catchment (3140 m a.s.l.) vegetation mainly consists of sub-páramo shrubs, adapted to higher wind speeds, lower temperatures and low nutrient availability (Beck et al., 2008). The micro-catchment M13 (Group 3) is representative for mixed conditions with moderate human impact. Anthropogenic impacts consist of extensive wood cutting, gravel mining in the river bed, a draining gravel road and extensive grazing. The catchment is primarily covered with montane cloud forest (73%), sub-páramo (15%) and extensive pastures (*Setaria sphacelata*) (Werner et al., 2005).

### 2.3.3 GEOLOGY

The micro-catchment M3 is located on the Pisayambo Fm. composed of compacted pyroclastic deposits with basaltic, andesite and rhyolitic composition dating from the Pliocene age. The geology of the micro-catchments M1, M2 and M4 to M7 belongs to the Late Oligocene to Early Miocene Saraguro Fm. with lavas and andesitic volcanoclastic deposits compacted by glacier activity during the last ice age (Coltorti and Ollier, 2000; Hungerbühler et al., 2002). The hydraulic conductivity of the Pisayambo and Saraguro Fm. is low (Buytaert et al., 2005), and their lithology similar (Kennerley, 1980). The micro-catchments M8 to M11 are located on the Quimsacocha Fm. (Pratt et al., 1997). Covered by volcanic and volcanoclastic rocks, the formation consists of basalt flows with plagioclase, feldspar phenocrysts and andesitic pyroclastic deposits. According to IAMGOLD (2006) the age of the deposits is not defined; hydraulically they are nearly impermeable and possess a low density of fissures in the top layer of the formation. The micro-catchments M12 and M13, located in the Cordillera Real on the Amazonian side, correspond to the Chiguinda unit, which is mainly composed of Paleozoic metamorphic rocks such as semipelite, phyllite and

quartzite with low alteration (Litherland et al., 1994; Hungerbühler, 1997; Bendix et al., 2008). Observations and findings (Buytaert et al., 2005; Buytaert et al., 2007; Bücker et al., 2010; PROMAS/IAMGOLD, 2009) tend to suggest that (i) the geological impact on the runoff generation process is minimal, (ii) in most of the catchments only a minor fraction of the water in the soil reservoir percolates into the bedrock, and (iii) in local depressions of the bedrock a non-permanent water table is found.

#### 2.3.4 SOILS

The main soil types in the study catchments are Andosol, Leptosol, Histosol, Cambisol and Regosol (FAO/ISRIC/ISSS, 1998). Table 2-1 depicts the soil distribution per catchment, and Table 2-2 summarizes per horizon the soil properties. The cold and wet climate and the low atmospheric pressure, characteristic for highlands, favor organic matter accumulation. This, together with the volcanic ash accumulation, is responsible for the dark, humic and acid soils, with an open pore structure, classified as Andosols. Andosols typically have a high organic matter content (13-36%), low bulk density (0.2-0.8 g cm<sup>-3</sup>) and high water retention capacity (0.64-0.93 cm<sup>3</sup> cm<sup>-3</sup> at saturation) (Buytaert, 2004). The depth of the organic horizon varies between 40 and 104 cm. The sequence of Ah1, Ah2, A, and C horizons are typically for Andosols under páramo, below forest the Ah1 horizon is replaced by an O (organic litter) horizon. The horizons are acid with a pH ranging between 4 and 6.

Leptosols are shallow with the O or Ah horizon lying directly on top of the parent material. Both horizons have fairly similar properties, are 15-25 cm deep, have a pH of 5.6 to 6.0, an organic matter content in the range of 6-20%, and a bulk density varying between 0.5 and 1.0 g cm<sup>-3</sup>. Histosols typically contain a high fraction of non-decomposed plant fibers, particularly in the páramo belt (Beck et al., 2008). The main properties of the soils are very high organic matter (21-66%), low bulk density (0.1-0.3 g cm<sup>-3</sup>), and high water retention between saturation and field capacity. The higher situated Histosols (above 3500 m a.s.l.) are on average 90 cm deep, typically composed of a H1, H2 and A horizon with high organic matter content. The Histosols under cloud forest (below 3500 m a.s.l.) are less deep with main horizons O, H, Ah and C (Makeschin et al., 2008; Wilcke et al., 2002).

The 120 cm deep Cambisols under pasture (M3) are characterized by three horizons (A, Bw and C) with decreasing saturated hydraulic conductivity, respectively 54.6, 23.4 and 16 mm h<sup>-1</sup>. The bulk density varies between 1.0 and 1.3 g cm<sup>-3</sup>. The soil organic matter content decreases with depth, fluctuating between 4 and 28% in the A and 0.3 to 13% in the Bw horizon. As a consequence of the overall lower organic matter content, the water retention capacity in both horizons is less than in the organic rich horizons of the Andosols and Histosols (see Table 2-2). The Cambisols in the M12 and M13 catchments are typical Dystric or Humic Cambisols with the horizon sequence O, Ah, Bw and C under forest (Wilcke et al., 2002). As observed by Makeschin et al. (2008) the change in land cover from forest to shrub and pasture strongly reduces the thickness and the properties of the O horizon. Huwe et al. (2008) reported a significant reduction in the saturated hydraulic conductivity under pasture. Regosols are only present in the M12 and M13 catchments, mainly situated below 2100 m a.s.l. The typical horizon sequence of Regosols under forest is O, Ah and C, with the O horizon significantly reduced under shrubs or ferns and completely lost under pasture (Makeschin et al., 2008). The horizon properties are very similar to the properties of the Cambisols; however the Ah horizon is less developed (14 to 20 cm thick).

## 2.4 RESULTS AND DISCUSSION

### 2.4.1 STREAMFLOW PATTERN

Analysis of the rainfall timeseries reveals that rainfall throughout the year is fairly uniformly distributed in the micro-catchments belonging to Group 2 and 3. The rainfall timeseries of the micro-catchments in Group 1 reflect the presence of a rainy and dry season. Intensity of most storm events, below 10 mm h<sup>-1</sup> for the micro-catchments in Group 1 and 2 and below 15 mm h<sup>-1</sup> for the catchments in Group 3, is less than the saturated hydraulic conductivity of the top layer, which for Group 1 and 2 varies between 8 and 32 mm h<sup>-1</sup> and Group 3 between 160 and 167 mm h<sup>-1</sup>. Similar results were found by Buytaert et al. (2007), Crespo et al. (2008), Crespo et al. (2010) and PROMAS/IAMGOLD (2009). Given the low to moderate rainfall intensities it is very unlikely that Horton overland flow occurs. Fleischbein et al. (2006) also excluded the occurrence of Horton overland flow based on the results obtained from a field survey

nearby the M12 and M13 micro-catchments. Blume et al. (2007) and Buytaert et al. (2007) came to the same conclusion for a forested and páramo catchment in the south of Chile and Ecuador.

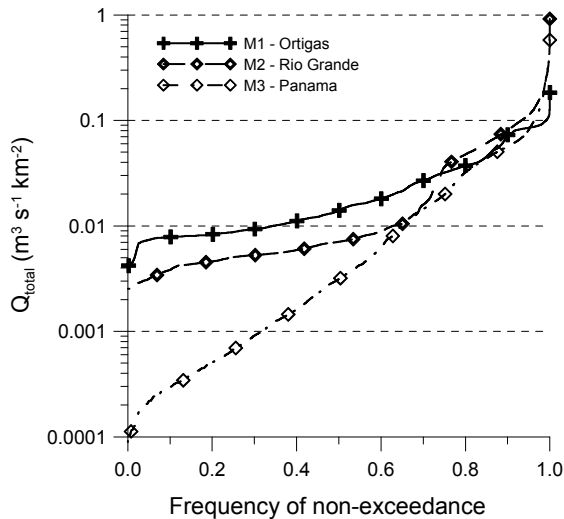


Figure 2–2a: 1-hour FDCs of the micro-catchments M1, M2 and M3 (Group 1) situated in the Pacific climate zone

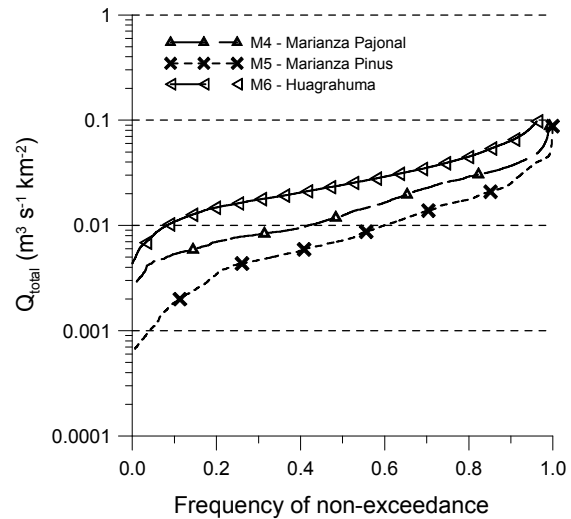


Figure 2–2b: 1-hour FDCs of the micro-catchments M4, M5 and M6 (Group 2) situated in the inter-valley climate zone

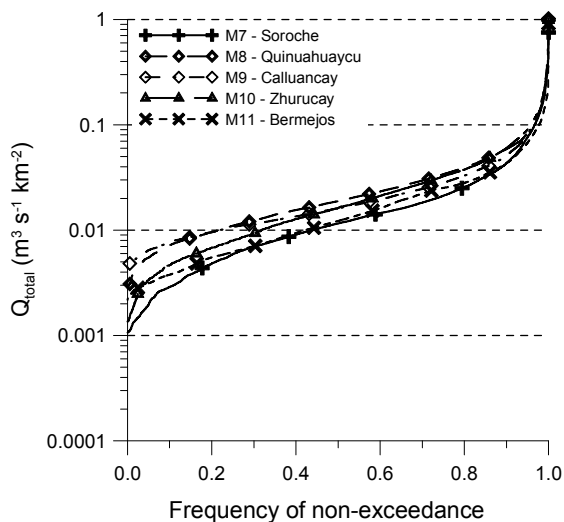


Figure 2–2c: 1-hour FDCs of the micro-catchments M7, M8, M9, M10 and M11 (Group 2) situated in the inter-valley climate zone

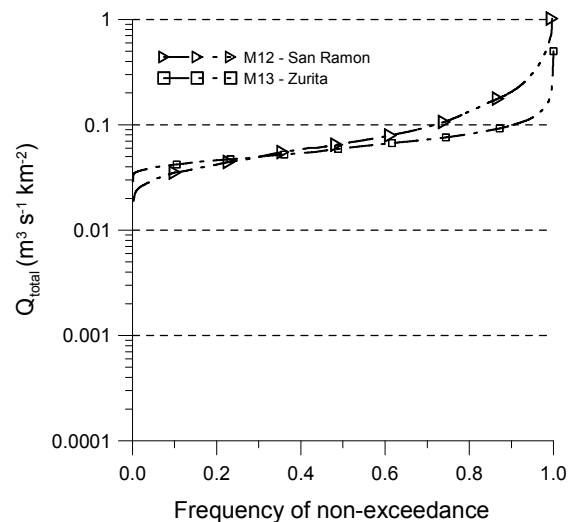


Figure 2–2d: 1-hour FDCs of the micro-catchments M12 and M13 (Group 3) situated in the Amazon climate zone

Figures 2-2a to 2-2d depict the 1-hour flow duration curve (FDC) of the studied micro-catchments. The x-axis lists the probability of non-exceedance and the y-axis the total streamflow expressed in  $\text{m}^3 \text{s}^{-1} \text{km}^{-2}$ . The FDCs of the catchments in Group 1 (Pacific climate zone), 2 (Inter-valley climate zone) and 3 (Amazon climate zone), except M3,

have similar shapes. This suggests that the same processes control the runoff generation notwithstanding the difference in climate and catchment properties. As can be derived from Table 2-3 streamflow is dominated by the slow flow component, representing 60.9 to 96.4% of the total flow, confirming that overland flow occurs only very occasionally. The larger hydraulic conductivity of the top soil in M1, M4 and M5 is responsible for the fact that slow flow represents respectively 96.4, 87.2 and 91.5% of the total flow. The slow flow component in M13 represents a larger fraction of the average total flow than in M12, respectively 89.0 versus 69.9%, notwithstanding similarity in catchment properties. This is likely due to the larger lateral flow contribution of the C horizon and the cracks in the upper zone of the bedrock for low streamflow in M13 than M12, as suggested by Bücken et al. (2010), and the higher precipitation in M12 which enhances the quick flow contribution as fast lateral flow through the organic horizon. The fraction of the slow flow in the remaining micro-catchments (M2, M3 and M6 to M11) varies between 60.9 to 75.9% of the total flow, very much in concordance with other studies (Célleri ,2007; Germer ,2008; Mortatti et al., 1997; Fujieda et al., 1997).

Above the non-exceedance probability level of 70% the observed distribution of high flows is almost the same in M1, M2 and M3. Differences in streamflow distribution below this level can be attributed to the following:

- (i) The average annual rainfall in M1 is higher than in M2 and M3 (4.7 mm d<sup>-1</sup> versus 3.5 a 3.6 mm d<sup>-1</sup>) compensating the interception losses caused by the relative high degree of basin area covered by forest but still resulting in more runoff;
- (ii) The lower flow-values for M3 as compared to M1 and M2, below the 70% non-exceedance probability, can be explained by the difference in geology and the anthropogenic impact (71% of the area in M3 is pasture and cropland versus 24 and 33% in M1 and M2). M3 is underlain by the Pisayambo Fm. whereas M1 and M2 are situated on the Saraguro Fm. It is possible that locally the top of the Pisayambo Fm. is semi-pervious capturing a fraction of the infiltrating precipitation. Unfortunately data to confirm this are not available. In addition in M3 a considerable fraction of the runoff water is tapped for irrigation water in the dry season reducing the runoff volume. Furthermore the soil physical properties degrade by the conversion of forest and shrub land to pasture or cropland (see Table 2-2). Similarly Bruijnzeel (2004), Buytaert (2004) and Vignola (2005) reported that intensive grazing and crop farming negatively affect the soil water

retention capacity. Morales (2008) and Tobón et al. (2006) stated that human impact is the main cause of a drop in discharge during dry spell periods as a consequence of a drop in soil water retention and hydraulic conductivity.

The FDCs of the micro-catchments in Group 2, although alike were split in two subgroups, respectively the micro-catchments M4 to M6 (Figure 2-2b) and the micro-catchments M7 to M11 (Figure 2-2c). Comparing both figures it is clear that the FDCs of the subgroup M7 to M11 are situated within a narrow range; the FDCs of the subgroup M4, M5 and M6 are much more different. The largest differences between both subgroups are: (i) the average basin slope which for the first subgroup varies between 37 and 45%, and between 18 and 20% for the second subgroup, and (ii) there is a higher variability in the partitioning of the flow between slow and quick flow across M4 to M6 than within M7 to M11. Difference in behavior of the micro-catchments M4-M6 as compared to the catchments M7-M11 can be explained by the fact that minor differences in rainfall and basin properties are more strongly reflected in the FDC due to the steep average slope of those catchments, on average 40% versus 20%. The mild slope of the micro-catchments M7-M11 masks local differences in precipitation pattern and basin properties. The higher flow-values of M6 in Figure 2-2b is the consequence of the overall higher rainfall in this micro-catchment as compared to the other micro-catchments in Group 2, being the consequence of the higher situation of this micro-catchment in the Andes mountain range. On the other hand the fact that in Figure 2-2b the FDC of M5 is positioned lowest can, as stated by Buytaert et al. (2007), be explained by the high degree of afforestation, 90% of the basin is covered with *Pinus patula*. Pine strongly intercepts precipitation which during dry spell periods evaporates reducing the fraction of rainfall contributing to runoff.

The FDCs of M12 and M13 (Group 3), situated in the Amazon climate zone, are shown in Figure 2-2d. The flow values of both FDCs are larger than the flow values of the FDCs of all other micro-catchments in the survey simply due to the fact that the rainfall in the Amazonian region is 2 to 3 times as high. Furthermore, the shape of the FDCs of both micro-catchments is more flat indicating that rainfall is fairly uniform. The larger fraction of quick flow in M12 than in M13 is due to the higher annual rainfall in M12, 3799 versus 2672 mm.

## 2.4.2 WATER YIELD AND ACTUAL EVAPOTRANSPIRATION

As depicted in Table 2-3, the average water yield of the micro-catchments in Group 1 (M1-M3), the Pacific climate zone, varies between 1.74 and 2.42 mm d<sup>-1</sup>, representing 46 to 68% of the precipitation. The micro-catchments in the Amazon climate zone (Group 3, M12-M13) have a much higher water yield varying between 5.78 and 8.43 mm d<sup>-1</sup>, equivalent to 79 to 81% of the rainfall. The average water yield of the micro-catchments situated in the inter-valley climate zone, Group 2 (M4-M11), varies between 0.99 and 2.94 mm d<sup>-1</sup>, corresponding to 28 to 74% of the precipitation, respectively.

The average rest term of the water balance, considered as an approximation of the actual evapotranspiration, is highest for the catchments M1 (2.50 mm d<sup>-1</sup>), M5 (2.51 mm d<sup>-1</sup>), M12 (1.98 mm d<sup>-1</sup>), M4 (1.68 mm d<sup>-1</sup>) and M13 (1.54 mm d<sup>-1</sup>). Foregoing can be explained by the high coverage of forest varying between 14 to 100% of the basin area, causing the interception of rainfall and fog followed by evaporation (Wilcke et al., 2008). The difference in evapotranspiration between M2 and M3 is due to the re-use of runoff water for irrigation in M3. The actual evapotranspiration of M1 closely matches the average evapotranspiration value of 2.68 mm d<sup>-1</sup> reported by Bruijnzeel (2001) for lower montane cloud forest. The average actual evapotranspiration of the micro-catchments M6 to M11 is lower varying between 0.9 and 1.4 mm d<sup>-1</sup>. The lower level can be explained by the overall lower average annual rainfall and the low transpiration rate of tussock grass. The leaf morphology of tussock grass and the sunken position of the stomata are considered responsible for the lower level of physiology and transpiration (Ramírez et al., 2006). The average value of the evapotranspiration for M12 and M13 is smaller than the range published by Bruijnzeel (2001) for tropical lowland forest (2.43 to 4.40 mm d<sup>-1</sup>) and larger than the range found for upper montane cloud forest (0.85 to 1.07 mm d<sup>-1</sup>). Fleischbein et al. (2006) on the other hand reported an average value for the evapotranspiration of 4.06 mm d<sup>-1</sup> for upper montane cloud forest, which is twice as large as the value derived in this study for M12. These authors conducted their experiments on two small catchments, respectively 8 and 9 ha large, in the vicinity of the M12 micro-catchment and used the same assumption for the water balance, i.e. actual evapotranspiration can be approximated as the rest term of the water balance. However, the difference is presumably due to the large gaps in the streamflow data; up to 80% of the monitoring period was missing and reconstructed using

TOPMODEL (Fleischbein et al., 2006). This might have led to an underestimation of the outflow and consequently and overestimation of the rest term.

Table 2–3: Average terms of the catchment water balance

Catchment	Used data window	P (mm d <sup>-1</sup> )	Q <sub>total</sub> (mm d <sup>-1</sup> )	Q <sub>average</sub> (m <sup>3</sup> s <sup>-1</sup> )	P-Q <sub>total</sub> (mm d <sup>-1</sup> )	Q <sub>slow</sub> %	Q <sub>quick</sub> %	RC
M1	06/09/2005 - 15/07/2008	4.7	2.2	0.025	2.5	96.4	3.6	0.46
M2	20/02/2006 - 01/01/2008	3.6	2.4	0.154	1.2	67.9	32.1	0.68
M3	23/11/2005 - 12/03/2008	3.5	1.7	0.200	1.8	67.4	32.6	0.50
M4	21/10/2005 - 27/06/2007	3.3	1.6	0.019	1.7	87.2	12.8	0.49
M5	19/10/2006 - 23/09/2008	3.5	1.0	0.007	2.5	91.5	8.5	0.28
M6	13/08/2003 - 29/10/2008	4.0	2.9	0.088	1.0	75.9	24.1	0.74
M7	11/05/2002 - 29/09/2003	3.0	1.9	0.034	1.1	60.9	39.1	0.63
M8	10/11/2006 - 11/11/2008	3.5	2.6	0.150	0.9	67.8	32.2	0.74
M9	10/11/2006 - 11/11/2008	3.8	2.4	0.122	1.4	69.0	31.0	0.64
M10	26/10/2006 - 11/11/2008	3.4	2.5	0.039	0.9	65.8	34.2	0.74
M11	25/10/2006 - 11/11/2008	2.9	1.8	0.452	1.1	61.6	38.4	0.62
M12	23/04/2007 - 24/08/2008	10.4	8.4	0.451	2.0	69.9	30.1	0.81
M13	23/04/2007 - 24/08/2008	7.3	5.8	0.761	1.5	89.0	11.0	0.79

Legend: RC, fraction of the rainfall leaving the catchment as streamflow (runoff coefficient); M1-M3, Pacific coastal climate; M4-M11, inter-valley climate zone; M12-M13, Amazonian climate

The difference between our data and the published data of Bruijnzeel (2001) and Fleischbein et al. (2006) is not unique. An analysis of the literature reveals that a large divergence exist between published average values of the evapotranspiration, partly because experimental conditions are not always comparable and literature is not always clear on the assumptions on which the rest term of the water balance is derived. For instance Hutley et al. (1997) found an average evapotranspiration value of 3.45 mm d<sup>-1</sup> for a highly fog-influenced Australian subtropical rainforest, while Motzer (2003) reported for similar conditions an average value of 1.54 mm d<sup>-1</sup>. The difference in reported values underlines the importance for the long-term monitoring of the water balance terms of properly selected representative catchments, but also a better representation of the high spatial variability of precipitation inputs.

Table 2–4: Eigenvectors of the variables retained in the three first principal components

Variables	PC1 42%	PC2 32%	PC3 10%
Slope	<b>0.372</b>	-0.026	-0.157
BD>20	-0.057	<b>-0.375</b>	<b>-0.385</b>
BD<20	<b>0.348</b>	-0.192	-0.077
Ks>20	<b>0.407</b>	0.102	-0.077
Ks<20	<b>0.357</b>	<b>0.205</b>	-0.049
Ks-C	0.140	<b>-0.381</b>	<b>0.339</b>
AWC	-0.029	-0.182	<b>-0.754</b>
P	<b>0.372</b>	<b>0.216</b>	-0.052
RC	0.033	<b>0.457</b>	-0.053
ET	<b>0.276</b>	<b>-0.325</b>	0.010
%Q <sub>slow</sub>	<b>0.245</b>	<b>-0.291</b>	<b>0.346</b>

Legend: PC1, PC2 and PC3, principal components of the original variables; Slope in percent; BD, bulk density; Ks, saturated hydraulic conductivity; AWC, water content at saturation of the organic horizon; P, average annual precipitation; RC, runoff coefficient; ET, actual evapotranspiration, equal to the rest term of the water balance; %Q<sub>slow</sub>, average percentage of slow flow contribution to the total discharge; >20, below 20 cm depth in the organic horizon; <20, above 20 cm depth; C, C horizon; bold numbers in grey shaded cells have an eigenvector value larger than 0.20 or smaller than -0.20

### 2.4.3 HYDROLOGICAL PROCESSES

For the assessment of the causal factors the correlation matrix between streamflow and the variables depicted in the Tables 2-2 and 2-3 was examined. Unfortunately the analysis did not yield any significant correlation, not enabling to get a clear picture of the variables controlling the rainfall-runoff process. Given the likelihood that streamflow in

the studied micro-catchments is the result of a group of variables a principal component analysis (PCA) was conducted. Table 2-4 lists the variables retained after elimination of the correlated variables and the eigenvector value for the 1<sup>st</sup>, 2<sup>nd</sup> and 3<sup>rd</sup> most important principal component. The three principal components explain 84% of the variance in hydrologic response. Of the three streamflow variables, Q<sub>total</sub>, %Q<sub>quick</sub> and %Q<sub>slow</sub>, only %Q<sub>slow</sub> was retained in the analysis, given the belief that the lateral subsurface flow through the organic horizons is dominant in the transfer of rainfall into runoff. As illustrated in Table 2-4 the contributing variables to the first principal component (PC) explain 42% of the total variance. The variables retained and positively correlated in the 1<sup>st</sup> PC, ranked according to their importance as expressed by the eigenvector value, are precipitation, average surface slope, the saturated hydraulic conductivity of the top and bottom layer of the organic horizon, the bulk density of the top horizon and to a lesser

extent the rest term of the water balance and the contribution of slow flow to the total streamflow. The significant variables associated with PC2, explaining 32% of the variance, are the runoff coefficient, precipitation and the saturated hydraulic conductivity of the top horizon; other retained variables in PC2 but negatively correlated are the bulk density of the soil profile, the saturated hydraulic conductivity of the C horizon, precipitation, evapotranspiration and  $\%Q_{\text{slow}}$ . PC3 still explains 10% of the variance in hydrologic response and is positively correlated to the saturated hydraulic conductivity of the C horizon and  $\%Q_{\text{slow}}$ , and negatively with the bulk density of the upper organic horizon and the soil water content at saturation of the organic horizons. Based on the retained variables and their positive, respectively negative correlation within each of the principal components the following physical meaning is attributed to each of the PC's:

- (i) PC1 represents the wet basin condition, i.e. when the soils are near saturation or saturated following a period of intense rainfall. Under this condition the different horizons in the soil profile contribute to the lateral subsurface flow of which the flow is controlled by the gradient of the surface and the hydraulic conductivity of the subsequent horizons. The organic horizons are very permeable and therefore contribute most, explaining the fast rise of total streamflow and the large fraction of the slow flow in the total streamflow component.
- (ii) PC2 stands for the wet to moderate dry conditions of the soil profile whereby the effect of rainfall becomes less significant. When evapotranspiration increases soil wetness reduces explaining the negative correlation, depleting first the litter and/or top organic horizon. Subsurface flow continuous primarily through the organic horizons, and limited through the mineral horizon as indicated by the negative correlation of PC2 with the bulk density and the saturated hydraulic conductivity of the C horizon. The fraction of slow flow in the total flow increases due to the reduction of overland flow. Runoff still can be important during wet periods. The soil physical parameters increasingly control the flow process.
- (iii) PC3 describes the phenomenon under moderate to dry condition whereby the quick flow component is zero or negligible and the drainage to the river network entirely consists of slow flow, produced by the mineral C horizon and the cracks in the top layer of the bedrock, and to a much lesser extent by the lower organic horizons. This is confirmed by the negative correlation of PC3 with the water content at saturation in the organic horizons.

Figure 2-3 depicts the ordination plot of the micro-catchments as a function of PC1 and PC2. This plot reveals that the hydrologic response of the 13 micro-catchments can be grouped into 3 clusters (I, II and III). Cluster I contains the micro-catchments M12 and M13, both situated in the San Francisco River Basin with Amazon climate, and with the average annual rainfall two to three times as large as the average annual rainfall recorded in all other studied micro-catchments. Both catchments, covered with upper montane cloud forest, have the highest average discharge and an average rest term of the water balance varying between 1.5 and 2.0 mm d<sup>-1</sup>. The position of Cluster I in the ordination plot confirms that the runoff process in M12 and M13 is mainly controlled by rainfall and the soil physical factors. Rainfall is fairly uniformly distributed throughout the year, such that most of the rainfall infiltrates keeping the soil moisture content in wet to moderate wet condition favoring the subsurface flow through the litter layer and the underlying organic horizons. Elsenbeer (2001), Goller et al. (2005) and Fleischbein et al. (2006) subscribed the flow in catchments similar to the catchments M12 and M13 as “organic horizon flow”, by which these authors refer to the fast lateral flow in the organic horizons.

Cluster II groups the micro-catchments M2 and M6 to M11. These micro-catchments are with the exception of M2, situated in the inter-valley climate zone at the east flank of the cordillera. M2 is situated at the west flank where climate is dominated by the Pacific Ocean. Common for these catchments is the similarity in average actual evapotranspiration, ranging between 0.90 and 1.38 mm d<sup>-1</sup>, and the relative large area under tussock grass and/or shrubs. The fraction under pasture and cropland is small to nonexistent. The position of this cluster in the ordination plot indicates that the hydrology of the micro-catchments in Cluster II mainly is controlled by the variables constituting PC2, it is climate characterized by rainfall and evapotranspiration, and the soil physical properties of the lower half of the organic horizons. The relative high contribution of the runoff coefficient in PC2 is the consequence of the relative high flows occurring during extreme wet conditions.

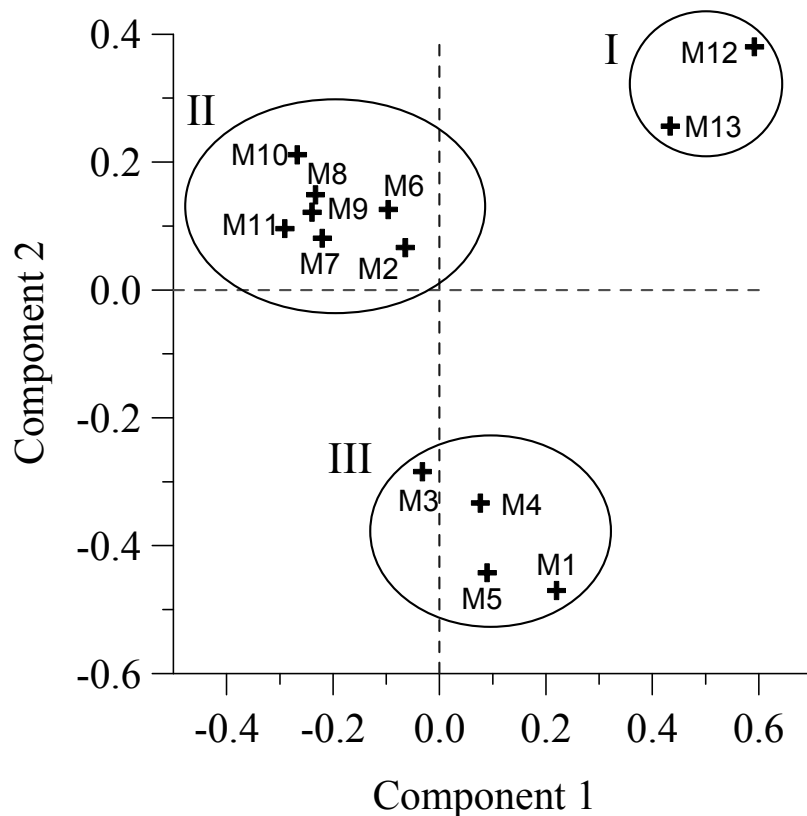


Figure 2–3: Ordination plot of the study micro-catchments according to the principal components 1 and 2

Cluster III is composed of the micro-catchments M1, M3, M4 and M5, which are, with the exception of M3, predominantly covered with upper montane forest, páramo and pine forest. M3 has a strong anthropogenic influence; 73% of the basin area has been converted to pasture and cropland. As stated above, a considerable fraction of the runoff water in this catchment is re-used as irrigation water. The 4 micro-catchment have in common that slow flow is a large proportion of the total flow, varying between 87 and 97%. Furthermore all 4 micro-catchments are steep with an average surface slope in the range of 37 to 44%. The position of this cluster in the ordination plot (Figure 2-3) is slightly controlled by PC1 and strongly, but negatively, controlled by PC2. The steepness of the basins, the shallowness of the soils, the permanent vegetation, and the high permeability of the top soil suggests that subsurface flow dominates the rainfall-runoff process.

The original variables in the three PCs, explaining 84% of the variance, reveal that the magnitude of the runoff and its distribution are controlled by precipitation, slope, bulk density of the top layer, lateral saturated hydraulic conductivity of the upper and lower

horizons, rest term of the water balance and  $\%Q_{\text{slow}}$ . Vegetation does not seem to have an effect on the rainfall-runoff process, except on the evapotranspiration when interception of rainfall and fog are important. Notwithstanding the sometimes high average basin slope, overland flow is not that significant as a consequence of flush vegetation, the low bulk density of the top layer of the Andosols and Histosols, and the high lateral saturated hydraulic conductivity. This and the fact that the basins are underlain by bedrock suggests that the infiltrating precipitation percolates relatively quickly to the bottom of the shallow to medium deep soil profiles, start filling up the soil layers from the bottom to the top, and as a layer saturates water starts flowing lateral by gravity towards the drainage network. That the soil composition is actually controlling the hydraulic response of the micro-catchments is confirmed by the main contributing variables in the 2<sup>nd</sup> and 3<sup>rd</sup> principal component. The analysis also reveals that human interference in the studied basins does not strongly modify the temporal streamflow distribution, although it affects the soil physical properties, the interception and the evapotranspiration. And even if it does modify the streamflow distribution, the affected area within the basin is relatively small with respect to the unaffected basin area or the density of the impact is limited (e.g. number of cattle per ha is still at the low side) as to become clearly visible in the shape of the FDC.

## 2.5 CONCLUSIONS

The hydrology of the studied micro-catchments is in addition to the average annual rainfall depth, rainfall regime and slope primarily controlled by the horizon sequence and the lateral saturated hydraulic conductivity of each horizon. It is realistic to assume that under dry-tropic conditions the slow flow component consists of the lateral flow in the C horizon and contributions of the top layer in the bedrock, if any, the so-called baseflow. Under wet conditions the slow flow component represents the lateral flow in the organic horizon(s) and litter layer, which could be considered as a form of intermittent flow. Overland flow most probably occurs primarily by saturation excess. Albeit it seems that in all studied micro-catchments, in addition to the magnitude of rainfall and variety of catchment properties, the hydrological response is dominated by the physical soil properties. The antecedent soil water content controls which layer of the soil profile mostly contributes to the slow flow component of streamflow, being in

all studied micro-catchments the major contributor to total streamflow. It is most probable that those findings, representative for the area in which the 13 micro-catchments are situated, apply to the entire Andes Cordillera above 2500 m a.s.l. stretching from Riobamba to the border with Peru, a distance bird-flight of 600 km.

### 3 PRELIMINARY EVALUATION OF THE RUNOFF PROCESSES IN A REMOTE MONTANE CLOUD FOREST BASIN USING MIXING MODEL ANALYSIS AND MEAN TRANSIT TIME

#### Abstract

In this study the Mean Transit Time and Mixing Model Analysis methods are combined to unravel the runoff generation process of the San Francisco River basin (75.3 km<sup>2</sup>) situated on the Amazonian side of the Cordillera Real in the southernmost Andes of Ecuador. The montane basin is covered with cloud forest, sub-páramo, pasture and ferns. Nested sampling was applied for the collection of streamwater samples and discharge measurements in the main tributaries and outlet of the basin, and for the collection of soil and rock water samples. Weekly to biweekly water grab samples were taken at all stations in the period April 2007 - November 2008. Hydrometric data, Mean Transit Time and Mixing Model Analysis allowed preliminary evaluation of the processes controlling the runoff in the San Francisco River basin. Results suggest that flow during dry conditions mainly consists of lateral flow through the C-horizon and cracks in the top weathered bedrock layer, and that all subcatchments have an important contribution of this deep water to runoff, no matter whether pristine or deforested. During normal to low precipitation intensities, when antecedent soil moisture conditions favor water infiltration, vertical flow paths to deeper soil horizons with subsequent lateral subsurface flow contribute most to streamflow. Under wet conditions in forested catchments streamflow is controlled by near surface lateral flow through the organic horizon. Exceptionally saturation excess flow occurs. By absence of the litter layer in pasture streamflow under wet conditions originates from the A horizon, and overland flow.

#### Published as

Crespo, P., A. Búcker, J. Feyen, K. Vaché, H-G. Frede, L. Breuer, 2011. Preliminary evaluation of the runoff processes in a remote montane cloud forest basin using Mixing Model Analysis and Mean Transit Time. *Hydrological Process.*, doi: 10.1002/hyp.8382

### 3.1 INTRODUCTION

According to Myers et al. (2000) the tropical Andes belongs to the 25 hotspots of biodiversity on earth; cloud forests being ranked as one of the most species rich ecosystems. The geochemistry, biology and ecology of these ecosystems are strongly controlled by the water that passes through (Boy et al., 2008; Neill et al., 2006). Disturbance of the hydrology of these ecosystems will therefore directly affect all water dependent processes. In this regard understanding of the hydrology is essential as to conserve in a more effective way these ecosystems. Despite scarce funding and the poor accessibility several research groups recently deployed considerable efforts in collecting data in pristine Andean basins. Most studies have been carried out on micro-basins of less than 10 km<sup>2</sup> with a monotonic landuse and cover (Buytaert, 2004; Buytaert et al., 2007; Boy et al., 2008; Goller et al., 2005; Fleischbein et al., 2006). However, to examine the effect of anthropogenic pressures requires studying the hydrology of larger basins where people converted forested areas into productive agricultural land and/or partly urbanized pristine areas for living. The highly spatial variability of climate, topography and other catchment properties on small scales, typical for the Andean region, prohibits extrapolation of findings obtained at the scale of micro-catchments with monotonic landuse to basins with different types of landuses. In addition, the hydrology of larger, medium or even small basins might be governed by other processes than the processes controlling the rainfall-runoff at small basin scale, justifying the need to analyze the hydrological processes at the scale of medium to large catchments (Céleri, 2007; Mortatti et al., 1997; Bücken et al., 2010).

Hydrological processes here are defined as the processes controlling the conversion of precipitation into streamflow. This definition encompasses questions such as: (i) Which hydrological components contribute to streamflow (overland, soil, subsoil, shallow and deep aquifers)?, (ii) How are the different storage reservoirs interconnected?, (iii) What is the residence time of the water in the different hydrologic components?, and (iv) To what extent reflect water in the different reservoirs the geochemical composition of the source area? For inference of the hydrological processes multiple techniques are used, such as hydrometric data (e.g., Kirkby, 1978; McDonnell, 1990; Bonell, 1993; Montanari

et al., 2006), isotopical tracers (e.g., Dincer et al., 1970; Niemi, 1977; Payne and Schroeter, 1979; Sklash and Farvolden, 1979; Maloszewski et al., 1983; Turner et al., 1987; Buttle, 1994; Mortatti et al., 1997), chemical tracers (e.g., Christophersen et al., 1990; Hooper et al., 1990; Robson and Neal, 1990; Hensel and Elsenbeer, 1997), modeling (e.g., Stephenson and Freeze, 1974; Beven and Kirkby, 1977; Dunne, 1983; Beven et al., 1995; Beven, 2001a; Buytaert and Beven, 2011) or a combination of previous methods (e.g., Pearce, 1990; Bonell and Fritsch, 1997; Kendall and McDonnell, 1998; Wels et al., 1991; Giusti and Neal, 1993). Buytaert et al. (2004), Buytaert et al. (2007) and Celleri (2007) analyzed the rainfall-runoff process of Andean highland ecosystems using solely hydrometric data. Research of Payne and Schroeter (1979), Schellekens et al. (2004), Goller et al. (2005), Blume et al. (2008), Chaves et al. (2008) and Bückner (2010) demonstrated that combining different techniques leads to a more accurate understanding of the rainfall-runoff process. The main advantage of monitoring the isotope and geochemical composition in different compartments of the hydrological cycle is that in a relative short period on the basis of a limited amount of data a fairly accurate reconstruction can be made of the water contributing areas and flow paths under variable rainfall conditions and landuses.

In line with previous the authors objective was deriving a preliminary impression of the streamflow generating processes in the San Francisco River basin (South Ecuador) using hydrometric, hydrochemistry and isotopic measurements. The underlying hypotheses were: (i) use of multi-approach techniques allows the tentative identification of the principal hydrological processes and permits identification of the main sources of water, (ii) the mean transit time (MTT, McGuire and McDonnell, 2006) of the streamwater in the San Francisco basin is short and not influenced by deep water contribution, (iii) the subsurface lateral flow through the organic horizon dominates the runoff generation during wet conditions, and (iv) monitoring of the isotope and geochemical composition of water samples in different parts of a basin yields in a relative quick and inexpensive way key features of the hydrology of ungauged or poorly gauged basins.

## 3.2 MATERIALS AND METHODS

### 3.2.1 STUDY AREA

The San Francisco River basin is located in on the Amazonian side of the Cordillera Real between 1800 and 3250 m above sea level (a.s.l.) in the southernmost Andes of Ecuador, latitude 03°58' S and longitude 79°04' W (Figure 3-1). The study basin is 75.3 km<sup>2</sup> and drains into the Amazon basin. The catchment is divided into a northern and a southern zone with distinct landuses. Natural forest in the north is replaced by extensive grazeland (*Setaria sphacelata*) (Werner et al., 2005), which when abandoned is replaced by ferns (*Pteridium aquilinum*, L). The southern basin area is covered with pristine montane cloud forest with trees up to 20 m high. The dominant plant species belong to the families Lauraceae, Euphorbiaceae, Melastomataceae and Rubiaceae (Homeier *et al.*, 2002). At the highest crest of the basin (3250 m a.s.l.) the vegetation mainly consists of a sub-páramo shrub land and an evergreen elfin forest, both of which are adapted to higher wind speed, lower temperatures and nutrient availability (Beck et al., 2008). Land cover distribution of the monitored subbasins is summarized in Table 3-1. Anthropogenic impacts in the north mainly consist of extensive wood cutting, river bed gravel mining, the existence and extension of gravel roads and grazeland, while a hydropower plant is located in the southern zone of the basin.

The climate is controlled by Amazonian air masses (Beck et al., 2008). The precipitation pattern is unimodal with moderate to low inter-annual variability. The main wet season is from April to September, and the dry season from October to December (Fleischbein et al., 2006). According to Rollenbeck (2006) precipitation is strongly positive correlated with altitude, and intensities based on 5 min data are low with 90% of all monitored precipitation rates less than 10 mm h<sup>-1</sup>. Precipitation is primarily caused by advective orographical clouds. In the period 1964-2008 annual precipitation varied between 900 and 4300 mm (Instituto Nacional de Meteorología e Hidrología, INAMHI) with an average of 2200 mm at an altitude of 1960 m; wind speeds being low and cloud cover less dense at this elevation. Annual average rainfall increases to 4700 mm (monitoring period 1994-2004) at the Cerro del Consuelo station located at the border of the catchment (3200 m a.s.l.) (Rollenbeck, 2006) and up to 6700

mm when taken horizontal rain and fog deposition into account (Bendix et al., 2008). Horizontal rain and cloud/fog water deposition contributes considerably to the total water input representing up to 41.2% of the basin water yield at 3180 m a.s.l.; below 2270 m a.s.l. water input consists only of vertical rain (Bendix et al., 2008). The mean annual temperature at 1952 m a.s.l. is 15.2 °C. The coldest months are June and July, with a mean temperature of 14.4 °C; the warmest month is November with a mean temperature of 16.1 °C. The average temperature gradient between the station at 1952 m and 2927 m a.s.l. is 0.66 °C per 100 m and the mean humidity is 86% (Fleischbein et al., 2006).

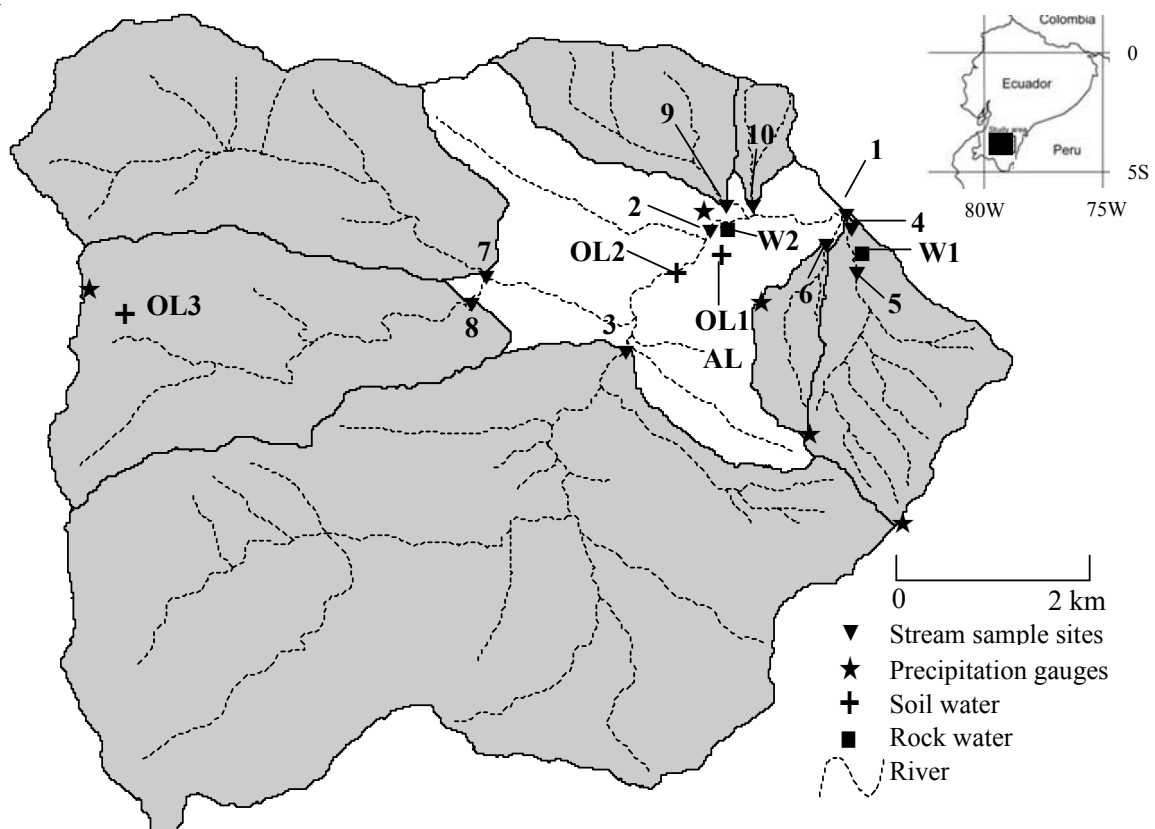


Figure 3–1: Location of the study area and nested subcatchments. 1 = PL, Planta (catchment outlet), 2 = SF, Rio San Francisco, 3 = FH, Rio San Francisco headwater, 4 = QR1, Quebrada Ramon 1, 5 = QR2, Quebrada Ramon 2, 6 = QM, Quebrada Milagro, 7 = QZ, Quebrada Zurita, 8 = QN, Quebrada Navidades, 9 = QP, Quebrada Pastos, 10 = QC, Quebrada Cruces, OL = soil water sampled in organic layer, AL = soil water sampled in A horizon layer, W = rock water.

The geology of the San Francisco catchment corresponds to the Chiguinda unit, which is composed of Paleozoic metamorphic rocks such as semipelite, phyllite and quartzite (Litherland et al., 1994; Hungerbühler, 1997). As stated by Mackeschin et al. (2008) the geology and soil mineralogy are fairly uniform in the basin. To the knowledge of the

authors no information on the rock permeability is available. The main chemical characteristics of the weathered and non-weathered rocks are listed in Table 3-2 (derived from the website of the DFG Research Unit FOR816, [www.tropicalmountainforest.org](http://www.tropicalmountainforest.org)). Generally, weathered rocks have lower concentration of all elements except Al of which the concentration is almost the same as in non-weathered rocks.

Table 3–1: Main characteristics of the San Francisco basin and subbasins. Acronyms for subcatchments are explained in Figure 3-1.

Catchment properties	Units	Subcatchment									
		PL	SF	FH	QR1	QR2	QM	QZ	QN	QP	QC
Topography											
Area	km <sup>2</sup>	75.3	64.2	34.8	4.6	4.6	1.3	11.3	10.0	3.4	0.8
Slope	%	55	55	55	61	61	48	55	53	59	49
Min elevation	m a.s.l	1742	1910	1900	1743	1872	1869	2025	2050	1914	1829
Max elevation	m a.s.l	3250	3250	3250	3150	3150	2650	3075	3025	2900	2550
Hydro-meteorology											
Mean precipitation	mm yr <sup>-1</sup>	3396	3200	3372	3799	3820	3423	2972	2962	2760	2700
Mean discharge	mm yr <sup>-1</sup>	2634	2378	2734	3090	3078	2764	2217	2307	2041	2050
Runoff coefficient		0.78	0.74	0.81	0.81	0.81	0.78	0.75	0.78	0.74	0.76
Geology											
Palaeozoic metamorphic rocks											
Land use											
Forest	%	68	65	67	80	80	90	72	65	63	22
Sub-páramo	%	21	21	29	18	19	9	15	17	10	10
Pasture/Bracken	%	9	12	3	1.8	0.8	0.8	12	16	26	67
Others	%	2	2	1	0.2	0.2	0.2	1	2	1	1
Soils											
Histosols	%	66	74	74	70	66	57	70	71	62	54
Regosols	%	16	15	15	18	18	25	18	16	21	24
Cambisols	%	11	7	7	8	10	13	8	8	11	14
Stagnasol	%	7	4	4	4	6	5	4	5	6	8

The main soil types in the basin are Histosols, Regosols, Cambisols and Stagnasols (FAO/ISRIC/ISSS, 1998). The soil distribution per subbasin is summarized in Table 3-1 (Ließ et al., 2009). Histosols typically contain a high fraction of non-decomposed plant fibers (Beck et al., 2008), are located in the sub-páramo under cloud forest and are the most common soil in the basin (Wilcke et al., 2002). The higher situated Histosols are on average 90 cm deep while Histosols under cloud forest are less deep (Makeschin et al., 2008; Wilcke et al., 2002). The area of Regosols and Cambisols decreases while the Stagnasol soil area increases with altitude (Ließ et al., 2009). Landslides are due to the

steepness of the terrain (slopes varying between 48 and 61%), the shallowness of the soils, the aboveground biomass and the plentiful precipitation year round. Open spaces in the landscape with time are covered by secondary forests.

Table 3-2 presents the main soil properties per landuse and horizon (data provided by the DFG Research Unit FOR816). The reader is referred to Makeschin et al. (2008) for a description of the laboratory analyses used. As depicted in Table 3-2 C, Ca, Mn and the saturated hydraulic conductivity (Ks) decrease with depth (from the O to the C horizon), but slightly increase under pasture and shrubland. It is noticed that the saturated hydraulic conductivity under pasture and shrub is considerably smaller than under zero anthropogenic interference (Huwe et al., 2008). As stated by Wilcke et al. (2008) Al, Fe and K increase with depth while Mg, Na and pH are very uniform throughout the soil profile. The O horizon significantly reduces under shrubs or ferns and disappears under pasture (Makeschin et al., 2008). Sub-páramo and forest soils are very similar. According to these authors, frequent burning of pasture results in a slight increase of the pH and a more significant increase in Al, Na, Fe, Mg and K.

### 3.2.2 FIELD SAMPLING AND LABORATORY ANALYSIS

A nested sampling approach was used for the collection of streamwater (Table 3-1 and Figure 3-1), with eight sampling points (subbasins) in the main tributaries, one in the main river (SF) and the outlet (PL) of the San Francisco River basin. The selection of the sites was restricted by landuse, land cover and accessibility. Four of the ten subbasins are representative for cloud forest (FH, QR1, QR2 and QM), two subbasins are covered mainly with pasture (QP and QC) and two subbasins show clear anthropogenic interference (QN and QZ). The gully Ramon (QR) is monitored at two locations, QR1 and QR2 respectively. QR2 is located just before the intake channel of the hydropower plant and QR1 downstream of the intake (Figure 3-1).

Precipitation was sampled for the characterization of the chemical composition in the lower part of the catchment at 1940 m a.s.l., using polyethylene bottles installed at 1.2 m above the surface. At higher altitudes (2825 m a.s.l.) the chemical signature of precipitation was reconstructed using historical information collected between 2003 and 2005 by Beiderwieden et al. (2005) and Rollenbeck et al. (2005).

Table 3-2: Soil physical and chemical properties (average value and range) per horizon of the main soils in the studied catchment.

Horizon	Horizon thickness (cm)	Ks (mm h <sup>-1</sup> )	pH	C	Al	Ca	Fe	Mg	Mn	K	Na
(g kg <sup>-1</sup> )											
Forest											
O	10-20	166	4.7 (3.4-6.7)	466	5.6 (0.2-37.5)	5.3 (0.2-29.8)	3.6 (0.02-46.9)	1.8 (0.2-10.2)	0.40 (0.01-2.3)	2.5 (0.7-14.4)	0.37 (0.01-6.0)
A	10-20	92	3.6 (3.3-4.1)	48.1	23.2 (12.7-44.1)	0.03 (0.02-0.18)	18.9 (11.7-34.6)	1.04 (0.5-1.9)	0.29 (0.21-0.4)	8.5 (3.9-15.7)	0.30 (0.16-0.55)
B	10-80	11	3.9 (3.6-4.5)	34.2	30.1 (10.7-55.8)	0.05 (0.02-0.12)	22.9 (11.5-38.2)	1.23 (0.5-2.3)	0.30 (0.4-0.18)	10.2 (4.8-16.9)	0.33 (0.16-0.58)
C	30-50	17.9	4.1 (3.7-4.8)	10.5	33.2 (13.7-79.1)	0.06 (0.02-0.11)	24.8 (13.8-41.3)	1.36 (0.5-2.3)	0.29 (0.16-0.4)	11.4 (3.9-17.6)	0.36 (0.19-0.57)
Sub-páramo											
O	10-20	135	4.7 (3.7-5.9)	446	5.5 (0.3-24.1)	4.2 (0.2-11.2)	2.6 (0.14-12.1)	1.3 (0.2-3.1)	0.68 (0.06-2.2)	2.3 (1.02-8.1)	0.17 (0.03-0.4)
A	10-40	91	4.2 (3.9-4.5)	89.3	20.6 (3.3-45.2)	0.17 (0.05-0.9)	13.6 (6.6-24.9)	1.1 (0.2-2.1)	0.15 (0.1-0.3)	6.48 (0.6-14.0)	0.23 (0.1-0.4)
B	30-60	11	4.4 (4.2-4.7)	44.3	26.1 (3.1-53.0)	0.08 (0.02-0.33)	17.3 (6.9-29.8)	1.4 (0.1-2.8)	0.15 (0.09-0.3)	8.1 (0.6-16.7)	0.24 (0.08-0.5)
C	20-50	-	4.7 (4.5-5.1)	16.2	33.5 (1.7-55.3)	0.04 (0.02-0.10)	24.3 (6.9-41.2)	1.7 (0.2-3.3)	0.15 (0.09-0.3)	11.2 (0.3-18.6)	0.28 (0.08-0.4)
Pasture/Shrubs											
A	10-50	14	5.0 (4.1-7.5)	50.3	45.6 (13.1-102.9)	4.3 (0.04-63.6)	31.2 (2.4-119.1)	3.1 (0.4-19.6)	0.41 (0.02-2.2)	9.8 (2.3-21.3)	0.63 (0.17-2.3)
B	30-60	17	4.9 (3.9-5.9)	37.6	38.4 (14.2-70.4)	0.21 (0.03-1.35)	26.2 (7.7-46.5)	1.5 (0.3-4.2)	0.24 (0.39-0.17)	11.3 (4.5-22.9)	0.67 (0.19-2.6)
C	20-50	30	5.0 (4.2-6.1)	14.6	41.7 (20.0-81.4)	0.15 (0.04-1.3)	27.9 (10.1-48.1)	1.7 (0.6-3.8)	0.24 (0.16-0.4)	12.0 (3.3-22.5)	0.70 (0.17-2.6)
Rocks											
Weathered	-	-	-	-	52.5 (9.2-112.3)	0.15 (0.02-1.19)	19.1 (7.4-34.4)	2.9 (0.2-6.2)	0.19 (0.07-0.5)	17.7 (2.9-36.1)	0.75 (0.19-2.9)
Non-weathered	-	-	-	-	53.9 (15.2-85.6)	0.80 (0.08-1.54)	27.6 (8.3-47.3)	5.6 (0.7-13.2)	0.29 (0.05-0.9)	22.3 (5.5-43.6)	9.5 (1.2-17.2)

At three locations in the catchment, two in forest (OL1 and OL3) and one in sub-páramo (OL2), soil water samples in the O horizon were collected using zero-tension lysimeter devices consisting of 0.2 x 0.2 m plastic boxes covered with a polyethylene net. Soil water data of the A horizon (AL1) were derived from Boy et al. (2008), who used mullite suction cups with an average pore size diameter of 0.1  $\mu\text{m}$ . Both, O and A horizon water samples are an average of several samples collected in Histosols and Regosols. Soil water of the organic horizon in sub-páramo sites was sampled from the free draining water. Due to admittance refusal by landowners' soil water samples in pastures/ferns sites, the subcatchments FH and QZ, could not be collected. The authors however assume that the monitored sites are representative for the basin given the relative uniform soil distribution.

Rock water samples were collected in two places of the catchment directly from springs emerging from rock fractures. Although the effort to find more springs it was not possible due to the inaccessibility of the terrain. One sampling site is located just below the QR2 site, while the second site is close to SF (Figure 3-1). These two points are considered representative for the area given the fairly uniformity of the geology. Piezometers for sampling the water in the underground could not be installed because of the compactness of the underlying rock formation.

Weekly to biweekly water grab samples were collected at all sites in the period April 2007 - November 2008. In line with the availability of historic water quality data, water grab samples of precipitation, streams, soil and rock were analyzed on the following chemical elements: Al, Ca, Fe, Mg, Mn, K and Na. All water samples were filtered in the field using 0.45  $\mu\text{m}$  polypropylene membrane filters (Puradisc 25 PP Syringe Filters, Whatman Inc.) and stored in acid washed PE bottles. Samples were acidified to a  $\text{pH} < 2$  within three hours after collection using nitric acid, were frozen and transported to Germany. Element concentrations were determined at the Institute for Landscape Ecology and Resource Management of the Justus-Liebig Universität Gießen with an inductive coupled plasma-mass spectrometer (ICP-MS, Agilent 7500ce, Agilent Technologies). The quality of ICP-MS measurements was frequently checked using certified samples (NIST 1643e and NRC-SLR4) and additional internal calibration

procedures. The pH and electrical conductivity (EC) were measured in the field using a WTW pH Cond340i handheld meter (Weilheim, Germany).

The  $^{18}\text{O}/^{16}\text{O}$  ratio was determined on streamwater samples, collected in tightly closed amber glass bottles (Th. Geyer GmbH & Co. KG, Germany) and analyzed in Gießen using a direct-inject liquid-water isotope analyzer (DLT100, Los Gatos Research, Mountain View, CA, US), with an analytical precision of  $\pm 0.2\%$ . Ratios of  $^{18}\text{O}/^{16}\text{O}$  are expressed in delta units,  $\delta^{18}\text{O}$  (‰, parts per mille).  $\delta^{18}\text{O}$  was not measured in precipitation throughfall samples because Goller et al. (2005) reported extreme small differences between the  $\delta^{18}\text{O}$  concentration in rainfall and throughfall. Since  $\delta^{18}\text{O}$  was not measured in precipitation, precipitation  $\delta^{18}\text{O}$  data was reconstructed in two ways. First,  $\delta^{18}\text{O}$  data collected in the Estación Científica San Francisco (**ECSF**), situated in the study basin, in the period August 2000 - August 2001 were derived from Wagner (2002) and Goller et al. (2005). Secondly, the online isotopes in precipitation calculator (OIPC) ([www.waterisotopes.org](http://www.waterisotopes.org)) was used to estimate the  $\delta^{18}\text{O}$  precipitation amplitude at different altitudes, as a basis for the analysis of the altitude influence (McGuire et al., 2005). The OIPC results were validated to in the ECSF station  $\delta^{18}\text{O}$  precipitation measurements. In Ecuador 20 climate stations are controlled by the International Atomic Energy Agency/World Meteorological Organization Global Network for isotopes with altitudes ranging from 6 to 3150 m a.s.l.  $\delta^{18}\text{O}$  is calculated using the Bowen and Wilkinson (2002) algorithm, refined by Bowen and Revenaugh (2003).

### 3.2.3 HYDROMETRIC MEASUREMENTS

The water level at the outlet of the basin and each subbasin was recorded with an accuracy of  $\pm 1$  mm with a 5 min interval using pressure transducers and capacitance probe gauges (Odyssey Capacitance Probes and Odyssey Pressure Data Recorder, Dataflow Systems PTY Ltd, NZ). All river cross sections with exception of the QC outlet section were stable. In this section a Thompson (V-notch) weir ( $90^\circ$ ) was installed. Discharge versus stage measurements were made frequently with a Flo-Mate 2000 device (Marsh-McBirney Inc., MD, US) and a Flow Probe 101 (Global Water Instrumentation Inc., CA, US). Power or polynomial stage-discharge relationships were developed. For the QC station the Kindsvater-Shen relation (US Bureau of Reclamation, 2001) was used to convert water level data to flow rate data. Precipitation data (rainfall

and fog) were provided by Bendix and Richter (personal communication) of the DFG Research Unit FOR816. A detailed description of the set up of the meteorological stations is given by Bendix et al. (2008). Four meteorological stations were used to derive volume weighted element values.

Due to harsh environmental conditions equipment failure occurred several times but never lasted longer than a few days. Hence, data gap filling for precipitation and discharge was applied. Hourly rainfall gap-filling was conducted applying regression analyses with other station data and bulked weekly rainfall measurements. Discharge gaps were filled using the relationship between rainfall and discharge data from neighboring catchments. Discharge data of October and November 2008 were not used because an extreme flood event changed the geometry of the measuring cross section. Hourly fog deposition data series were estimated based on fixed monthly ratios between rainfall and fog deposition.

#### 3.2.4 MIXING MODEL ANALYSIS

A Mixing Model Analysis technique based on the procedure outlined by Hooper et al. (1990) was used for the evaluation of the contribution of rainfall, soil water and rock water to streamflow, considered in this study as the three principal sources. End-members were selected using two dimensional (2-D) plots, called mixing diagrams, plotting one solute against another solute for all possible combinations of selected elements. If the different water sources mix conservatively most of the streamwater samples lie inside the triangle formed by the three selected end-members (Christophersen et al., 1990). Given the vastness of data only the element combinations that gave better results are presented. Whereas in many studies the tracer technique is used to quantify the contribution of the different water sources or to separate subflow events (Elsenbeer et al., 1995; Chaves et al., 2008; Soulsby et al., 2003; Mortatti et al., 1997; Robson and Neal, 1990; among others), in this study due to the inaccessibility of the basin the technique is used to identify the source areas contributing to streamflow. The authors recognize the uncertainty associated to the approach, but anticipate that using multiple techniques reduce the uncertainty on the findings. Furthermore, the results in this study will be used for the design and setting-up of a more detailed and effective monitoring scheme leading to more conclusive results.

### 3.2.5 MEAN TRANSIT TIME ESTIMATION

A exponential piston-flow model (EPM) using a simple sine-wave approach (Maloszewski et al., 1983; DeWalle et al., 1997), was used to estimate the Mean Transit Time (MTT) at basin scale (Soulsby et al., 2006; McGuire and McDonnell, 2006). The model assumes that the decrease in the  $\delta^{18}\text{O}$  amplitude of streamwater relative to precipitation provides a basis for determining the transit time (Unnikrishna et al., 1995). The model evaluation process described by McGuire and McDonnell (2006) was used for the parameter identification. The model optimization was performed using Monte Carlo simulations. The precipitation amplitude was estimated using the sine-wave function given in Eq. (3-1):

$$\delta^{18}\text{O} = X + Az1[\cos(ct - \theta)] \quad (3-1)$$

where  $\delta^{18}\text{O}$  is the predicted  $\delta^{18}\text{O}$ , X the mean annual  $\delta^{18}\text{O}$ , Az1 the annual amplitude of  $\delta^{18}\text{O}$  for precipitation, c the angular frequency constant ( $2\pi/365$ ), t the time in days after an arbitrary date and  $\theta$  the phase lag or time of the annual peak  $\delta^{18}\text{O}$  in radians. Amplitudes for precipitation at different altitudes were estimated, however minor to no difference was found between values.

The amplitude (Az2) and phase lag ( $\theta$ ) for streamflow were estimated using the Eqs. (3-2) and (3-3) respectively:

$$Az2 = Az1 \left( 1 + \frac{c^2 MTT^2}{\eta^2} \right)^{-1/2} \quad (3-2)$$

$$\theta = cMTT \left( 1 - \frac{1}{\eta} \right) - \arccos \left[ \left( 1 + \frac{c^2 MTT^2}{\eta^2} \right)^{-1/2} \right] \quad (3-3)$$

where c is the angular frequency constant ( $2\pi/365$ ) and  $\eta$  is a parameter describing the piston flow portion of the model.  $\eta$  is equal to the total volume of water in the system divided by the volume with an exponential distribution of transit times. For  $\eta = 1$ , the model is equivalent to a exponential model, while for  $\eta \rightarrow \infty$  the model approaches pure piston flow.

The MTT of water leaving the subcatchment or catchment is calculated by Eq. (3-4):

$$MTT = c^{-1} \eta \left[ \left( \frac{Az2}{Az1} \right)^{-2} - 1 \right]^{1/2} \quad (3-4)$$

Since water samples were collected on a weekly to biweekly interval, high flow samples are poorly represented with the consequence that the estimation of MTT corresponds to basically low (base and intermittent) runoff conditions. Evident samples collected during storm conditions were excluded, analogue to the approach followed by Soulsby et al. (2006). Due to the simplicity of the used model and the data limitation the results presented herein could contain high uncertainty and should therefore be considered as a first approximation of the MTT (Maloszewski and Zuber, 1993; McGuire and McDonell, 2006). However given the objectives of the study the MTT value could be considered as a reference for identifying deep water contribution.

### 3.3 RESULTS AND DISCUSSION

#### 3.3.1 RAINFALL-RUNOFF

Annual precipitation in the subbasins in the observation period April 2007 - November 2008 varied between 2700 and 3820 mm yr<sup>-1</sup>. As mentioned, the precipitation pattern has low inter-annual variability. Figure 3-2 depicts the seasonality in precipitation and streamflow of the PL station located at the outlet of the San Francisco basin. A similar behavior is found in all subbasins. A fast response of discharge to rainfall is noticed. As depicted in Table 3-1, the average water yield of the subbasins varies between 2041 and 3090 mm yr<sup>-1</sup>, representing 76 to 81% of precipitation. Small differences are found mainly due to the spatial variability of rainfall depth and fog interception. Chaves et al. (2008) analyzing rainfall-runoff of a small rainforest catchment in Rancho Grande, Brazil, found similar values.

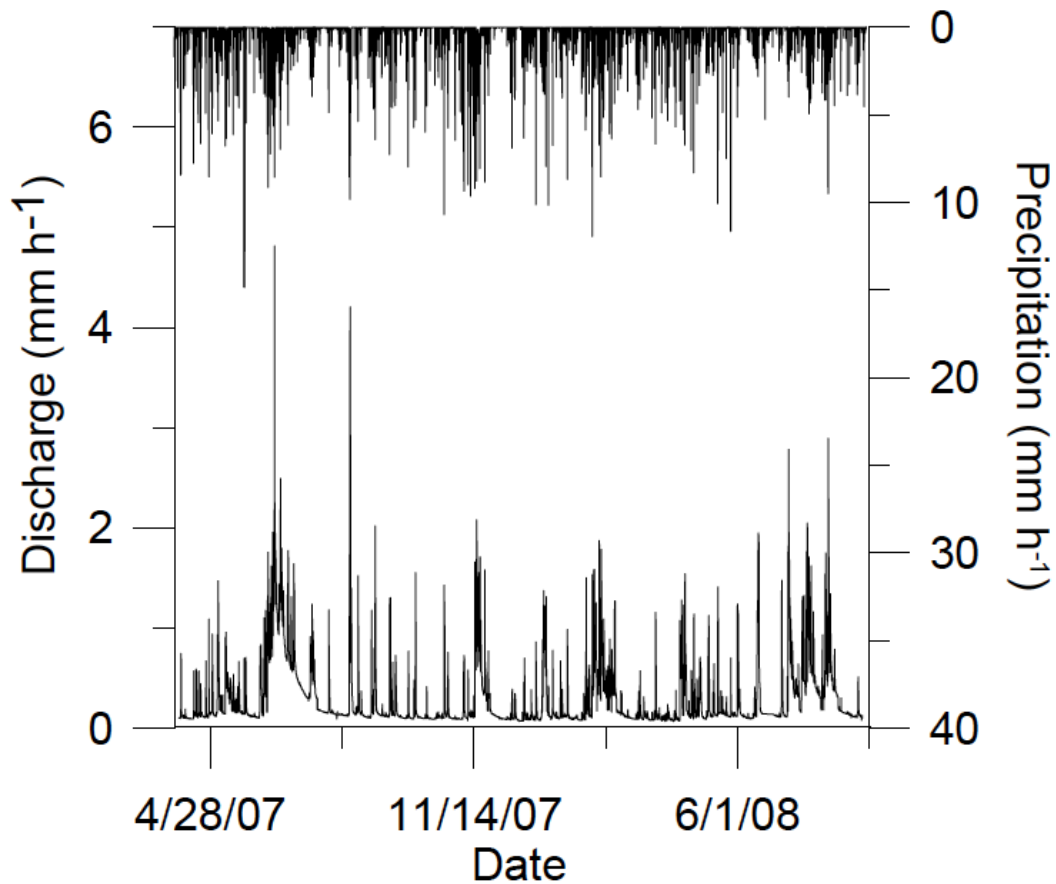


Figure 3–2: Hourly timeseries of rainfall and total streamflow in mm of the San Francisco basin.

Analysis of the rainfall timeseries reveals that the rainfall intensity of most events is less than the saturated hydraulic conductivity of the top layer, with averages values ranging between 91 and 166  $\text{mm h}^{-1}$  for forest and sub-páramo soils and 14 to 17  $\text{mm h}^{-1}$  for pasture soils (Table 3-2). In general, 90% of the rainfall intensities are less than 10  $\text{mm h}^{-1}$  (Rollenbeck, 2006). Given the overall low rainfall intensities Horton overland flow is unlikely to occur under forest and sub-páramo vegetation. However on grazeland infiltration excess overland flow is likely to occur during storm events given the low value of the saturated hydraulic conductivity of the top horizon. Future research in the study area is needed as to identify its importance and to verify if reinfiltration of excess overland flow occurs. Fleischbein et al. (2006), in a study conducted in a micro-catchment of the San Francisco basin cover with forest close to the gauging stations QM and FH (Figure 3-1), excluded the occurrence of overland flow (see also Boy et al., 2008; Búcker, 2010). Bogner et al. (2008) in a study conducted on slopes inside the QC subbasin, close to the QM gauging station, observed using dye tracers preferential flow close to the surface of pasture plots as a consequence of compaction of the top layer,

whereas under primary forest lateral flux was deeper and more evenly distributed in the soil profile. Based on the component analysis of streamflow during storms, the authors expect that saturation excess overland flow near to the river bed takes places and that on grazeland due to a reduction of the saturated hydraulic conductivity of the top horizon temporarily and locally saturation excess overland flow occurs.

### 3.3.2 HYDROCHEMISTRY

As depicted in Table 3-3 precipitation has low solute concentration compared to the other water sources. The pH is acid and EC is low. Both are relatively constant in all water sources ranging between 4.37 to 7.51, and 2 to 35  $\mu\text{S cm}^{-1}$ , respectively. Al concentration is highest in soil water of the A horizon with an average concentration of 526  $\mu\text{g l}^{-1}$  followed by the O horizon with 311  $\mu\text{g l}^{-1}$ . Instead of increasing with depth, the Al concentration is considerably lower in the rock water sources with averages of 10 and 19.4  $\mu\text{g l}^{-1}$  for W1 and W2, respectively. From this it can be concluded that Al is less mobile in mineral layers, and as stated by Makeschin et al. (2008), most likely to be retained by secondary minerals. Highest concentration of Ca and Mg were found in the soil water samples collected in the A horizon (average values of 1167 and 467  $\mu\text{g l}^{-1}$ ) and rock water (average values of 1175-1190  $\mu\text{g l}^{-1}$  and 527-654  $\mu\text{g l}^{-1}$ ) but lower in the organic horizon with average concentrations of 135 to 685  $\mu\text{g l}^{-1}$  and 176 to 302  $\mu\text{g l}^{-1}$  for Ca and Mg, respectively. Na concentration is almost three times higher in rock water than in soil water sources. Water from O horizon has higher concentration of Mn than mineral layers, with average concentrations ranging between 14.0 and 52.2  $\mu\text{g l}^{-1}$ . K concentration is almost constant in all water types except for W1 where the concentration is nearly two orders of magnitude higher. The concentration of the major solutes in the soil and rock water samples, except Al and Ca, is very similar to the concentration trend of the elements in the solid phase. Same results were found by Boy et al. (2008) in a study conducted in three micro-catchments (8 to 13 ha) close to the San Fransisco head gauging station FH (Figure 3-1).

Table 3-3: Chemical characteristics (average and range) of rainfall (volume weighted), rock and streamwater.

Sample location	n	pH	EC ( $\mu\text{S cm}^{-1}$ )	Al	Ca	Fe	Mg ( $\mu\text{g l}^{-1}$ )	Mn	K	Na
Rainfall	35	5.7 (4.6-6.4)	8 (2-35)	6.4 (0.6-22.0)	143 (44.14-335)	5.5 (1.7-22.1)	21 (4-206)	1.9 (0.6-5.5)	123 (40-303)	113 (33-556)
Soil water										
OL 1	14	5.1 (4.7-5.5)	16 (10-27)	311 (172-423)	685 (40-1939)	34.7 (11.5-72.7)	302 (41-469)	52.2 (0.5-160)	299 (38-843)	120 (41-579)
OL 2	10	5.5 (5.2-5.8)	8 (7-9)	185 (165-209)	140 (30-168)	197 (183-216)	293 (255-352)	14.0 (3.5-25.5)	198 (64-219)	627 (591-740)
OL 3	10	4.6 (4.4-4.9)	19 (18-23)	321 (297-359)	135 (103-229)	560 (450-660)	176 (144-189)	17.9 (10.5-28.2)	153 (66-376)	202 (67-452)
AL	-	-	-	526 (250-1000)	1166 (200-2000)	-	467 (400-1500)	9.0 (4-15)	201 (75-700)	465 (270-500)
Rock water										
W1	24	5.94 (5.7-6.8)	20 (19-22)	10 (1.2-49.1)	1176 (913-4147)	10.2 (0.6-68.3)	527 (465-738)	2.9 (0.4-4.1)	502 (383-2020)	1640 (1367-3034)
W2	14	6.44 (6.2-7.5)	24 (21-27)	19.4 (7.6-49.1)	1190 (921-2149)	29 (7.7-58.5)	654 (575-760)	3.9 (0.5-15.1)	277 (177-474)	2495 (2254-3093)
Streamwater										
PL	56	7.1 (5.5-7.5)	16 (7-36)	80.4 (7.6-358)	1297 (815-3228)	104 (26.7-574)	414 (279-1241)	18.2 (2.7-336)	375 (210-2446)	1383 (629-2339)
SF	54	7.2 (6.5-7.7)	21 (3-34)	94.8 (5.5-707)	1608.59 (883-2809)	133 (34.5-832)	511 (240-813)	16.4 (2.1-192)	398 (253-1209)	1646 (508-2776)
FH	47	7.1 (6.4-7.5)	13 (7-22)	93.3 (17.3-762)	886 (624-1664)	137 (18.8-1223)	314 (236-551)	31.8 (1-649)	308 (178-807)	1139 (407-1580)
QR1	41	6.90 (5.7-7.7)	12 (4-37)	55.3 (2.1-268)	639 (252-1052)	44.8 (6.1-182)	339 (134-526)	1.2 (0.1-5.7)	368 (175-628)	1134 (183-1785)
QR2	52	6.7 (6.2-6.8)	6 (5-8)	56.2 (25-162)	231 (195-334)	46.6 (23.1-114)	143 (125-185)	0.6 (0.4-1.1)	225 (187-250)	616 (449-616)
QM	51	6.5 (4.9-7.7)	6 (4-15)	95.7 (12.3-327)	242.74 (129-910)	124 (53.5-424)	176 (109-441)	4 (1.5-17.2)	317 (143-2012)	673 (156-1909)
QZ	45	7.21 (6.1-7.6)	23 (13-31)	77.9 (6-413)	2059 (1350-8559)	69.6 (11.8-611)	532 (394-745)	3 (0.7-17.7)	401 (225-1206)	1579 (812-2616)
QN	43	7.1 (6.4-7.6)	24 (13-36)	79.8 (9.9-294)	2064 (1147-3316)	278.2 (36-6898)	487 (270-2528)	20.2 (7.4-150)	386 (256-1548)	1471 (567-1813)
QP	52	7.3 (6.2-8.2)	28 (17-39)	67.9 (10-349)	1907 (1393-6360)	88.4 (28.7-306)	794 (530-941)	5.7 (2.6-17)	469 (301-840)	2441 (1109-3104)
QC	40	7.5 (6.1-8.4)	29 (18-36)	71.7 (10-361)	1843 (1080-2814)	120 (29.8-435)	784 (464-948)	8.3 (2.5-22.3)	605 (416-934)	2617 (1245-3295)

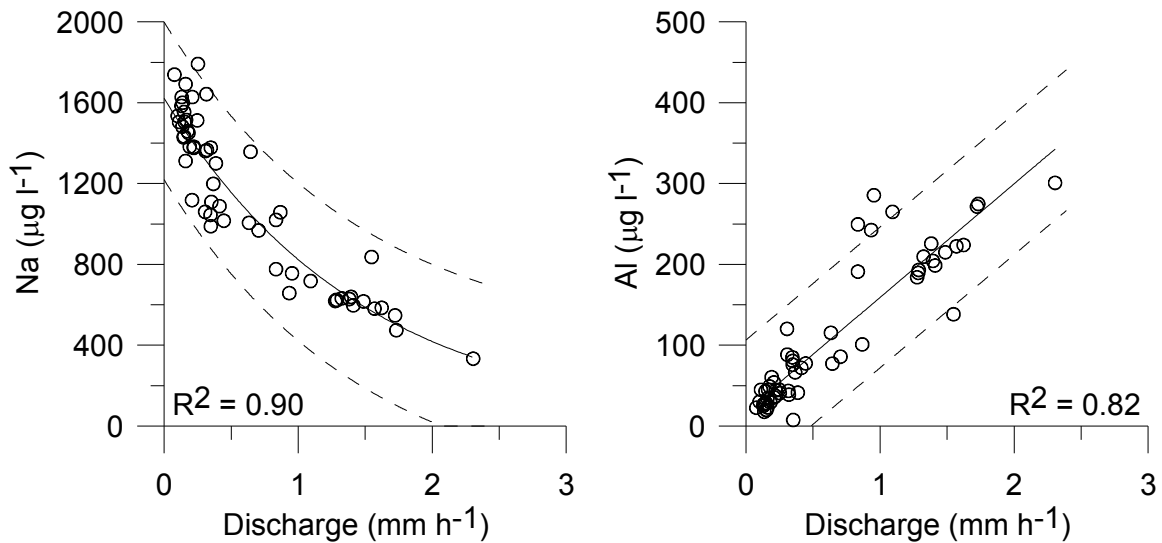


Figure 3–3: Correlation between discharge and streamwater Na and Al concentration at the outlet (PL) of the San Francisco basin

Concentration versus discharge was evaluated for all streamwater sampling stations where streamflow data were available. Only the results for the PL station for respectively Al and Na are shown in Figure 3-3. Details for the other subcatchments and solutes concentrations are listed in Bückner (2010). Results reveal that Al and Na are always significantly related to discharge, while this relation is variable and less visible for Ca, Mg, Mn and K. Na concentrations decrease with an increase in discharge, while Al increases (Figure 3-3). Ca and Mg behave similar to Na, decreasing with discharge. However no relation with water flow was found for the subcatchments QZ, QN, QM and QR. Concentrations of Mg in QM and QR are invariably related to discharge. For K no relation to water flow was observed, with exception in the subbasins QC and QP where K concentration increases with discharge. Observations are generally in line with what several studies report, namely a decline in Ca, Mg and Na concentration when flow rate increases (Anderson et al., 1997; Elsenbeer et al., 1994; Grimaldi et al., 2004; Tsujimura et al., 2001). Also McDowell and Asbury (1994) and Newbold et al. (1995) derived negative relations for Ca, Na and Mg with discharge and no relation for K as observed in the present study. On the other hand Lorieri and Elsenbeer (1997) report that Al and Mn concentrations increase with discharge. In general, drops in concentrations during storm flows are attributed to a dilution of streamwater, whereas an increase of concentration during storm flow is ascribed to a flushing of accumulated material (Elsenbeer et al., 1994). The analysis revealed that Al and Na are the only

solutes with the same hydrochemical behavior in all monitored catchments, and therefore suitable tracers for defining the hydrograph component composition using mixing model analysis.

### 3.3.3 ISOTOPIC TRACERS AND MEAN TRANSIT TIME

The mean, maximum and minimum values of  $\delta^{18}\text{O}$  concentration in precipitation and streamwater are listed in the Table 3-4 and presented in Figure 3-4. Given the similarity in streamflow isotopic composition between stations, Figure 3-4 shows only the  $\delta^{18}\text{O}$  values of 6 out of 10 streamwater sampling sites together with the fitted sine curve. The seasonal  $\delta^{18}\text{O}$  pattern for the two sources of precipitation data used in this study is depicted at the top of Figure 3-4, with both data sets being representative for the same location. Each of them shows a seasonal pattern typical for the Andean mountain range, more diluted in the wet season and a higher  $\delta^{18}\text{O}$  concentration in the dry season, with values ranging between -12.6 to -1.2‰, -12.8 to -5.6, -13.9 to -6.1 and -14.3 to -6.3 for stations located at 1957, 2270, 2669 and 2825 m a.s.l. Goller et al. (2005), based on the correlation between the  $\delta^{18}\text{O}$  concentration of rainfall and the synoptic wind directions, stated that variations in  $\delta^{18}\text{O}$  values are due to the influence of air masses originating from different source regions. The values of the  $\delta^{18}\text{O}$  concentration generated with OIPC are slightly lower and the peak is situated 50 days earlier than the peak using the Wagner (2002) and Goller et al. (2005) data for a station located at 1957 m a.s.l.. The difference in the position of the regressions is likely the consequence of the high variation in intra-annual precipitation and because data cover different periods.

The seasonal pattern of  $\delta^{18}\text{O}$  concentration in streamwater of the San Francisco basin and subbasins is similar to the  $\delta^{18}\text{O}$  pattern of precipitation water. Throughout the observation period, i.e. from April 2007 to November 2008, only small variations in  $\delta^{18}\text{O}$  concentration of streamwater were measured ranging between -10.05 and -6.21‰. Difference in  $\delta^{18}\text{O}$  pattern between the subbasins is small, as shown in Figure 3-4. The streamwater isotopic composition measured at 1980 m a.s.l. is more diluted than the isotopic composition of precipitation water, suggesting a contribution of water with lower isotopic composition from higher altitudes in the basin. Goller et al. (2005) report similar  $\delta^{18}\text{O}$  values for streamwater ranging between -8.7 and -5.8‰. Streamwater isotope values for all catchments are more damped and less responsive to precipitation

likely because (i) the low temporal sampling resolution that prevented registration of all extreme values, and/or (ii) the piston flow type of response, i.e. precipitation pushes the old water out of the system that then is recorded as streamwater.

Table 3–4: Mean, maximum and minimum  $\delta^{18}\text{O}$  values, modeled amplitude and mean residence times of the San Francisco basin and subbasins.

Sampling location	$\delta^{18}\text{O}$ measured			Amplitude (‰)	$\eta$	$R^2$	Mean Transit Time (days)	
	n	Mean (‰)	Min (‰)					Max (‰)
Precipitation								
OIPC								
1957 m a.s.l.	12	-6.08	-12.60	-1.20	3.00		0.85	
2270 m a.s.l.	12	-8.80	-12.80	-5.60	3.00		0.82	
2669 m a.s.l.	12	-9.54	-13.90	-6.10	3.10		0.87	
2825 m a.s.l.	12	-9.80	-14.30	-6.30	3.10		0.80	
Wagner (2002) and Goller et al. (2005)	24	-6.08	-1.20	-12.6	3.20		0.45	
Streams								
PL	35	-7.97	-9.82	-6.71	1.01	2.02	0.41	330
SF	35	-8.02	-9.55	-6.29	0.98	1.71	0.56	285
FH	30	-7.91	-9.49	-6.23	0.79	1.47	0.35	313
QR1	30	-7.59	-8.82	-6.67	0.64	1.34	0.38	354
QR2	27	-7.83	-9.10	-6.97	0.66	1.78	0.47	263
QM	27	-7.42	-8.22	-6.23	0.93	1.52	0.36	269
QZ	27	-8.20	-9.79	-6.83	1.00	2.06	0.53	336
QN	27	-8.10	-9.44	-6.87	1.05	1.87	0.35	288
QP	30	-7.92	-9.73	-6.21	0.93	1.52	0.32	267
QC	26	-7.80	-10.05	-6.43	0.73	1.20	0.40	276

A first approximation of the mean transit time is derived using a model optimization performed using Monte Carlo simulations. The amplitude for precipitation water varies between 3 and 3.2‰ with values for  $R^2$  of 0.80 and 0.85 for the data derived with the OIPC calculator for stations with altitudes in the range 1957 and 2825 m a.s.l, while the amplitude using Wagner (2002) and Goller et al. (2005) data is 3.2‰ at 1957 m a.s.l. The results show that OIPC data yield similar results as the data collected by Wagner (2002) and Goller et al. (2005). Based on the similarity between both data sets the authors used the OIPC data for the calculation of the MTT for the different subbasins. Due to the similar estimated precipitation amplitudes at different altitudes, a value of 3.0‰ was selected for all the subbasins to estimate MTT. The amplitude and  $\eta$  values and the correlation coefficient for streamwater are listed in the Table 3-4, with

amplitudes ranging between 0.64 and 1.05 ‰,  $\eta$  values from 1.20 to 2.06 and  $R^2$  values between 0.32 and 0.56.

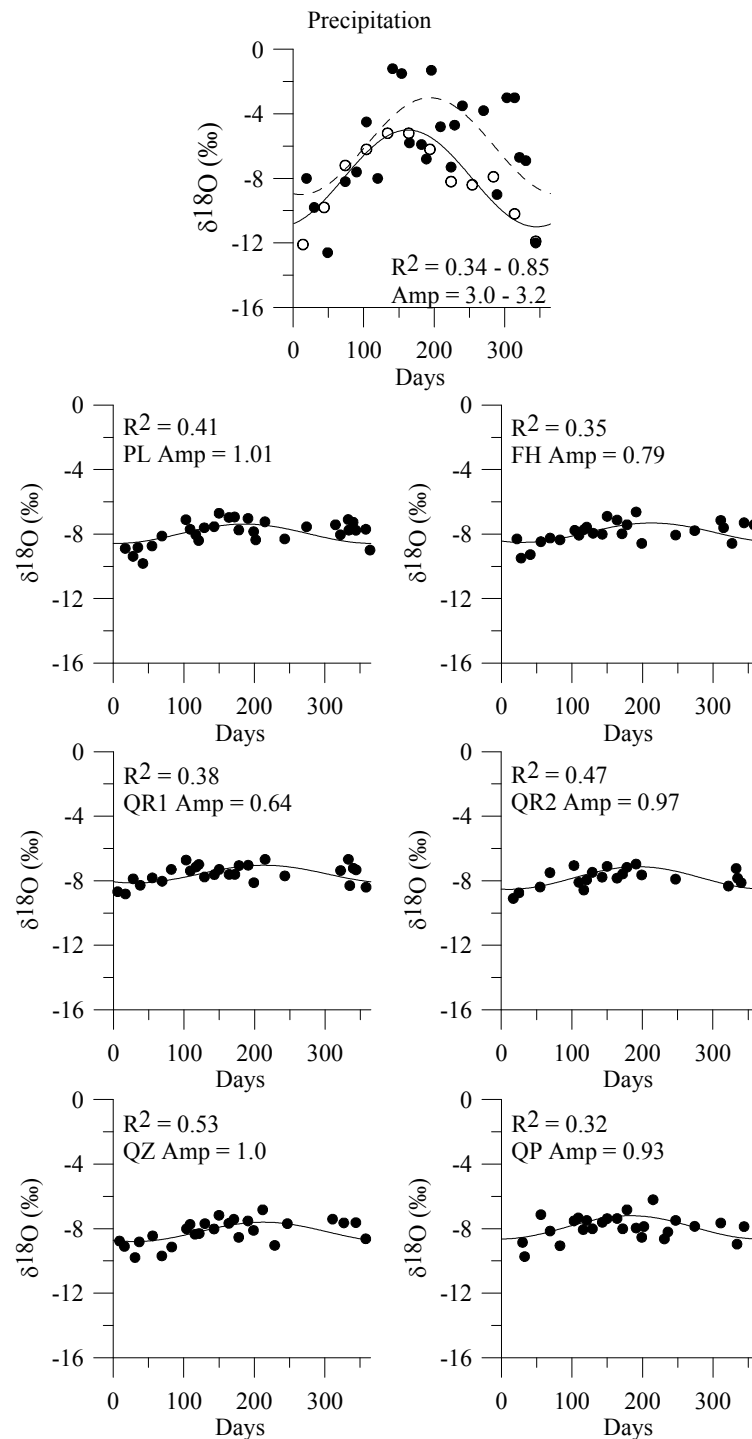


Figure 3-4: Sine-wave regression models for  $\delta^{18}\text{O}$  in precipitation (filled points with dashed regression line derived from Wagner (2002) and Goller et al. (2005) data, solid points with solid regression line derived from OICP data) and streamwater for the San Francisco basin (PL) and subbasins (FH, QR1, QR2, QZ, QP). Acronyms for subbasins are provided in Figure 3-1.

Figure 3-5 shows the results of the Monte Carlo simulations for the estimation of the MTT for 6 of the 10 subbasins. Results show for each subbasin a rapid decrease of the mean absolute error (MAE) for values below the optimum estimation (solid diamond in Figure 3-5), while for values above the uncertainty in the estimation of MTT increases, mainly due to the short length of the available data series (McGuire and McDonnell, 2006). As an initial estimate, given the complexity of the study basin, the authors believe that the obtained results are quite acceptable and in line with the output of similar studies. It is evident that the found MTT values in the range of 263 to 354 days (Table 3-4) need to be interpreted with care.

QR1 has the highest MTT value with 354 days. The MTT value for PL, SF, FH, QZ and QN subbasins vary from 285 to 336 days, while for QR2, QM, QP and QC subbasins MTT fluctuates between 263 and 276 days. Our study shows no correlation between MTT and basin area ( $R^2 < 0.1$ ) suggesting that MTT is controlled by subsurface contact time and not by basin scale transport (Wolock et al., 1997). Some studies show a positive correlation between basin area and MTT (DeWalle et al., 1997; McDonnell et al., 1999) while others report that basin area is not related to MTT (McGuire et al., 2002; McGuire et al., 2005; Rodgers et al., 2005). Due to the similarity in geology, differences in MTTs between basins are attributable to the contribution of water from different sources. Although QR1 and QR2 are located relatively close to each other with an altitudinal difference of 129 m, MTTs are different with 354 and 263 days, respectively, suggesting that QR1 is receiving water from deeper horizons with longer contact time. As stated by Bückner (2010) spring rock water (W1) downstream QR2 is influencing QR1 during low flow conditions. Less deep rock water contribution is observed in QR2, QM, QP and QC.

Similarity in derived MTTs, independent of the vegetation cover of the subbasin, suggests that during low flows landuse does not or minimal affect runoff generation. This assumption is supported by the low correlation observed between the percentage of forest and MTT ( $R^2 < 0.05$ ). Notwithstanding the uncertainty on the derived MTT values it can be concluded that during low flow conditions subsurface flow from rock layers and/or C soil horizon is the main contributor to streamflow.

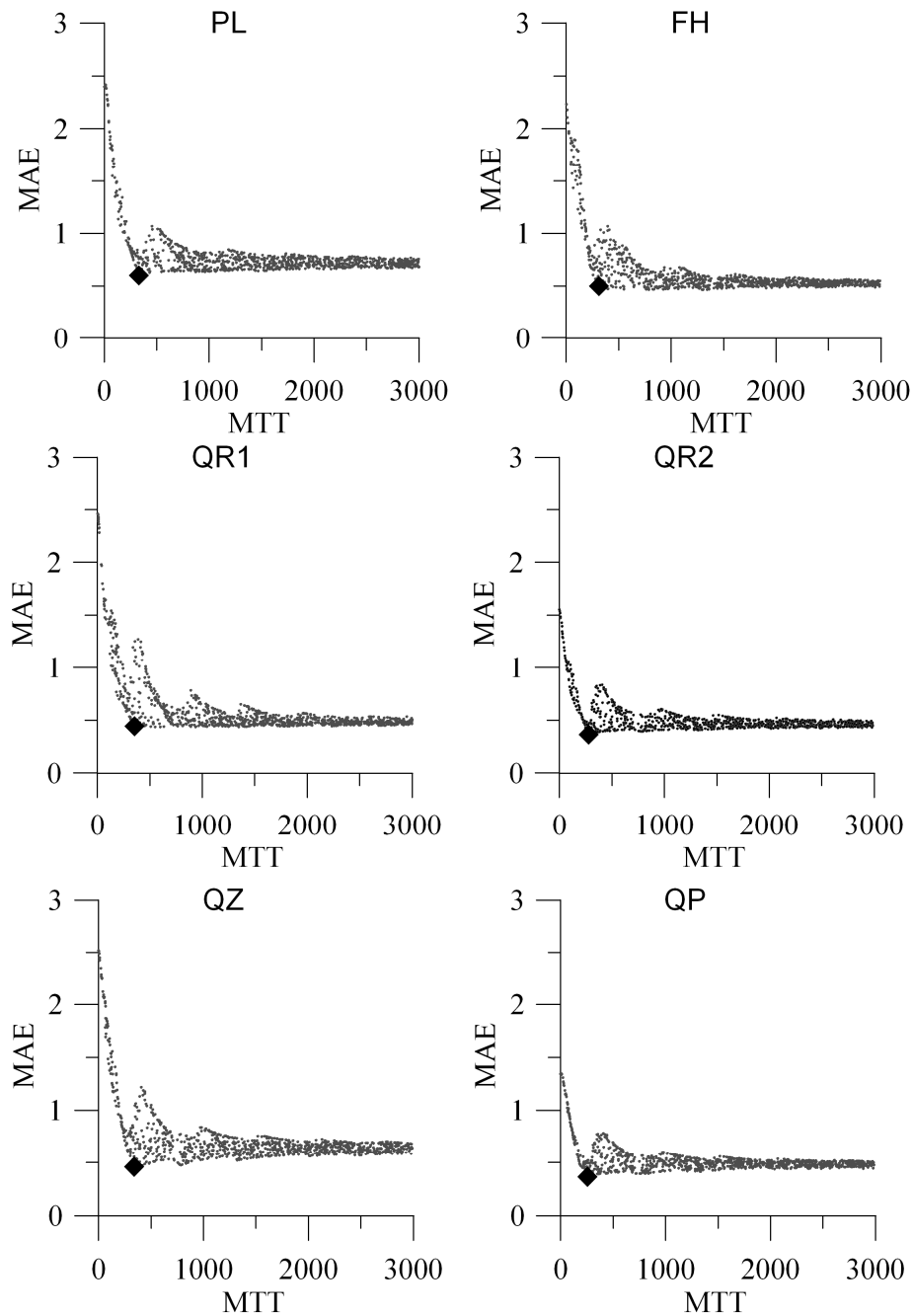


Figure 3–5: Scatterplots of MTT versus Mean Absolute Error (MAE) for 2000 Monte Carlo simulations for streamflow  $\delta^{18}\text{O}$  using the EPM.

### 3.3.4 END-MEMBER IDENTIFICATION

The chemical characteristics of soil, rock and streamwater are listed in Table 3-3 and the correlation between Al and Na concentration measured in water extracted from the O and A soil horizon as well as from bed rock for different flow rates are shown in Figure 3-4. For the application of mixing analysis, the chemical components Al and Na

were selected because of their representativeness for the hydrochemistry of the San Francisco basin as mentioned in the Section 3.2. In addition, the analysis revealed that the combination of Al and Na provides the best separation of water sources in the two dimensional mixing plots. In the analysis the chemical signature of rainfall was used given the similarity of Al and Na concentration between precipitation and throughfall (Boy et al., 2008). The chemical signature of precipitation represents also the chemical composition of infiltration excess overland flow. The Al and Na concentration in precipitation is low and therefore selected as one end-member in Figure 3-6. This end-member point is situated in the origin of each graph presented in this figure.

Given the similarity in soil distribution of Histosols and Regosols in the study basin, it is correct stating that the water samples collected at the sites OL1, OL2 and OL3 are representative for the study basin and the water flow through the litter layer, also called the organic near-surface flow and/or the saturation excess overland flow. High concentration of Al and the absence or the low concentration of Na is typical. The water samples collected in OL1 and OL3 have similar Al and Na signatures, whereas the water samples in OL2 have a lower Al and higher Na content. The latter suggests that the organic near surface water flow in OL2 seeps through soils with higher mineral content. Water samples collected in the AL site are representative for the lateral flow through the A horizon and in general for the A horizon in the basin. These samples are rich in Al and poor in Na. According to Boy et al. (2008) and Lorieri and Elsenbeer (1997) Al is mobilized and transported as organometallic complex, typical for near surface flow in litter and subsurface flow in topsoil with high organic matter content.

Rock water samples collected at the W1 and W2 sites represent the flow through the mineral C horizon and cracks in the top layer of the bedrock. As explained in Section 3.3 this flow is the major contributor to streamflow under dry conditions and based on the long MTT it is likely that the infiltrating rainfall replaces old water in the C horizon and the cracks in the top layer of the bedrock. The end-member of rock water is characterized by a high concentration of Na and zero to low concentration of Al. Boy et al. (2008) states that the origin of Na in the rock water is chemical weathering of the deeper subsurface layers. Our data strongly support this finding. Reduction in the contribution of deeper water sources to total flow, as happens during storm flow, would explain the observed pattern of decreasing concentrations during storm flow (see also

Bücker et al., 2010). The Na concentration in the water samples collected at W1 is higher than in the water samples taken at W2 suggesting that the W2 rock water represents the flow through deeper rock layers with higher mean transit time.

### 3.3.5 MIXING MODEL ANALYSIS

As shown in Figure 3-6 the Al and Na concentration of streamflow of the selected subbasins are well bounded by the chemical signature of the end-members precipitation, organic soil water and rock water with exception of the subbasins QP and QC (data not shown because the similarity with QP) where the A horizon is considered instead of the organic soil water. The studied basin and subbasins could be divided in three groups based on the end-member analysis. The station located at the outlet (PL) the main river (SF), and the subcatchments (FH, QR1, QZ, QN) belong to Group 1, the subbasins QR2 and QM form Group 2 and Group 3 consists of the subbasins QC and QP.

The chemical signature of the subbasins in Group 1 during low flow conditions is strongly related to the Al and Na load of the rock water collected in site W1, which is representative for the water seeping through shallow weathered rock with high density of shallow cracks. It is supported by the MTT values varying between 285 and 354 days. The subbasin QR1 is clearly more influenced by rock water contribution than the other subbasins. When the wetness of the soil increases the chemical signature of streamflow samples of the subbasins in Group 1 tend to be more oriented towards the chemical composition of the soil water in the O and A horizon. During storm events or when the soil profile is close to saturation the chemical fingerprint of streamwater is closely related to the chemical signature of the water flowing laterally through the organic soil horizons. Under those conditions the concentration of Ca decreases in favor of an increase of the Al concentration, as confirmed by Bücker et al. (2010). Given the high hydraulic conductivity of the litter layer and organic horizons infiltration excess overland flow does not occur in the subbasins of Group 1.

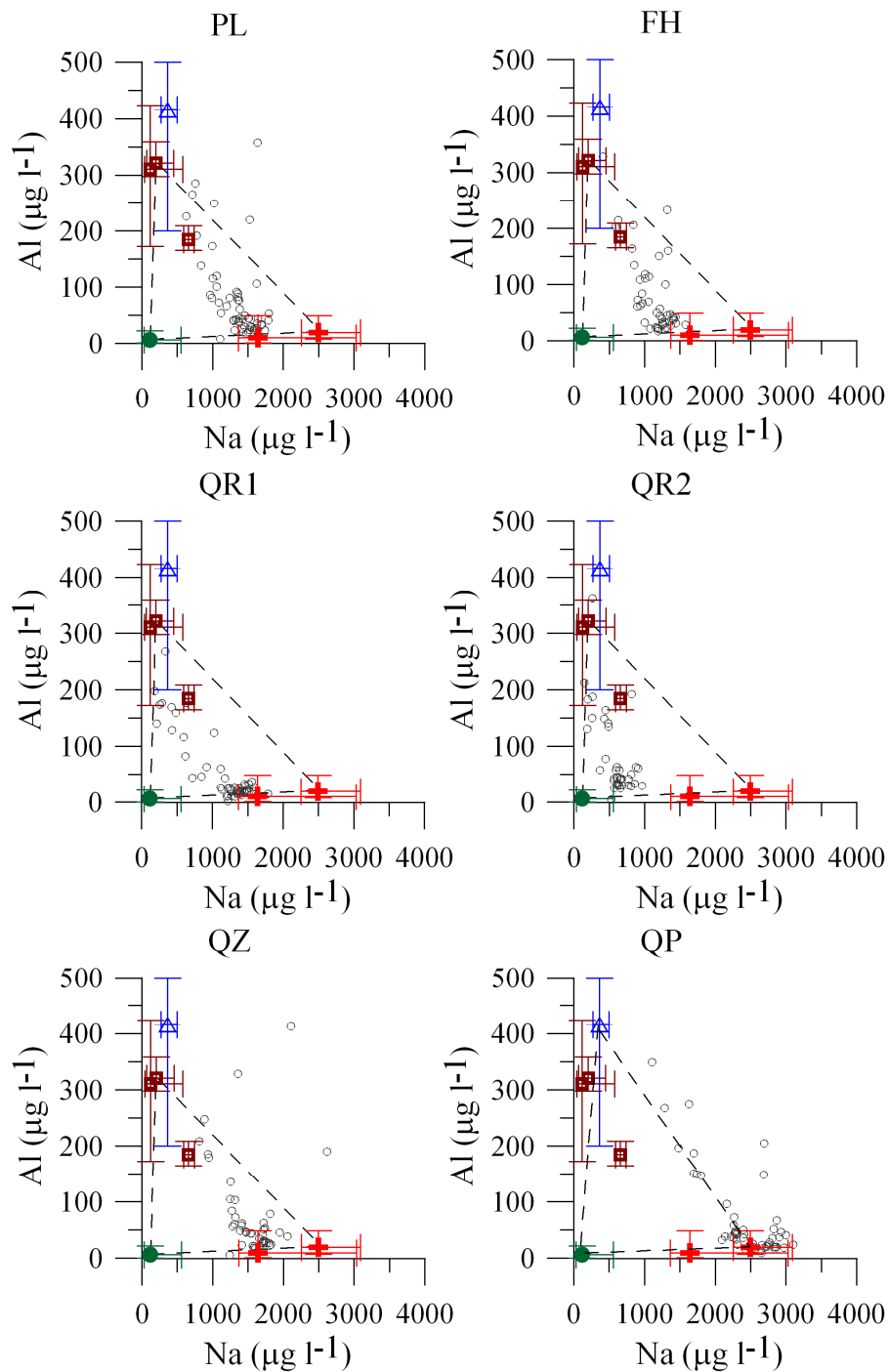


Figure 3–6: Mixing diagrams for Na and Al concentration for the San Francisco basin outlet (PL) and subbasins FH, QR1, QR2, QZ and QP. End members (including maximum and minimum) are represented by green circle = precipitation; brown square = OL, soil water in organic layer horizon; blue triangle = AL, soil water in A horizon layer; red cross = rock water.

The chemical fingerprint of the streamwater of the two subbasins in Group 2 is less similar to rock water at site W1 suggesting that streamflow under dry conditions is dominated by water from the C horizon and/or superficial weathered rock layers. This finding is in concordance with the lower value for MTT than the values found for the

subbasins in Group 1, 263 and 269 days for QR2 and QM, respectively. As discharge increases the contributing water is coming from the same source areas, the upper soil horizons, as in the subbasins of Group 1. For the subbasins in Group 1 and 2, the chemical signature of streamwater during storm events is dominated by the water flowing through the litter and organic horizons. Here too there is no evidence of infiltration excess overland flow in these subbasins.

The two subbasins in Group 3, QP and QC, have the largest area grazeland, varying between 26 and 67% of the total subbasin area. Mixing diagrams reveal that during low flow conditions the streamflow samples are apparently more related to deeper rock water contribution (W2). However, lower MTT values were registered in these catchments. This apparent contradiction could be explained by the increase of Al and Na concentrations in soils under pastures as a consequence of burning. Verification shows an increase of Al and Na of nearly 100 to 700% with respect to the Al and Na content of the A horizons under forest. Similarly an increase of the Al and Na content in the B and C horizons was observed but to a lower degree for Al (Makeschin et al., 2008). Although soil water and rock water samples in grazeland could not be collected by refusal of trespassing by the landowners, the mixing diagram (QP in Figure 3-6) suggests that during low flow the chemical signature of streamwater is dominated by lateral subsurface flow through the C horizon and the superficial weathered rock layers. When discharge increases, due to the degradation of the O horizon the chemical signature is increasingly controlled by the water lateral seeping through the A horizon. It is believed that the top soil horizons mainly contribute to the runoff generation by increasing discharge and that during storm events lateral flow through the A horizon is dominant. However, when the discharge increases, most of the streamwater samples fall outside the mixing domain determined by the three selected end-members. This can be the consequence that the authors were not able to sample soil and bedrock water at the pasture sites, and/or that all potential end-members were not successfully sampled. The mixing domain reveals that infiltration excess overland flow is not occurring. This is in concordance with the results of the study conducted by Zimmermann (2007) in the same area using hydrometric data at plot scale. However, due to the limitations in the data no strong conclusion can be drawn, justifying the need for further research.

### 3.4 CONCLUSIONS

The study revealed that the collection of hydrometric data, the chemical signature of water samples and isotopic tracers, and mixing model analysis provide crucial information on the processes dominating the runoff generation at basin scale in cloud forested areas, as stated in *hypothesis 1* of this study. The applied nested approach showed to be a relevant method for the determination of the spatial variability of the processes. A combination of the methods enabled reducing the limitation of each technique and when used together results provided a more exact and coherent picture of the hydrological system. Furthermore, tracers in contrast with hydrometric data lead to a considerable reduction in the length of the monitoring period and associated costs. The approach offers promising possibilities for the hydrologic analysis of ungauged or poorly gauged basins, as projected in *hypothesis 4*. In addition, the study suggests that more research on the geochemistry, complemented with the analysis of biological processes, in connection with the traditional hydrological approaches might provide far more reaching knowledge on the functioning of complex tropical ecosystems in a shorter period and at less cost.

The mixing diagrams and MTT values suggest that in the studied basin deep water contributes significantly to streamflow, and that these contributions are relatively unaffected by landuse or topography in contradiction with the *hypothesis 2*. The streamflow of all subbasins is mainly composed by subsurface flow. The analysis revealed that overland flow does not, or only exceptionally occurs in grazeland. The inclusion of spring water samples in the analysis enabled to identify differences in deep water contribution along the subbasins. As such it highlighted the relevance of including spring, seep and well water in tracer studies of tropical mountainous areas (Bücker et al., 2010; Soulsby et al., 2007).

The *3rd hypothesis*, which states that under wet conditions the runoff generation process is controlled by subsurface lateral flow through the organic horizons notwithstanding the steep topography, is confirmed by the analysis. The small differences in the generally long MTTs between catchments suggest that old water in the different storages of the basin is pushed out when new water enters.

## 4 DEVELOPMENT OF A CONCEPTUAL MODEL OF THE HYDROLOGIC RESPONSE OF TROPICAL ANDEAN MICRO-CATCHMENTS IN SOUTHERN ECUADOR

### Abstract

This paper presents a lumped conceptual model designed for simulating the rainfall-runoff response of mountain micro-catchments with natural vegetation, located in the south of Ecuador. The conceptual model is mimicking the soil hydrology and consists of a maximum of three linear reservoirs in series. A two and three reservoir model structure were tested, respectively. A GLUE uncertainty analysis was applied to assess the model performance. Simulation results of the discharge confirmed the applicability of the soil-based conceptual model structure for the selected study areas, during model calibration and validation. The three reservoir model best predicted the runoff, nevertheless the two reservoir model well captures the rainfall-runoff process of the micro-catchments with páramo vegetation. Although differences in climate regime, vegetation, and soil of the selected catchments, runoff is strongly controlled by the precipitation and soil type, and the horizons contributing to runoff are defined by their antecedent wetness. Results confirm that the discharge is mainly controlled by lateral subsurface flow through the organic horizons, while during dry conditions the C-horizon and the bedrock mainly contribute to discharge. Lateral transport through the densely rooted top horizon and the litter layer occurs during storm events, being under those conditions the major discharge component. Overland flow is a local phenomenon, negligible in comparison to the other flow components.

### Submitted as

Crespo, P., J. Feyen, W. Buytaert, R. Célleri, L. Breuer, H-G. Frede, M. Ramírez. Development of a conceptual model of the hydrologic response of tropical Andean micro-catchments in southern Ecuador. *Hydrological Earth Science System Discussion*, 9, 1-37.

## 4.1 INTRODUCTION

Mountain ecosystems sustain freshwater resources, human livelihoods and well-being, in particular of Southern America and Ecuador. They provide shelter to wildlife, resilience to rainfall variability and play an important role in climate change mitigation and adaptation (Celleri and Feyen, 2009). The natural functioning of these ecosystems are increasingly at risk not only as a consequence of global warming but also due to the continuing expansion of human activities (Buytaert et al., 2007; 2011). It is expected that understanding of the hydrology of the Andean mountain ecosystems will provide knowledge on how best to manage these systems to secure their existing fresh water supplies (Bruijnzeel, 2001; Feddema et al., 2005). Notwithstanding the ecological and economic importance of these ecosystems understanding of the hydrological functioning is still incomplete, especially the prediction of the rainfall-runoff response is complex as a consequence of the high spatial variability of climate, soils, and vegetation (Crespo et al., 2011a).

According to Buytaert et al. (2006a) the runoff variability of páramo ecosystems is strongly masked by the topography, soil and vegetation. Buytaert (2004), Zimmermann and Elsenbeer (2008) and Crespo et al. (2011a) confirmed this hypothesis and found that streamflow mainly is sustained by lateral subsurface flow in the soil matrix. Goller et al. (2005), Boy et al. (2008) and Crespo et al. (2011b) came to the same conclusion monitoring geochemical and isotopic tracers in forested subcatchments of the San Francisco basin in southern Ecuador. Their findings are confirmed by Elsenbeer et al. (1995), Elsenbeer (2001), Schellekens et al. (2004), Buytaert et al. (2006b) and Blume et al. (2008) on the basis of detailed flow monitoring in tropical ecosystems. Other publications report that runoff in tropical forested catchments predominantly is characterized by overland flow (Elsenbeer and Lack, 1996; Johnson et al., 2006; Chaves et al., 2008).

Crespo et al. (2011a,b), in their survey of the rainfall-runoff response of small catchments in the tropical Andes of southern Ecuador, found that during dry periods streamflow mainly is the result of lateral flow through the C-horizon of the

soil profile and the weathered top of the underlying bedrock. These authors further assumed that the unweathered bedrock does not contribute to streamflow, although locally depending from the geological characteristics it might be possible that a fraction of streamflow is generated by the water stored in bedrock fissures. The water draining from the C-horizon and the weathered top of the bedrock originates from the excess rainfall percolating below the overlying organic horizons. During average precipitation events the soil profile gradually saturates yielding an increasing fraction of lateral subsurface flow (Buytaert, 2004; Boy et al., 2008; Crespo et al., 2011a). Zimmermann and Elsenbeer (2008) found that under moderate rainfall conditions, in a study area situated in the same area as the research conducted by Crespo et al. (2011a), most of the streamflow is composed of the lateral flow through the top horizons of the soil. Under intense storm events streamflow is dominated by the lateral flow through the rooted organic horizon and litter layer, as stated by Goller et al.(2006), Boy et al.(2008) and Bücken et al. (2010). Research further revealed that during wet soil conditions and near rivers, overland flow most probably occur by saturation excess. Due to the overall low rainfall intensity and the high saturated hydraulic conductivity of the top layer it is unlikely that Hortonian overland flow happens, although Crespo et al. (2011a) found that locally in páramo ecosystems overland flow during extreme events can arise. Zimmermann and Elsenbeer (2008) and Bogner et al. (2008) concluded that Hortonian flow only seldom occurs in cloud forests in southern Ecuador. Similarly Buytaert et al. (2007) and Blume et al. (2007) came to the same conclusion for páramo ecosystems in Ecuador and Chile.

The paper presents a conceptual model for simulating the runoff response to rainfall of Andean micro-catchments in southern Ecuador, based on the hypotheses formulated in previous research (Crespo et al., 2011a,b). Underlying assumptions implemented in the conceptual model are: (i) deep water hardly contributes to streamflow; (ii) during prolonged dry spell periods streamflow mainly consists of lateral flow through the C-horizon and bedrock; (iii) lateral flow through the organic horizons and/or litter layer mostly characterizes streamflow in rainy periods; and (iv) saturation excess flow only locally occurs during extreme storm events. A step-wise increase in complexity of conceptual model was applied and

tested, with the objective to define which level of complexity most adequately mimics the runoff response in the studied catchments.

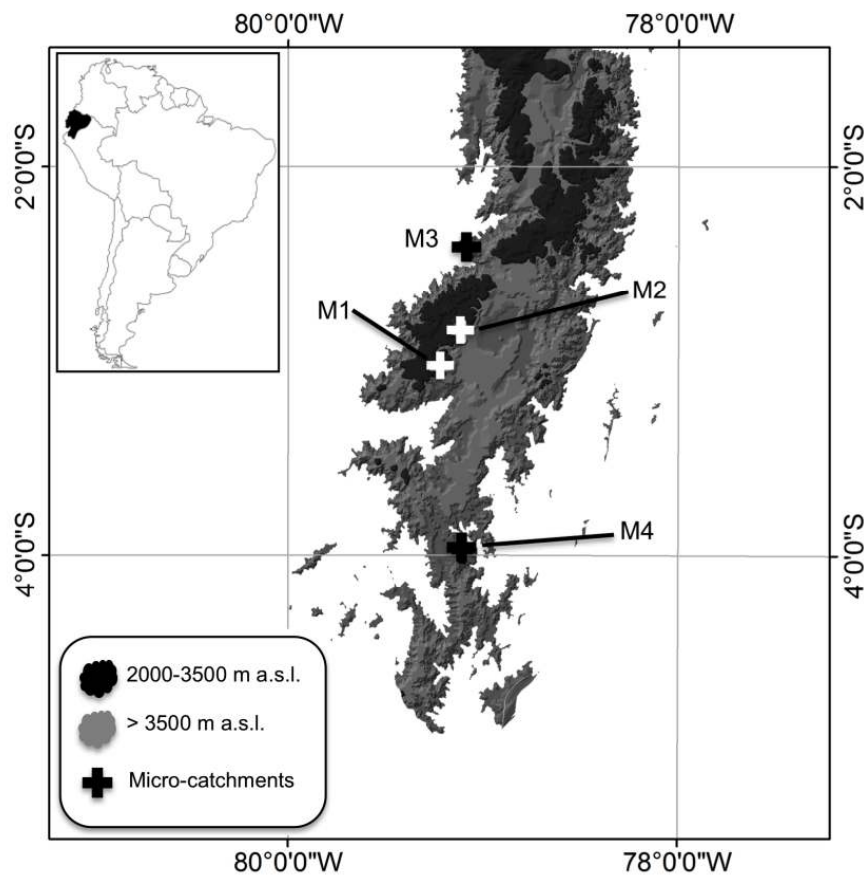


Figure 4–1: Location of the four study micro-catchments

## 4.2 MATERIALS AND METHODS

### 4.2.1 CASE STUDY CATCHMENT DESCRIPTION

Four micro-catchments were selected, representing pristine conditions in the wet páramo, upper montane and cloud forest region of southern Ecuador. The micro-catchments are situated between  $2^{\circ}24'$  and  $3^{\circ}58'$  latitude. The elevations vary between 1743 and 4100 m a.s.l. and the catchment area between 0.99 and 4.62 km<sup>2</sup> (Figure 4-1 and Table 4-1). The micro-catchments Zhurucay (M1) and Ortigas (M3) drain to the Pacific Ocean and are located on the east slope of the Cordillera Occidental while the Huagrahuma (M2) and San Ramon (M4) are tributaries to the Amazonian River Basin, whereby M2 is located on the western slope of the Cordillera Occidental and M4 on the western slope of the Cordillera Real. M1 is

located in the upper basin of the Jubones river, M2 is a tributary to the Paute river, M3 drains into the BuluBulu river basin, and M4 discharges into the Zamora river basin. The shape of M2 (2.58 km<sup>2</sup>) and M3 (0.99 km<sup>2</sup>) is stretched oval with an average surface slope of 43 to 45%. The basin area of M1 and M4 is 1.34 and 4.62 km<sup>2</sup> and the average surface slope is 18 and 61%, respectively. The catchment shape of both these micro-catchments is elongated oval to rectangular and circular to oval (see Table 4-1).

Table 4–1: Main catchment characteristics

Characteristic	Unit	Catchment			
		M1 Zhurucay	M2 Huagrahuma	M3 Ortigas	M4 San Ramon
Area name		Quimsacocha	Huagrahuma	Ortigas	San Francisco
Area	km <sup>2</sup>	1.34	2.58	0.99	4.62
Altitude	m a.s.l	3680-3900	3690-4100	2305-2880	1743-3150
Slope	%	18	45	43	61
Shape		EOR	SO	SO	CO
Geology		Quimsacocha Fm.: volcanic and volcanoclastic rocks	Saraguro Fm.: lavas and andesitic volcanoclastic deposits		Chiguinda unit: palaeozoic metamorphic rocks
Soil distribution	%	Andosol (85), Histosol (15)	Andosol (100)	Andosol (74), Leptosol (26)	Histosol (60), Cambisol (30), Regosol (10)
Vegetation cover	%	Tussock grass (71), shrubs (2), Pasture (27)	Tussock grass (100)	Upper montane forest (76), pasture (20), cropland (4)	Upper montane cloud forest (80), sub-páramo (18), shrubs (2)
Landuse		Extensive grazing	Natural	Natural, extensive grazing	Natural
Observation period		26/10/06- 11/11/08	08/08/01- 16/06/05	16/01/06- 15/07/08	23/04/07- 25/08/08
Length	days	747	1408	911	490
Precipitation	mm y <sup>-1</sup>	1241	1460	1715	3796
Discharge	mm y <sup>-1</sup>	913	1059	803	3066
Runoff coefficient		0.74	0.74	0.46	0.81

Legend: SO, stretched oval; CO, circular to oval; EOR, elongated oval to rectangular

M1 and M2 belong to the wet páramo ecosystem (neotropical alpine grassland) covering the Andes region above 3500 m a.s.l. with a landscape build up of relative flat to concave valleys (Luteyn, 1992; Hofstede, 1995; Medina and Vásquez, 2001). Both micro-catchments represent good pristine conditions; only sporadic extensive grazing by free roaming animals is observed in the lower part of both catchments. Tussock grass, cushion plants and low shrubs are the dominant vegetation (Table 4-1) (Buytaert et al., 2006b). Although the similarities between both, these catchments were selected for the difference in average surface slope, respectively 18 and 43%. Primary protected upper montane forest covers 76% of M3 (*Asteraceae*, *Boraginaceae*, *Coriaceae*, *Euphorbiaceae*, *Junglandaceae*, *Fabaceae*, *Melastomataceae*, *Scrophulariaceae*, *Solanaceae*, *Verbenaceae*) (Bruijnzeel, 2001; Crespo et al., 2008). Canopy height varies between 5 and 10 m, occasionally exceeding 15 m (Bussmann, 2005); stems are covered with lichens and epiphytes (Balslev and Øllgard, 2002). Fog interception at this altitude is negligible according to Bendix et al. (2008). Anthropogenic impacts are mainly present in the upper and remaining part of the basin consisting of deforestation for grazing (*Penicetum clandestinum*) and the cultivation of maize and potatoes. M4 is covered with pristine montane cloud forest (80%) with trees of the families *Lauraceae*, *Euphorbiaceae*, *Melastomataceae* and *Rubiaceae*, on average 20 m tall (Homeier et al., 2002). The basin area above 3140 m, representing 18% of the basin area, is covered with sub-páramo evergreen elfin forest (Beck et al., 2008; Homeier et al., 2002). The area is very susceptible for landslides, as a consequence of terrain steepness, the relative shallowness and high moisture content of the soils (Bussmann et al., 2008). Open spots, occupying 2% of the basin area, created by landslides are with time covered by secondary forest growth. A more detailed description of the four micro-catchments can be found in Buytaert et al. (2006b, 2007) and Crespo et al. (2010, 2011a).

The climate in M1 and M2 is affected by the Pacific coastal regime from the west and the continental and tropical Atlantic air masses from the east (Vuille et al., 2000). The resulting precipitation pattern is bimodal, with a major wet season in December to February and a less pronounced wet season from August to September interrupted by dry spell periods of less than 16 days (Buytaert et al., 2005; Crespo et al., 2011a). The mean annual precipitation in the period 1964-2008 (INAMHI)

varies from a maximum of 1600 mm to a minimum of 900 mm. Mean annual precipitation in M3 in the period 1970-2008 fluctuates between 500 and 1900 mm. The inter-annual seasonality is unimodal and influenced by the Pacific coastal regime. The wet season stretches from December to May yielding 60 to 80% of the annual precipitation, and a dry season from June to November. Continuous dry periods of two months and longer are not an exception. The climate in M4 is affected by air masses originating in the Amazonian basin (Beck et al., 2008). The precipitation pattern is unimodal with relative constant inter-annual seasonality. The main wet season is from April to September with dry spells mainly occurring for less than 10 consecutive days (Fleischbein et al., 2005). In the period 1964-2008 annual precipitation varied from 900 to 4300 mm (INAMHI) with an average of 2200 mm at an altitude of 1960 m; however average rainfall increases to 4700 mm (1994-2004) at the Cerro del Consuelo station located at 3150 m a.s.l., at the fringe of the catchment (Rollenbeck, 2006; Bendix et al., 2008). Horizontal rain and cloud/fog water deposition contributes up to 41.2% of the basin water yield (Bendix et al., 2008). Rainfall intensity is low in all four study basins with 90% of the rains having intensities less than 10 (M1, M2 and M4) and 15 mm h<sup>-1</sup> (M3). A more detailed description of the climate in each of the micro-catchments is available in Buytaert et al. (2006a, 2007) and Crespo et al. (2008).

The geology of M1 and M3 belongs to the Late Oligocene to Early Miocene Saraguro Fm., with lavas and andesitic volcanoclastic deposits compacted by glacier activity during the last ice age (Coltorti and Ollier, 2000; Hungerbühler et al., 2002). According to Buytaert et al. (2005) hydraulic conductivity of the Saraguro Fm. is low. The micro-catchment M2 is located on the Quimsacocha Fm. (Pratt et al., 1997). Covered by volcanic and volcanoclastic rocks, the formation consists of basalt flows with plagioclase, feldspar phenocrysts and andesitic pyroclastic deposits. According to IAMGOLD (2006) the age of the deposits is undefined; hydraulically they are nearly impermeable and possess a low density of fissures in the upper layer of the formation. The geology in M4 correspond to the Chiguinda unit, which is mainly composed of Paleozoic metamorphic rocks such as semipelite, phyllite and quartzite with low alteration (Litherland et al., 1994; Hungerbühler, 1997; Bendix et al., 2008).

Table 4-2: Horizon properties of the main soils in the catchments

Catchment/horizon	Depth (cm)	Bulk density (g cm <sup>-3</sup> )	pH	SOM (%)	Ks (mm h <sup>-1</sup> )	pF = 0 (cm <sup>3</sup> cm <sup>-3</sup> )	pF = 2 (cm <sup>3</sup> cm <sup>-3</sup> )	pF = 4.2 (cm <sup>3</sup> cm <sup>-3</sup> )	Sand (%)	Silt (%)	Clay (%)
<b>M1 (Zhurucay)</b>											
Ah	20-40	0.21-0.35	4.3-4.8	15-31	8-12	0.7-0.85	0.67-0.82	0.36-0.44	67-80	17-30	12-34
H	22-31	0.1-0.21	4.4-4.7	33-50	5-12	0.85-0.90	0.84-0.90	0.15-0.39	56-64	20-30	14-26
A	16-50	0.2-0.5	4.5-5.7	24-44	5-33	0.74-0.89	0.72-0.86	0.30-0.52	34-53	30-44	12-38
C	-	0.76-1.11	4.3-6.0	0.4-4.7	7.9-41	0.63-0.66	0.58-0.63	0.18-0.40	42-74	24-30	4-36
<b>M2 (Huaqhahuma)</b>											
Ah	18-25	0.29-0.44	4.6-4.8	16.7-31.0	9-38	0.85-0.90	0.84-0.90	0.13-0.39	29-40	43-49	11-28
A	18-30	0.25-0.37	4.8-5.0	17.5-31	10-34	0.66-0.86	0.50-0.83	0.15-0.74	26-32	35-43	25-41
C	-	0.75-1.3	4.5-4.9	0.4-8.6	2-28	0.71-0.79	0.65-0.72	0.32-0.50	64-67	16-23	10-20
<b>M3 (Ortigas)</b>											
O	15-30	0.1-0.2	5.6-6.0	23-60	28-105	0.66-0.77	0.59-0.71	0.18-0.58	38-50	43-50	12-35
A	13-30	0.4-0.6	4.0-6.0	16-29	22-60	0.71-0.93	0.65-0.89	0.48-0.49	28-42	45-47	11-27
Bw	40-50	0.3	5.6-6.0	1-8	23-60	0.64-0.76	0.59-0.76	0.33-0.59	41-68	27-37	5-22
C	-	0.44-1.4	5.7-6.0	1-8	26-60	0.60-0.74	0.59-0.61	0.33-0.49	46-68	27-35	9-27
<b>M4 (San Ramon)</b>											
O	8-20	0.1-0.2	4.2-4.4	33-44	160-167	-	-	-	42	38	20
H	8-20	0.1-0.3	4.8	28	83-91	0.76	0.5	0.23	37	42	21
Ah	8-40	0.2-1.1	4.8-5.4	8-28	11-91	0.55-0.76	0.50-0.52	0.23-0.26	29-38	42	20-28
Bw	15-80	1.0-1.3	5.1-5.7	0.3-13	9-23	0.68-0.70	0.46-0.63	0.19-0.36	19-30	42-49	21-38
C	-	-	-	-	11-18	0.59	0.40	0.25	-	-	-

Legend: pH, soil acidity expressed as amount of H<sup>+</sup> cations in soil solution; SOM, soil organic matter in %; Ks, saturated hydraulic conductivity in mm h<sup>-1</sup>; pF, soil matric potential expressed as the log<sub>10</sub>(cm water column) respectively at saturation, field capacity and wilting point and corresponding soil water content in cm<sup>3</sup> cm<sup>-3</sup>; Sand, Silt and Clay, main particle size classes in percent

The main soils in the study catchments are Andosol, Leptosol, Histosol, Cambisol and Regosol (FAO/ISRIC/ISSS, 1998). The soil distribution per micro-catchment is listed in Table 4-1, while the soil properties of the main horizons are summarized in Table 4-2. The cold and wet climate and the low atmospheric pressure, characteristic for mountains, favor organic matter accumulation resulting in soils with high soil organic matter content, 15 to 50%, low bulk density ( $0.1$  to  $0.44$  g  $\text{cm}^{-3}$ ), high water content ( $0.63$  to  $0.9$   $\text{cm}^3$   $\text{cm}^{-3}$ ) at saturation, and low to moderate pH ( $4.3$  to  $6.0$ ) (Table 4-2). The horizon sequence of the Andosols in M1 and M2 is Ah, A and C, and of the Histosols in M1 is H, A and C. The depth of the organic horizon ranges from 36 to 90 cm in M1 and from 36 to 55 cm in M2. Andosols (74%) and Leptosols (26%) are present in M3 with horizon sequence O, A, Bw and C for Andosols, and O or Ah on top of the parent material for Leptosols. Leptosols are mainly located on steep slopes where the soils in general are less developed. The main soils in M4 are Histosols (60%), Cambisols (30%) and Regosols (10%). The Histosols under cloud forest are less deep having a horizon sequence of O, H, Ah and C (Makeschin et al., 2008; Wilcke et al., 2002). The Cambisols in M4 are located below 2100 m a.s.l. and are typical Dystric or Humic Cambisols with the horizon sequence O, Ah, Bw and C (Wilcke et al., 2002). Regosols are mainly situated below 2100 m a.s.l., decreasing in area with the altitude until 2300 m a.s.l. O, Ah and C are the typical horizon sequence of the Regosols. A detailed description of the soil characteristics are given in Crespo et al. (2011a).

#### 4.2.2 MONITORING

M1 and M3 were equipped with a weather station, and M4 with 3 weather stations. A weather station was present at the Chanlud dam, close to M2. Hourly data was available for M1, M3 and M4, while daily data for M2. Reference evapotranspiration (ET<sub>p</sub>) was estimated using the Penman-Monteith equation with constant canopy resistance (Allen et al., 1998). An intra-day curve was used to estimate hourly ET<sub>p</sub> for M2 and repeated for the entire monitoring period. This approach produces an acceptable hourly distribution of ET<sub>p</sub> due to the low seasonal climate variability, typical for páramo, as stated by Buytaert and Beven (2011). Additionally, in M1 and M3 two rainfall gauges (HOBO RG3 tipping bucket gauge with a resolution of 0.2 mm) were installed, respectively in the upper and lower part

of the basin, and three rainfall gauges relatively uniformly distributed over the basin area in M2 (same type of raingauge as in M1 and M3) and M4 (details on the equipment and protocol of rainfall and fog collection and data processing are given in Bendix et al., 2008). The precipitation data for all catchments were aggregated over time intervals of one hour. The short data gaps were filled using linear interpolation. The Thiessen polygon method was applied to derive areal precipitation data for the catchments M1 to M3, and the area weighted elevation method for the generation of the areal rainfall and fog for M4. A concrete Thompson (V-notch) weir (90°) with sharp metal edges was installed in the micro-catchments M1 to M3, while streamflow in the catchment M4 was measured in a natural stable river cross section. Each measuring site was equipped with pressure transducers, recording the water level with a 5 min interval and an accuracy of  $\pm 1$  mm. In M2 on 12/05/2002 a backup sensor was installed to replace the failing sensor. To reduce the uncertainty on streamflow measurements, particular during storm events, frequent control measurements were made. The Kindsvater-Shen relation (US Bureau of Reclamation, 2001) was used for the conversion of the water level to discharge for M1 to M3. An empirical stage-discharge relationship was developed for M4.

#### 4.2.3 DESCRIPTION OF THE CONCEPTUAL MODEL

The concept of the model for simulating the runoff of the micro-catchments M1 to M4 is based on the findings of Goller et al. (2006), Buytaert and Beven (2011) and Crespo et al. (2011a,b). Precipitation is split in canopy and surface interception and rainfall stored in the different soil horizons and top of the bedrock. The subsurface and groundwater flow components are mimicked by a maximum of 3 reservoirs. If present, overland or liter layer flow is calculated as a fraction of the rainfall. Figure 4-2 depicts the structure of the subsurface model assuming that the soil hydrology can be mimicked with 3 reservoirs (3-Res model structure). Total flow ( $Q_{total}$ ) is the sum of the outflow of each reservoir ( $Q1$ ,  $Q2$  and  $Q3$ ) and in the case of overland flow increased with the direct flow. The storage ( $S$ ) in each of the three linear reservoirs  $S1$ - $S3$  is governed by the water balance equations as shown in the Eqs. (4-1), (4-2) and (4-3):

$$S1(t) = S1(t-1) + P(t) - ET_a(t) - LL(t) - SOF(t) - Q1(t) - IS1(t) \quad (4-1)$$

$$S2(t) = S2(t-1) + IS1(t) - Q2(t) - IS2(t) \quad (4-2)$$

$$S3(t) = S3(t-1) + IS2(t) - Q3(t) \quad (4-3)$$

where  $P$  is the precipitation at time interval  $t$ ,  $ET_a$  the actual evapotranspiration,  $LL$  the overland or litter layer flow,  $SOF$  the saturated overland flow,  $Q$  the lateral outflow from the reservoir,  $IS1$  is the percolation from reservoir 1 into reservoir 2, and  $IS2$  the percolation from reservoir 2 into 3. Interception loss is calculated as a fraction of the precipitation below a threshold value representing the rainfall that saturates the canopy or fulfills surface storage. Threshold value for the canopy saturation was fixed at 10 mm, while the interception loss fraction was estimated between 25 to 52% of the incident precipitation, both according to the study conducted by Fleischbein et al. (2005; 2006) in the same area as M4.

Actual evapotranspiration ( $ET_a$ ) is satisfied by the water stored in the canopy and surface storage ( $IL$ -Interception loss). When the amount of water in  $IL$  is less than the actual demand, the remaining fraction is extracted from the first reservoir, the so-called rootzone, via transpiration.  $ET_a$  is proportional to the reference evapotranspiration  $ET_p$  varying linearly with the soil moisture content ( $SI/SI_{max}$ ) as depicted in Eq (4-4).

$$ET_a(t) = \frac{S1(t)}{S1_{max}} [ET_p(t) - IL(t)] + IL \quad (4-4)$$

The outflow  $Q(t)$ , Eq. (4-5), for each reservoir ( $i$ ) is simulated multiplying a transfer function for routing the model storage ( $f$ ) by a flow contribution equation ( $\chi$ ). Equation (4-6) shows the transfer function and Eq. (4-7) the flow contribution equation used in the conceptual model.

$$Qi(t) = f_{Qi} \times \chi_{Qi} \quad (4-5)$$

$$f_{Qi}(t) = \tau_{Qi}^{-1} \times \exp \left[ a_{Qi} \frac{Si(t)}{Si_{max}} \right] \quad (4-6)$$

$$\chi_{Q_i}(t) = [S(t) - T_{S_i}] \text{ for } S_i > T_{S_i} \text{ and } S_i < S_{i_{\max}} \quad (4-7)$$

where  $\tau$  is a time constant parameter,  $a$  is a model parameter for the different outflows,  $S_{i_{\max}}$  the upper water storage limit in reservoir  $i$ , interpreted as the maximum soil moisture content or the maximum water storage in the rock layer, and  $T_{S_i}$  is the minimum soil moisture content required to generate lateral outflow in reservoir  $i$ .  $S_{i_{\max}}$  for soils is derived as the difference between saturation and wilting point multiplied by the horizon depth. When  $S_i$  is less than  $T_{S_i}$ ,  $Q_i(t)$  is equal to 0 and  $S_i$  represents the non-mobile water in the reservoir.

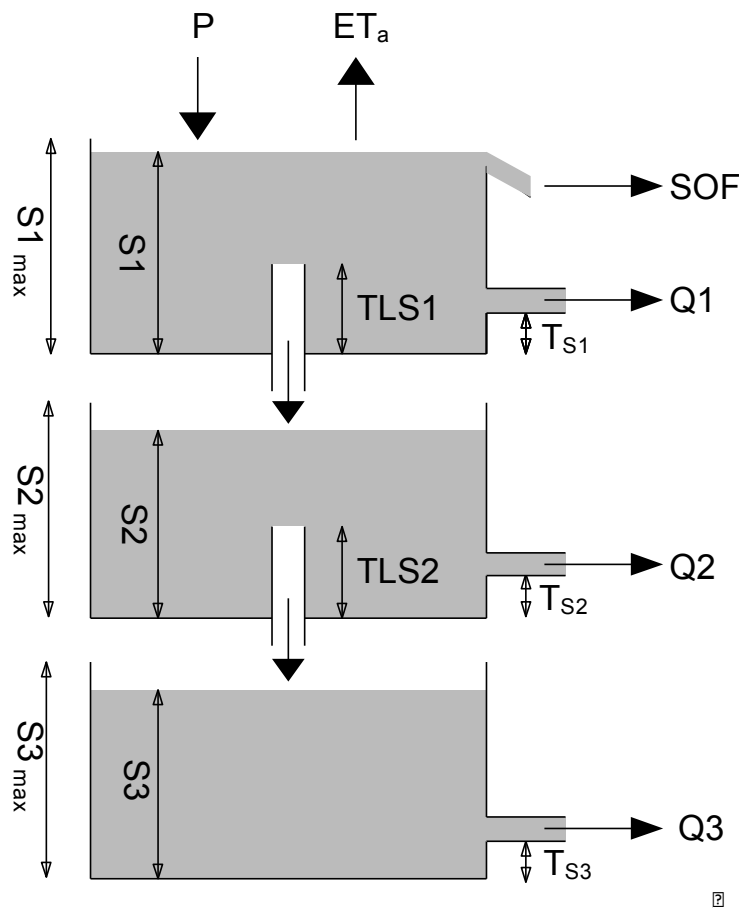


Figure 4–2: Schematic presentation of the concept of the 3-Res (3-reservoir) model (based on Crespo et al., 2011a,b)

Direct overland flow (*SOF*) and saturation excess in ponding areas and/or litter layer flow (*LL*) occur when the rainfall intensity is higher than the infiltration rate of the organic horizon. *LL* is estimated as a fraction of the rainfall and *SOF* is the

volume that exceeds the maximum storage ( $SI_{max}$ ) in the top reservoir, both multiplied by the runoff coefficient  $C_{LL}$ . Finally, the percolation ( $ISi$ ) from one reservoir into the underlying reservoir is calculated as the volume above a threshold value ( $TLSi$ ) assuming a linear variation with the soil moisture content ( $Si/Si_{max}$ ) (Eq 4-8).

$$Si(t) = [Si(t) - TLSi] \times \frac{Si(t)}{Si_{max}} \text{ for } Si > TLSi \text{ and } Si < Si_{max} \quad (4-8)$$

The number of parameters to calibrate is 14 when considering a 3-reservoir (3-Res) model, and 10 parameters when mimicking the runoff with a 2-reservoir (2-Res) approach. The number of parameters increases by 2 when including the model description of interception losses ( $IL$ ). The model was developed in the R programming language, using version 2.14.

#### 4.2.4 MODEL PERFORMANCE ANALYSIS

According to Klemeš (1986) the hourly rainfall dataset available per study catchment was split, respectively for model calibration and validation, as outlined in Table 4-3. Prior to calibration a warm-up period of 6 months was used for all micro-catchments. Two model set-ups, the 2- and a 3-Res (2 and 3 reservoirs) model were tested. Interception losses were only considered in the forested micro-catchments M3 and M4. Surface interception was considered negligible for the four micro-catchments. The Generalized Likelihood Uncertainty Estimation method (GLUE) (Beven and Binley, 1992) was used to generate uncertainty bounds. The behavioral limits were chosen such that the uncertainty range encompasses 90% of all used observations. Model performance was characterized by the Nash Sutcliffe efficiency coefficient (EF) (Nash and Sutcliffe, 1970). As stated by Buytaert and Beven (2011) uncertainty in modeling the hydrologic response of mountain micro-catchments comes primarily from the input data, as a consequence of the climate variability and heterogeneity in aerial precipitation. Since it was not possible to measure the uncertainty caused by model inputs, the authors just considered the total prediction uncertainty associated with input and model parameters. The

viability of the model structures, respectively the 2 or 3-Res model, was assessed comparing the simulation output with the 90% confidence interval.

## 4.3 RESULTS AND DISCUSSION

### 4.3.1 RAINFALL-RUNOFF

Table 4-1 depicts the annual precipitation and discharge for the four micro-catchments, as recorded during the corresponding observation periods. The runoff coefficient for M1 and M2 is 0.74, the result of an average annual observed precipitation of 1241 and 1460 mm  $y^{-1}$  and discharge of 913 and 1059 mm  $y^{-1}$ , respectively. The precipitation regime in M3 is well-marked by a wet and dry period. 80% of the precipitation falls during the wet season, yielding a runoff coefficient of 0.46; the result of 803 mm  $y^{-1}$  discharge and 1715 mm  $y^{-1}$  rainfall. According to Crespo et al. (2011a) the moderate runoff in this micro-catchment is the consequence of the moderate to high evapotranspiration rate during the dry season. Annual precipitation in M4 is close to three times higher than in the other 3 micro-catchments, with an average annual value during the observation period of 3796 mm  $y^{-1}$ . The fast response of the catchment to rain events results in an average annual discharge of 3066 mm  $y^{-1}$  during the observation period, leading to a the high runoff/precipitation ratio of 0.81.

Intensities of most storm events are smaller than 10 mm  $h^{-1}$  for the micro-catchments M1, M2 and M4 and below 15 mm  $h^{-1}$  for M3; less than the saturated hydraulic conductivity of the top layer, which for M1 and M2 varies between 8 and 38 mm  $h^{-1}$ , M3 from 28 to 105 mm  $h^{-1}$  and M4 between 160 and 167 mm  $h^{-1}$ . Given the low to moderate rainfall intensities it is very unlikely that Horton overland flow occurs, being the case very locally during high intensity rain events (Buytaert et al., 2006c ;Goller et al., 2005; Crespo et al. 2011a). The authors expect that saturation excess overland flow takes place near the river bed. In general all catchments show a quick response of discharge to rainfall, suggesting a fast transport of water through the litter and organic layers of the soils. During dry conditions the recession constant of discharge is high, suggesting a large water regulation capacity

of the soils, as displayed in Table 4-2. The foregoing is confirmed by Buytaert (2004), Buytaert et al., (2006c), Crespo et al. (2008), and Crespo et al. (2010).

### 4.3.2 MODEL CALIBRATION AND EVALUATION

The model performance indicators, bias, efficiency and accuracy (Moriassi et al., 2007) of the 2- and 3-Res model structure for each of the four micro-catchments are for the calibration and validation period listed in Table 4-3. Figure 4-3 shows the observed (dotted line) and the 90% confidence interval for the hourly flow duration curves (FDC) of the 2- (gray lines) and 3- (black lines) Res model. Figure 4-4 depicts for the microcatchments M1 to M4 the observed, the 90% uncertainty band on the predicted discharge, respectively for the 2- (left panels) and 3-Res (right panels) model. Results in Table 4-3 clearly show that for each of the four micro-catchments the 3-Res model outperforms the 2-Res model, and this during the calibration and evaluation periods. However, the difference in performance of both model structures is not significant for the M1 and M2 micro-catchments. Both model structures slightly better predict the observed discharge for M1 during the evaluation period, and perform equally well for M2 during the model calibration and validation period. The 3-Res model shows a statistically significant better prediction of the discharge for the M3 micro-catchment, and somehow less significant better than the 2-Res model structure for the M4 catchment. For both these catchments the model performance of both model structures in the calibration period was generally slightly better than during the model evaluation period.

The 5 and 95% uncertainty limits of the predicted discharge with application to the M1 micro-catchment, using the 2- and 3-Res model, envelopes the observed time series of discharge, as shown in the Figures 4-3 and 4-4. Both model structures seem to predict the hydrologic response well for the majority of precipitation events. The recession curves, the fast response to rainfall events in dry spell periods, and the time of peaks are in general correctly captured by both model structures (Figure 4-4). The 2-Res model seems to slightly underestimate peak flows during wet periods, while peaks during drier periods are overestimated or not simulated. Adding a 3rd reservoir on top of the 2-Res model structure, with low

residence time (18 hours), peak flows are better simulated, however considerably overestimated during dry periods (Figure 4-3). In line with findings of Nandakumar and Mein (1997) and Bruijnzeel and Veneklaas (1998) the incorrect prediction of peak flows during wet and dry periods is due to an underestimation of the areal precipitation, a well-known phenomenon in mountain areas (Celleri et al., 2007). Additionally, as suggested by Buytaert and Beven (2011), linear reservoir structures in general tend to have problems in simulating peaks. Another explanation might be that the lumped approach does not correctly mimic the dynamics between the hillslope and concave saturated plateaus and depressions, which according to Beven and Freer (2001) and Beven (2001a) during rain storms directly contribute to peak flow. The uncertainty interval is considerably wider during low flows than high flows, and adding a 3rd reservoir reduces the width of the 90% confidence interval. It is noticed that both the 2- and 3-Res models better predict streamflow during the model validation than calibration period.

Table 4–3: Model performance indicators

Model structure	Calibration				Evaluation			
	Data period	BIAS	EF	AC	Data period	BIAS	EF	AC
M1 (Zhurucay)								
2-Res	26/Oct/06 -	0.03	0.66	68	27/Mar/08 -	0.01	0.74	65
3-Res	26/Mar/08	0.02	0.68	79	11/Nov/08	0.01	0.75	77
M2 (Huagrahuma)								
2-Res	08/Aug/01 -	0.03	0.73	65	14/Aug/03 -	0.02	0.71	62
3-Res	07/Feb/03	0.02	0.74	73	16/Jun/05	0.01	0.73	71
M3 (Ortigas)								
2-Res	16/Jan/06 -	0.08	0.36	NA	17/Jan/07 -	0.05	0.28	NA
3-Res	16/Jan/07	-0.04	0.92	70	15/Jul/08	0.02	0.83	63
M4 (San Ramon)								
2-Res	23/Apr/07 -	0.09	0.63	56	23/Apr/07 -	0.01	0.60	47
3-Res	23/Apr/08	-0.01	0.71	69	23/Apr/08	0.03	0.69	71

Legend: EF, Nash-Sutcliffe Efficiency; AC, accuracy (% of observations within the prediction limits); NA, not applicable, uncertainty limits could not be generated because the maximum EF is lower than the threshold selected for the GLUE analysis

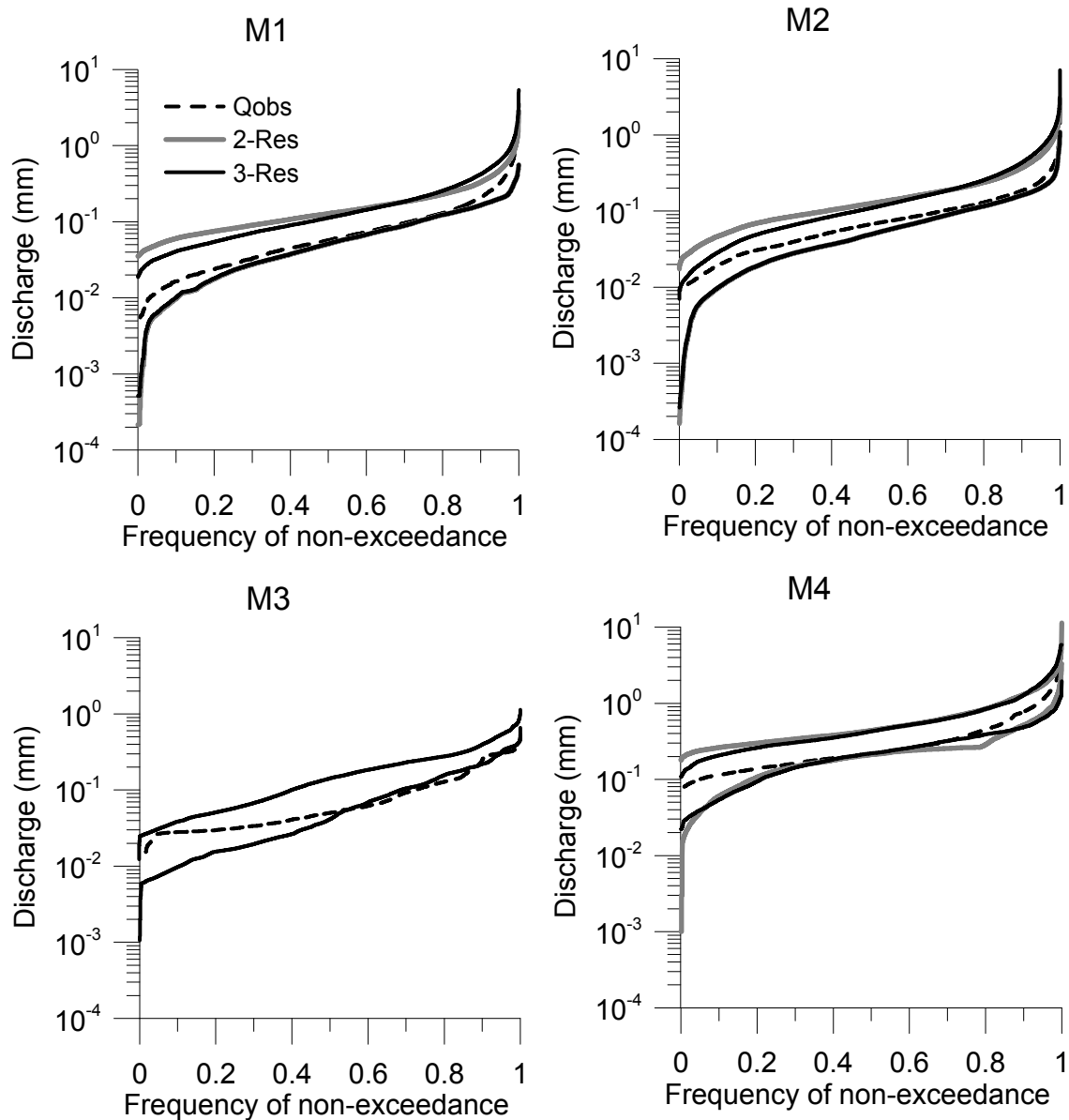


Figure 4-3: Hourly flow duration curves for the observed discharge and the 5 and 95% uncertainty limits of the four micro-catchments applying respectively the 2- and 3-Res model structure

The 2- and 3-Res model structures perform equally well in modeling the rainfall-runoff process of the M2 micro-catchment. Both model structures give similar EF and Bias values. Nearly the same value, varying between 0.71 and 0.74, was obtained for the modeling efficiency (EF) using the 2- and 3-Res model structure during model calibration and validation. Bias values for both periods and model structures are low, and in the range 0.01 and 0.03. The uncertainty limits are in general well capturing the observed discharge, with accuracy values ranging

between 62 and 65%, and 71 and 73% for the 2- and 3-Res model, respectively. As shown in Figure 4-3 for M1, the 5 and 95% uncertainty limits envelope the flow duration curve of the M2 micro-catchment. Both model structures represent properly most precipitation events and recession curves are well simulated, however the lower (5%) uncertainty limit significantly underestimates discharge values during low flows. The addition of a 3rd reservoir with high residence time (140 days), with the objective to simulate possible deep-water flow, did not improve the simulation results (data not shown). A plausible reason could be the overestimation of the evapotranspiration.  $ET_p$  was calculated using daily data from a station outside the catchment, situated at a lower - warmer - elevation. Another explanation could be the inability of linear reservoirs to correctly model the antecedent soil moisture content and soil drainage as explained earlier (Fenicia et al., 2008a,b; Lane et al., 2009). Buytaert and Beven (2011), in a study carried out in the same M2 micro-catchment using a 2 and 3 parallel linear reservoir model, were also not able of properly simulating low flows during dry conditions. On the other hand, the tested 2- and 3-Res model structures correctly mimic the fast response from low to peak flows following a transition from a non-rainy to a rainy period, suggesting that the reservoir storage concept correctly models the hydrology of the M2 micro-catchment. Whereas the 2-Res model correctly simulates the peaks during dry periods, it underestimates peak flows during wetter conditions. Adding a 3rd reservoir on top of the 2-Res model with low residence time (25 hours), the 3-Res model structure in general improves the simulation of the peak flows during wet conditions; however overestimate the peaks during drier periods. The latter could be attributed to the interception loss of the low intensity rains and the fact that the presented conceptual model does not account for the hydrological connectivity between slopes, small plateaus and depressions. As can be seen in Figure 4-4, the 3-Res model is capable of simulating more accurately low flows than the 2-Res model structure.

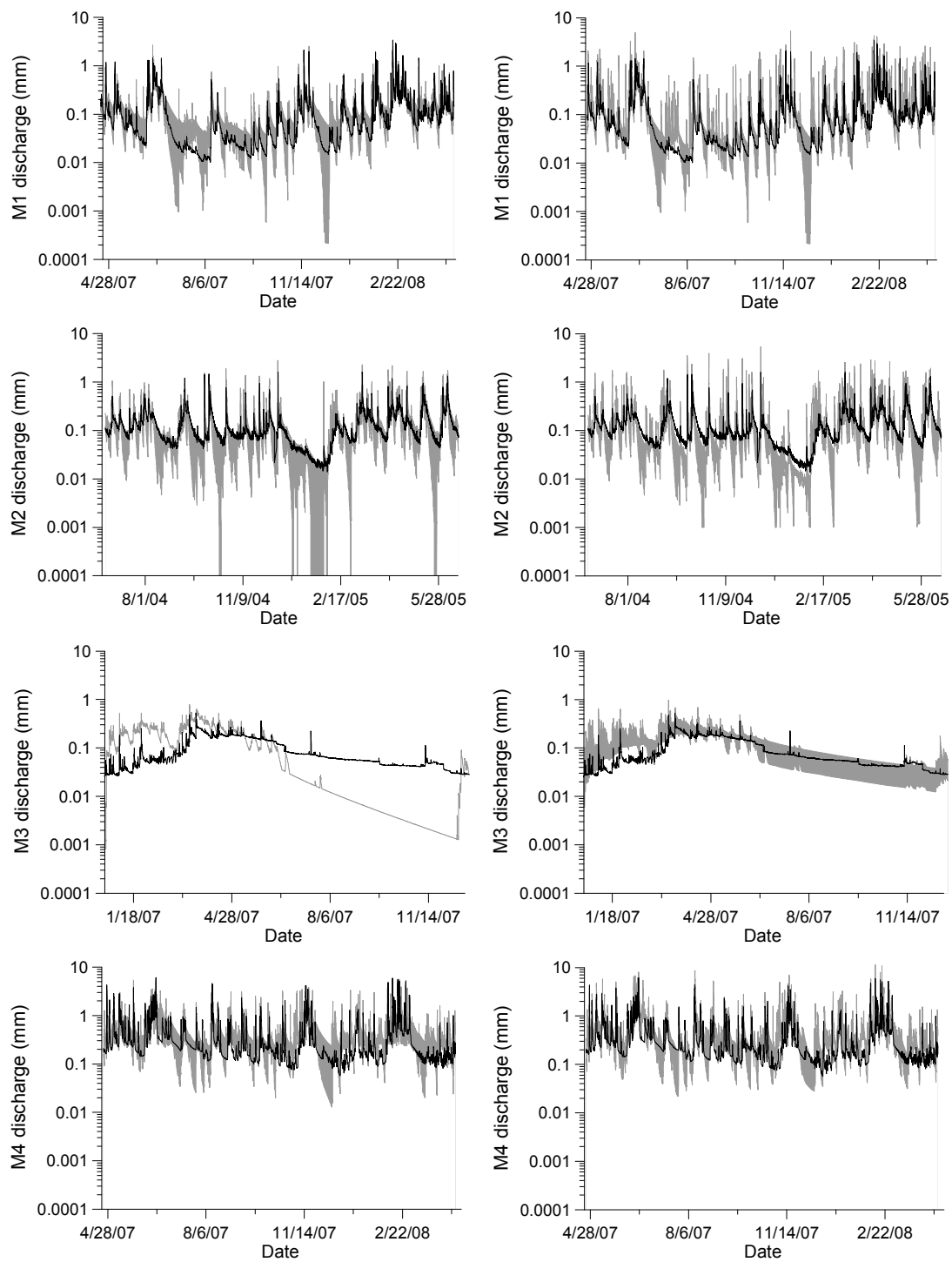


Figure 4–4: Observed discharge and the 5 and 95% uncertainty limits on the predicted discharge with application to the four micro-catchments. Left figures correspond to the 2-Res model structure, while right figures to the 3-Res model structure. 2-Res model results for M3 correspond to the best model simulation.

The model performance indicators for M3 in Table 4-3 clearly illustrates that the 2-Res model structure strongly underrates the prediction of the discharge. Modeling

efficiency is 0.36 and 0.28 for the calibration and validation period, respectively. Due to the selected threshold value for EF in the GLUE analysis ( $EF > 0.5$ ) the uncertainty bounds for the 2-Res model structure could not be generated. The 2-Res model consistently underestimates discharge during low flows, indicating that the recession curves are not well simulated (Figure 4-4). Additionally, the 2-Res model showed difficulties in correctly simulating the recession curves during wet and dry periods. Adding a 3rd reservoir, with a residence time of 398 days, considerably improved for the M3 micro-catchment the modeling of the runoff. It is noticed that low flows are better simulated during the wet season, than the dry season, indicating that during the wet season the streamflow contributing water source areas and the hydraulic connectivity of streamflow contributing areas are different (Staudinger et al., 2011). The 3-Res model structure quite accurately simulates the recession curves during the long dry season, a 6 month period totaling 20 to 40% of the annual precipitation. Crespo et al. (2008) in a study conducted in the same catchment reported difficulties simulating the recession curves and low flows using the SWAT model. These authors suggested a high contribution of the rock water as possible explanation. Roa-García et al. (2011) in a study conducted in the Andean region of Colombia found that natural forest basins store more water and release the stored water over a much longer period than grassland. Medium flows were in general underestimated, likely as a consequence of the incorrect modeling of the rainfall interception affecting the vertical water distribution and net rainfall spatial heterogeneity, resulting in the wet season in a moderate to large spatial variability of stored water (Fenicia et al., 2008b). Peak flows were overestimated and the time of peaks were simulated approximately 2 hours earlier than the observed, reflecting the effect of the delay caused by the litter layer, a layer not fully considered in the presented 2- and 3-Res model structures.

Application of the 3-Res model to the M4 micro-catchment yields similar model efficiency values as found for the M1 and M2 micro-catchments. The EF values are a bit lower using the 2-Res model structure for predicting the catchment runoff. Both model structures perform a little better during the calibration phase, respectively 0.63 versus 0.60 for the 2-Res model structure and 0.71 versus 0.69 for the 3-Res model structure. Whereas the lower (5%) and upper (95%) confidence limits of the 2- and 3-Res models envelop the cumulative frequency curve of the

observed hourly flows, application of the 3-Res model leads to a higher accuracy and this during both, the calibration and validation, periods. The accuracy of the 2-Res model structure in predicting the runoff is considerably less and is respectively equal to 56 and 47% during the calibration and validation period, versus 69 and 71% for the 3-Res model. Both model structures correctly predicted the major precipitation events, failed to model some of the observed peaks, and simulated peaks that were not directly associated with precipitation events. Similar deviations between observed and simulated discharge were reported by Plesca et al. (2011) in a study conducted in a basin where M4 is a tributary. According to these authors and in agreement with Rollenbeck (2006), deviations are likely due to the high spatial variability in rainfall and fog, and the poor spatial distribution of precipitation monitoring stations. As shown in Figure 4-2, the limits of the 90% confidence interval of the predictions of both models are in general very similar, notwithstanding recession curves during wetter periods were sometimes underestimated, but correctly simulated during drier periods. Application of the 2-Res model to predict for the M4 micro-catchment streamflow leads to a systematic overestimation of peak flows, while the low flows are significantly underestimated. Adding a 3rd reservoir with high residence time (365 days), mimicking the water contribution of the bedrock considerably improved the predictive capacity of the conceptual model during low flows, a finding in line with the results obtained by Crespo et al. (2011b) and Bückner et al. (2010, 2011), and as suggested by Plesca et al. (2011).

### 4.3.3 EVALUATION OF THE CONCEPTUAL MODEL

The modeling results and the performance indicators for all micro-catchments point out that the two conceptual model structures are variably capable of modeling the hydrology of the soil profile and the underlying bedrock. Although the vegetation cover, topography and climate regime of the four micro-catchments are different, they have in common that the rainfall-runoff process is controlled by the succession of organic rich horizons laying on a thin layer of weathered bedrock, on top of the bedrock (Crespo et al., 2011a; Bückner et al., 2011). As stated earlier, the 2- and 3-Res models show similar performances for the micro-catchments M1 and M2. Here, the upper reservoir of the 2-Res model represents the soil organic horizons

(Ah and H) with a soil organic matter content varying between 15 and 50%, densely rooted, and extreme low bulk density (in the range 0.1 to 0.44 g cm<sup>-3</sup>). The origin of the organic layers is very much different from the underlying mineral layer. The latter being the product of the weathering of the rock layer beneath the thick and dark, highly organic epipedons. The organic horizons are the result of the poor decomposition of organic matter because of the predominantly cold and wet climate. The water storage release of the mineral layer and top of the bedrock is presented by the second reservoir in the 2-Res model. No groundwater was considered neither for M1 or M2 as was suggested in previous research (Crespo et al., 2011a; Buytaert et al., 2006c). Adding a third reservoir (i.e. shifting from a 2- to a 3-Res model) results in an improvement of the peak flows. As stated by Buytaert and Beven (2011) and Crespo et al. (2011a) during peak flows the fast response of both catchments is mainly controlled by the interaction between the hillslopes, the dynamic zones in the catchments, and the stagnant zones in the valley bottoms, the overland flow in saturated areas and the fast lateral flow through the rooted organic horizon. Whereas the first phenomenon is not represented by the model, the second is mimicked in the model by the estimation of *SOF* and *LL*, and the third phenomenon is indirectly mimicked by introducing a third shallow reservoir with small storage capacity and low transit time. Table 4-4 summarizes the cumulative contribution of the different reservoirs to the total flow assuming a 3-Res model concept. For the micro-catchments M1 and M2, 31 and 28% of the total discharge is contributed by the upper reservoir by subsurface flow through the rooted organic horizon, 57 and 60% of the streamflow is delivered by the non-rooted organic horizon, and 11 and 10.8% is the result of the lateral flow through the weathered mineral layer on top of the bedrock, respectively. Good estimation of the antecedent soil moisture content during both peak and slow flows seems to be important, as stated by Crespo et al. (2011a); Buytaert et al. (2006c); and Celleri (2007).

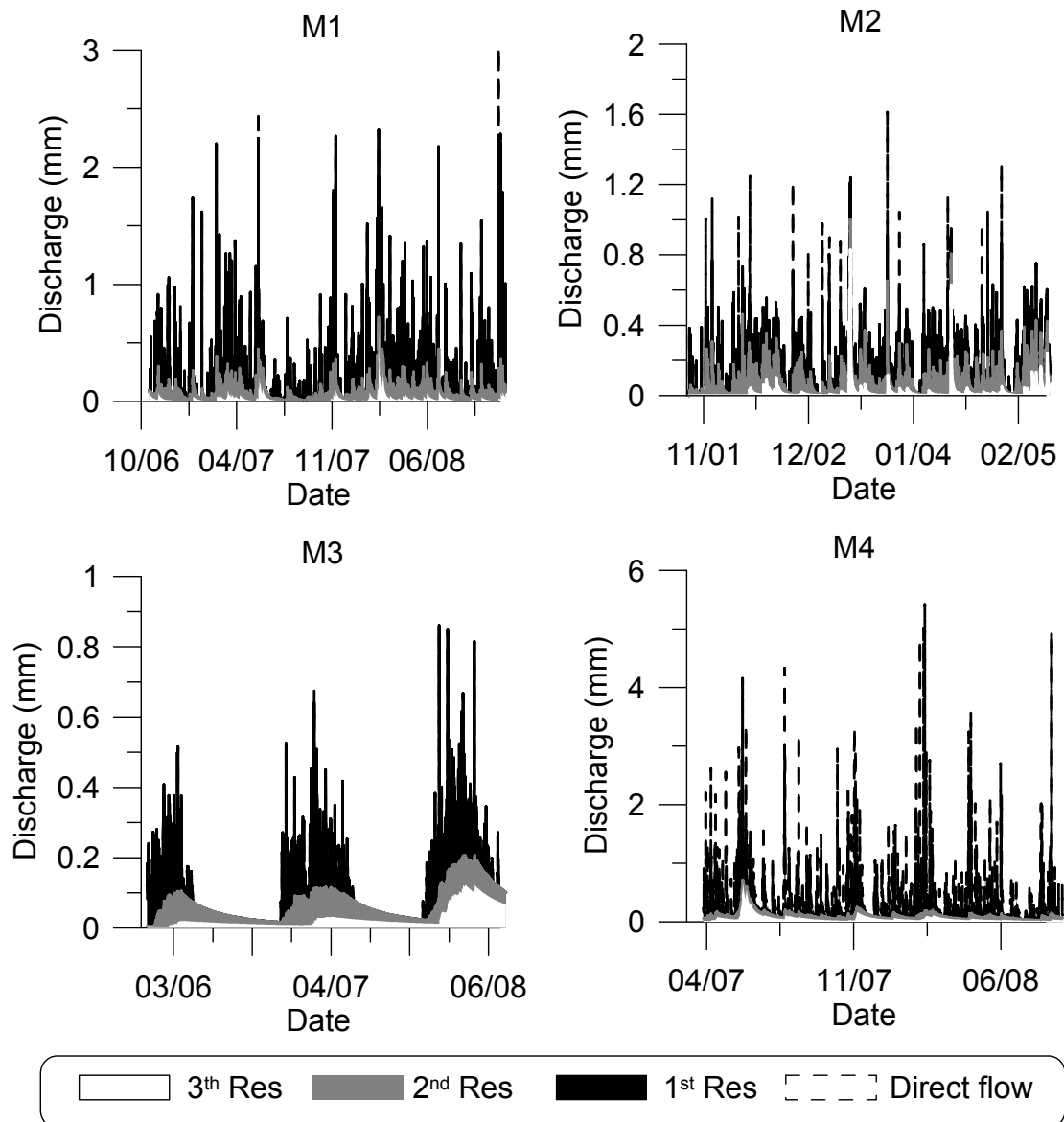


Figure 4-5: Discharge components according to the 3-Res model structure, with application to the four micro-catchments

The simulation results for the M3 micro-catchment show the relevance of adding a third reservoir with high transit time, representing the contribution of the bedrock, yielding 30% of the total discharge (Table 4-4). The third reservoir captures the runoff generation during dry periods. The relative contribution of the second reservoir, being the mineral soil layer, is more significant during dry periods being less important during wet conditions as is depicted in the Figure 4-5. The second reservoir generates on average 26% of the total discharge. However, during wet periods the first reservoir (organic soil layer) dominates the runoff process with an average contribution of 44%. Direct flow is unimportant contributing only 0.2% of

the total discharge. The low lateral flow contribution of the litter layer is likely the consequence of the high infiltration rate of this layer. Crespo et al. (2011a) in a study carried out in the same basins, concluded that under dry conditions the slow flow component mainly is generated by the lateral flow in the C-horizon and contributions of the bedrock, the so-called baseflow. This conclusion is supported by the simulation results of the 3-Res conceptual model presented herein. Results however indicate that the model concept underestimates the contribution of the top of the rock layer. The high hydraulic conductivity of the O and A horizons suggests the rapid infiltration of the rainfall during wet periods, replenishing the shallow watertable on top of the bedrock, filling also the fissures in the top of the bedrock. It is this water that feeds runoff during dry periods. During wet conditions the lateral flow through the litter layer and organic horizon are the main components of the total discharge in the M3 micro-catchment.

Table 4–4: Reservoir flow contribution (%)

Flow	M1 Zhurucay	M2 Huagrahuma	M3 Ortigas	M4 San Ramon
Direct	0.5	1.2	0.2	10.2
First reservoir	31.0	28.0	43.8	66.3
Second	57.3	60.0	26.0	10.2
Third reservoir	11.2	10.8	30.0	13.3

Similarly, for the M4 micro-catchment adding a third reservoir with high residence time improves the simulation of the low flows and peaks, suggesting a significant contribution of the bedrock representing on average 13% of the total discharge, confirming earlier findings of Crespo et al. (2011b) and Bücke et al. (2010; 2011). These authors also showed that the weathering of the top of the bedrock not only influences runoff generation during low flows, but also contributes to the discharge in wet periods. The mineral soil layer (second reservoir) contributes on average 10% to total discharge. The lateral subsurface flow through the organic soil horizons is the major flow source, representing on average 66% of the discharge. Direct flow through the litter layer represents around 10% of total flow, primarily sustaining the peaks during wet conditions. Overland flow is low to non-existent as suggested by Fleischbein et al. (2006) and Crespo et al. (2011b). Goller et al.

(2005) in a study close to M4 obtained similar results in a flow separation experiment based on stable water isotopes. They found that the water flow paths are dominated by the vertical flow through the soil profile, while during rainstorm events mainly lateral flow through the organic layers take place. These authors identified the high contribution of a near-surface flow (through litter layer) during intense rain storm events. Similar results were obtained by Wilcke et al. (2002); Fleischbein et al. (2006); Boy et al. (2008); Crespo et al. (2011b). All these findings fits well with the results generated by respectively the 2- and 3-Res conceptual model.

## 4.4 CONCLUSIONS

Based on the calculated performance indicators the 2- and 3-Res models perform equally well using the times series of the micro-catchments M1 and M2. In general both models are capable of predicting the runoff slightly better during model validation than calibration. Basically the bottom reservoir represents the water release of the mineral horizon and the bedrock layer sustaining the basin discharge during dry periods. The top reservoir of the 2-Res model concept mimics the lateral subsurface flow through the highly organic epipedons. During wet conditions most of the runoff is generated by the lateral flow in the organic rich horizons. Addition of a 3rd reservoir, representing the flow through the upper rooted layer of the organic horizons, results to a better prediction of the peak flows. To make the predictions of the runoff of the M3 micro-catchment acceptable using the soil-based conceptual model, the model structure should include at least three reservoirs. The upper reservoir mimics the lateral flow through the O and A, organic rich, horizons during wet periods, the 2nd reservoir the flow through the mineral Bw horizon 40 to 50 cm thick, and the bottom, the 3rd reservoir the flow in the C-horizon, the weathered top of the bedrock, and the bedrock. Baseflow dominates runoff during dry spell periods. For the simulation of the runoff timeseries of the M4 micro-catchment, acceptable results are obtained applying the 2-Res model structure. However, the 3-Res model structure considerably improves the model accuracy during the model calibration and validation period. The 3rd reservoir added to the

2-Res model structure represents the contribution to the runoff by the bedrock layer, being particular important during dry periods. Simulation results reveal that by adding a 3rd reservoir with high residence time improves the simulation of the low flows and peaks.

In general, the modeling exercise confirms that the soil-based concept is a valid approach for simulating the rainfall-runoff process of the four studied Andean micro-catchments. With the model the flow contribution of the different soil compartments, represented by either 2 or 3 linear reservoirs, can be characterized as a function of the overall wetness of the soil profile. Findings are in line with the observations mentioned by several authors having studied the hydrology of high mountain micro-catchments in the Andean cordillera. Not only the simplicity of the modeling concept is an advantage, but its relation with the soil enables in principle to apply the approach on ungauged micro-catchments analyzing in detail the profile composition. Delineating topographically medium sized basins in a series of micro-basins and routing the predicted outflow of each of the micro-catchments, using either the 2- or 3-Res modeling concept, might result in realistic estimates of the runoff of meso-scale basins.

---

## 5 REFERENCES

- Anderson, S., Dietrich, W., Torres, R., Montgomery, D., Loague, K., 1997. Concentration-discharge relationships in runoff from a steep, unchanneled catchment. *Water Resour. Res.* 33(1), 211-225.
- Allen, R.G, Pereira, L.S., Raes, D., Smith, M., 1998. Crop evapotranspiration guidelines for computing crop water requirements. *FAO Irrigation and Drainage Paper 56*, FAO, Rome, 300 pp.
- Bacuilima, F. L., Bacuilima, J. C., Bermeo, W. A., 1999. Caracterización de clima por microcuencas en el Austro Ecuatoriano. Master thesis, Universidad de Cuenca, Ecuador, 120pp.
- Baquero, F., Sierra, R., Ordóñez, L., Tipán, M., Espinosa, L., Rivera, M. B., Soria, P., 2004. La Vegetación de los Andes del Ecuador. Memoria explicativa de los mapas de vegetación: potencial y remanente a escala 1:250.000 y del modelamiento predictivo con especies indicadoras. *EcoCiencia/CESLA/Corporación EcoPar/MAG SIGAGRO/CDC - Jatun Sacha/División Geográfica - IGM*.
- Balslev, H., Øllgaard, B., 2002. Mapa de vegetación del sur de Ecuador, in: Aguirre, Z. M., Madsen, J. E., Cotton, E., Balslev, H. (Eds.), *Botánica Austroecuatorialiana - Estudios sobre los recursos vegetales en las provincias de el Oro, Loja y Zamora-Chinchipec*. Abya-Yala, Quito, Ecuador, pp. 51-64.
- Barthold, F.K., 2010. Large scale application of an environmental tracer approach: spatio-temporal patterns of hydrochemistry in a semi-arid grassland. PhD dissertation, University of Giessen, Giessen, Germany, 115pp.
- Beck, E., Makeschin, F., Haubrich, F., Richter, M., Bendix, J., Valarezo, C., 2008. The ecosystem in the Reserva Biológica San Francisco, in: Beck, E., Bendix, J., Kottke, I., Makeschin, F., Mosandl, R. (Eds.), *Gradients in a tropical mountain ecosystem of Ecuador*. Ecological Studies, Springer Verlag, Berlin, Germany, pp. 1-14.
- Beiderwieden, E., Wrzesinsky, T., Klemm, O., 2005. Chemical characterization of fog and rain water collected at the eastern Andes cordillera. *Hydrol. Earth Syst. Sc.*, 9,185-191.
- Bendix, J., Rollenbeck, R., Richter, M., Fabian, P., Emck, P., 2008. Climate, in: Beck, E., Bendix, J., Kottke, I., Makeschin, F., Mosandl, R. (Eds.), *Gradients in a tropical mountain ecosystem of Ecuador*. Ecological Studies, Springer Verlag, Berlin, Germany, pp. 63-74.
- Beven, K.J., Kirkby, M.J., 1977. Considerations in the development and validation of a simple physically-based, variable contributing area model of catchment hydrology, in: Morel-Seytoux, H.J. (Eds.), *3<sup>rd</sup> Int. Hydrol. Symp. Surface and subsurface hydrology*, Water Resour. Publ., Fort Collins, 23-36.

- Beven, K.J., Binley, A., 1992. The future of distributed models: model calibration and uncertainty prediction. *Hydrol. Process.*, 6, 279-298.
- Beven, K.J., Lamb, R., Quinn, P., Romanowics, R., Freer, J., 1995. TOPMODEL, in: Singh, V.J. (Eds.), *Computer models of watershed hydrology*, Water Resour. Publ., 627-668.
- Beven, K.J., Freer, J., 2001. Equifinality, data assimilation and uncertainty estimation in mechanistic modelling of complex environmental systems using the glue methodology. *J. Hydrol.*, 249, 11-29.
- Beven, K.J., 2001a. *Rainfall-runoff modeling: the primer*. Wiley and Sons, New York.
- Beven, K.J., 2001b. On hypothesis testing in hydrology. *Hydrol. Process.*, 15, 1655-1657.
- Beven, K., 2002. Towards a coherent philosophy for modeling the environment, *Proc. R. Soc. London, Ser. A*, 458, 2465–2484.
- Blume, T., Zehe, E., Bronstert, A., 2007. Rainfall runoff response, event-based runoff coefficients and hydrograph separation. *Hydrol. Sci. J.*, 52(5), 843-862.
- Blume, T., Zehe, E., Reusser, D.E., Iroumé, A., Bronstert, A., 2008. Investigation of runoff generation in a pristine, poorly gauged catchment in the Chilean Andes I: A multi-method experimental study. *Hydrol. Process.*, 22(18), 3661-3675
- Bogner, C., Engelhardt, S., Zelinger, J., Huwe, B., 2008. Visualization and analysis of flow patterns and water flow simulations in disturbed and undisturbed tropical soils, in: Beck, E., Bendix, J, Kottke, I., Makeschin, F., Mosandl, R. (Eds.), *Gradients in a tropical mountain ecosystem of Ecuador*. Ecological Studies, Springer Verlag, Berlin, Germany, 75-86.
- Bonell, M., 1993. Progress in the understanding of runoff generation in forest. *J. Hydrol.*, 150, 217-275.
- Bonell, M., Fritsch, J.M., 1997. Combining hydrometric-hydrochemistry methods: a challenge for advancing runoff generation process research. *Hydrochemistry*. IAHS Publ., 244, 165-184.
- Boy, J., Valarezo, C., Wilcke, W., 2008. Water flow paths in soil control element exports in an Andean tropical montane forest. *Eur. J. Soil Sci.*, 59(6), 1209-1227.
- Bowen, G.J., Wilkinson, B., 2002. Spatial distribution of  $\delta^{18}\text{O}$  in meteoric precipitation. *Geology*, 30(4), 315-318.
- Bowen, G.J., Revenaugh, J., 2003. Interpolating the isotopic composition of modern meteoric precipitation. *Water Resour. Res.*, 39(10), 1299. doi:10.129/2003WR002086.

- Bruijnzeel, L.A., Veneklaas, E.J., 1998. Climatic conditions and tropical montane forest production: the fog has not lifted yet. *Ecology*, 79, 3-9.
- Bruijnzeel, L. A., 2001. Hydrology of tropical montane cloud forests: a reassessment. *Land Use and Water Resources Research*, 1, 1.1-1.18.
- Bruijnzeel, L. A., 2004. Hydrological functions of tropical forests: not seeing the soil for the trees? *Agric. Ecosyst. Environ.*, 104, 185-228.
- Bücker, A., Crespo, P., Frede, H. G., Vaché, K., Cisneros, F., Breuer, L., 2010. Identifying controls on water chemistry of tropical cloud forest catchments - combining descriptive approaches and multivariate analysis. *Aquat. Geochem.*, 16(1), 127-149.
- Bücker, A., 2010. Chemical and biological water quality in tropical cloud forest streams under different land-use. PhD dissertation, Justus-Liebig Universität Gießen, Giessen, Germany, 93 pp.
- Bücker, A., Crespo, P., Frede, H-G., Breuer, L., 2011. Solute behaviour and export rates in remote neotropical mountain catchments under different land-uses. *J. Trop. Ecol.*, 27, 305-317.
- Bussmann, R., 2005. Bosques andinos del sur de Ecuador, clasificación, regeneración y uso. *Rev. Peru. Biol.*, 12(2), 203-216.
- Bussmann, R.W., Wilcke, W., Richter, M., 2008. Landslides as important disturbance regimes—causes and regeneration, in: Beck, E., Bendix, J, Kottke, I., Makeschin, F., Mosandl, R. (Eds.), *Gradients in a tropical mountain ecosystem of Ecuador. Ecological Studies*, Springer Verlag, Berlin, Germany, 319-330.
- Buytaert, W., 2004. The properties of the soils of the south Ecuadorian páramo and the impact of land use changes on their hydrology. PhD dissertation, Katholieke Universiteit Leuven, Leuven, Belgium, 228 pp.
- Buytaert, W., De Bièvre, B., Wyseure, G., Deckers, J., 2005. The effect of land use changes on the hydrological behaviour of Histic Andosols in south Ecuador. *Hydrol. Process.*, 19(20), 3985-3997.
- Buytaert, W., Célleri, R., Willems, P., De Bièvre, B., Wyseure, G., 2006a. Spatial and temporal rainfall variability in mountainous areas: A case study from the south Ecuadorian Andes. *J. Hydrol.*, 329, 413-421.
- Buytaert, W., Celleri, R., De Bièvre, B., Hofstede, R., Cisneros, F., Wyseure, G., Deckers, J., 2006b. Human impact on the hydrology of the Andean páramos. *Earth-Sci. Rev.*, 79, 53-72.
- Buytaert, W., Iniguez, V., De Bièvre, B., 2007. The effects of afforestation and cultivation on water yield in the Andean páramo. *Forest Ecol. Manag.*, 251, 22-30.

- Buytaert, W., Beven, B., 2009. Regionalisation as a learning process. *Water Resour. Res.*, 45, W11419, 13pp.
- Buytaert, W., Vuille, M., Dewulf, A., Urrutia, R., Karmalkar, A., Célleri, R., 2010. Uncertainties in climate change projections and regional downscaling: implications for water resources management. *Hydrol. Earth Syst. Sci.*, 14, 1247-1258.
- Buytaert, W., Cuesta-Camacho, F., Tobon, C., 2011. Potential impacts of climate change on the environmental services of humid tropical alpine regions. *Global Ecol. Biogeogr.*, 20(1), 19-33.
- Buytaert, W., Beven, K., 2011. Models as multiple working hypotheses: Hydrological simulation of tropical alpine wetlands. *Hydrol. Process.*, 25(11), 1784-1799.
- Buttle, J.M., 1994. Isotope hydrograph separations and rapid delivery of pre-event water from drainage basin. *Prog. Phys. Geog.*, 18,16-41.
- Castaño, C., 2002. Páramos y ecosistemas alto andinos de Colombia en condición hotspot y global climatic tensor. IDEAM, Bogotá, Colombia, Open file Rep., 65pp.
- Chapman, T., 1991. Comment on: Evaluation of automated techniques for base flow and recession analyses by R. J. Nathan, and T. A. McMahon. *Water Resour. Res.*, 27(7), 1783-1784.
- Célleri, R., 2007. Rainfall variability and rainfall-runoff dynamics in the Paute river basin - southern Ecuadorian Andes. Ph.D. dissertation, Katholieke Universiteit Leuven, Leuven, Belgium, 125 pp.
- Célleri, R., Willems, P., Buytaert, W., Feyen, J., 2007. Space-time variability of rainfall in the Paute river basin of South Ecuador. *Hydrol. Process.*, 21, 3316-3327.
- Célleri, R., Feyen, J., 2009. The hydrology of tropical Andean ecosystems: Importance, knowledge status and perspectives. *Mt. Res. Dev.* 29(4), 350-355.
- Chaves, J., Neill, C., Germer, S., Neto, S.G., Krusche, A., Elsenbeer, H., 2008. Land management impacts on runoff sources in small Amazon watersheds. *Hydrol. Process.*, 22, 1766-1775.
- Christophersen, N., Neal, C., Hooper, R.P., Vogt, R.D., Andersen, S., 1990. Modelling streamwater chemistry as a mixture of soilwater end-members – a step towards second generation acidification models. *J. Hydrol.*, 116, 307-320.
- Christophersen, N., Hooper, R.P., 1992. Multivariate analysis of stream water chemical data: the use of principal components analysis for the end member mixing problem. *Water Resour. Res.*, 28(1), 99-107.
- Coltorti, M., Ollier, C. D., 2000. Geomorphic and tectonic evolution of the Ecuadorian Andes. *Geomorphology*, 32, 1-19.

- Crespo, P., Coello, C., Iñiguez, V., Cisneros, F., Ramirez, M., 2008. Implementación de un modelo hidrológico en microcuencas del Río BuluBulu. PROTOS/SENDAS, Universidad de Cuenca, Cuenca, Ecuador, Tech. Rep., 160 pp.
- Crespo, P., Célleri, R., Buytaert, W., Iñiguez, V., Borja, P., De Bievre, B., Cisneros, F., Feyen, J., 2010. Land use change impacts on the hydrology of Andean páramo ecosystems, in: Status and Perspectives of Hydrology in Small Basins. IAHS Publ. 336, pp. 71-76.
- Crespo, P., Feyen, J., Buytaert, W., Bücken, A., Breuer, L., Frede, H-G., Ramírez, M. 2011a. Identifying controls of the hydrological response of small catchments in the tropical Andes (Ecuador). *J. Hydrol.*, 407, 164-174.
- Crespo, P., Bücken, A., Feyen, J., Vaché, K., Frede, H-G, Breuer, L., 2011b. Preliminary evaluation of the runoff processes in a remote montane cloud forest basin using Mixing Model Analysis and Mean Transit Time. *Hydrol. Process.*, in press, doi: 10.1002/hyp.8382.
- Crespo, P., Coello, C., Iñiguez, V., Cisneros, F., Ramirez, M. 2008. Implementación de un modelo hidrológico en microcuencas del Río BuluBulu. PROTOS/SENDAS, Universidad de Cuenca, Cuenca, Ecuador, Tech. Rep., 160 pp.
- DeWalle, D.R., Edwards, P.J., Swistock, B.R., Aravena, R., Drimmie, R.J., 1997. Seasonal hydrology of three Appalachian forest catchments. *Hydrol. Process.*, 11,1895-1906.
- Dincer, T., Payne, B.R., Florkowski, T., Martinec, D., Tongiorgi, E., 1970. Snowmelt runoff from measurements of tritium and oxygen-18. *Water Resour. Res.*, 6,110-124.
- Dunne, T., 1983. Relation to field studies and modeling in the prediction of storm runoff. *J. Hydrol.*, 65: 25-48.
- Elsenbeer, H., Lorieri, D., Bonell, M., 1995. Mixing model approaches to estimate storm flow sources in an overland flow-dominated tropical rain forest catchments. *Water Resour. Res.*, 31(9), 2267-2278.
- Elsenbeer, H., Lack, A., 1996. Hydrometric and hydrochemical evidence for fast flowpaths at La Cuenca, western Amazonia. *J. Hydrol.*, 180(1-4), 237-250.
- Elsenbeer, H., West, A., Bonell, M., 1994. Hydrologic Pathways and Stormflow Hydrochemistry at South Creek, Northeast Queensland. *J. Hydrol.*, 162(1-2), 1-21.
- Elsenbeer, H., 2001. Hydraulic flowpath in tropical rainforest soil scapes: A review. *Hydrol. Process.*, 15, 1751-1759.
- FAO/ISRIC/ISSS, 1998. World Reference Base for Soil Resources. World Soil Resources Report 84, FAO, Rome, 88 pp.
- FAO, 2006. Global forest resources assessment 2005. Progress towards sustainable forest management. Forestry Paper 147, FAO, Rome, 320 pp.

- Feddema, J.J., Oleson, K.W., Bonan, G.B., Mearns, L.O., Buja, L.E., Meehl, G.A., Washington, W.M., 2005. The Importance of Land-Cover Change in Simulating Future Climates. *Science*, 210, 1674-1678.
- Fenicia, F., McDonnell, J.J., Savenije, H.H.G., 2008. Learning from model improvement : On the contribution of complementary data to process understanding. *Water Resour. Res.*, 44, W06419, doi:10.1029/2007WR006386.
- Fenicia, F., Savenije, H.H.G., Matgen, P., Pfister, L., 2008. Understanding catchment behavior through stepwise model concept improvement. *Water Resour. Res.*, 44, W01402, doi:10.1029/2006WR005563.
- Fleischbein, K., Wilcke, W., Boy, J., Valarezo, C., Zech, W., Knoblich, K., 2005. Rainfall interception in a lower montane forest in Ecuador: effects of canopy properties. *Hydrol. Process.*, 19, 1355-1371.
- Fleischbein, K., Wilcke, W., Valarezo, C., Zech, W., Knoblich, K., 2006. Water budgets of three small catchments under montane forest in Ecuador: experimental and modelling approach. *Hydrol. Process.*, 20, 2491-2507.
- Franks, S., Sivapalan, M., Takeuchi, K., Tachikawa, Y., (Eds.) 2006. Predictions in Ungauged Basins: International Perspectives on the State of the Art and Pathways Forward, IAHS Publ., 301, 348 pp.
- Fujieda, M., Kudoh, T., de Cicco, V., Calvarcho, J. L., 1997. Hydrological processes at two subtropical forest catchments: the Serra do Mar, Sao Paulo, Brazil. *J. Hydrol.*, 196, 26-46.
- Genereux D.P., 1998. Quantifying uncertainty in tracer-based hydrograph separations. *Water Resour. Res.*, 34, 915-919.
- Germer, S., 2008. Near-surface hydrology and hydrochemistry under contrasting land cover. Ph.D. dissertation, Potsdam University, Potsdam, Germany, 121 pp.
- Giusti, L., Neal, C., 1993. Hydrological pathways and solute chemistry of storm runoff at Dargall Lane, southwest Scotland. *J. Hydrol.*, 142, 1-27.
- Goller, R., Wilcke, W., Leng, M. J., Tobschall, H. J., Wagner, K., Valarezo, C., Zech, W., 2005. Tracing water paths through small catchments under a tropical montane rain forest in south Ecuador by an oxygen isotope approach. *J. Hydrol.*, 308, 67-80.
- Grimaldi, C., Grimaldi, M., Millet, A., Bariac, T., Boulegue, J.. 2004. Behaviour of chemical solutes during a storm in a rainforested headwater catchment. *Hydrol. Process.*, 18(1), 93-106.
- Hamilton, L.S., Juvik, J.O., Scatena, F.N., 1995. The Puerto Rico tropical cloud forest symposium: introduction and workshop synthesis, in: Hamilton, L.S., Juvik, J.O., Scatena, F.N. (Eds.). *Tropical Montane Cloud Forests*. Ecol. Stud. 110, Springer-Verlag, New York, pp. 1-23.

- Henderson, A., Churchill, S.P., Luteyn, J.L., 1991. Neotropical plant diversity. *Nature*, 351, 21-22.
- Hensel, D., Elsenbeer, H., 1997. Stormflow generation in tropical rainforest: a hydrochemical approach. *Hydrochemistry*, IAHS Publ., 244, 227-234.
- Hofstede, R. G. M., 1995. The effects of grazing and burning on soil and plant nutrient concentrations in Colombian páramo grasslands. *Plant Soil*, 173, 111-132.
- Hofstede, R., Segarra, P., Mena, P.V., 2003. *Los Páramos del Mundo*. Global Peatland Initiative/NC-IUCN/EcoCiencia, Quito.
- Homeier, J., Dalitz, H., Breckle, S. W., 2002. Waldstruktur und Baumartendiversität im momentanen Regenwald der Estación Científica San Francisco in Südecuador. *Ber Reinhold-Tüxen Ges.*, 14, 109-118.
- Hooper, R.P., Christophersen, N., Peters, N.E., 1990. Modelling streamwater as a mixture of soilwater end-members – an application to the Panola mountain catchment, Georgia, USA. *J. Hydrol.*, 116, 321-343.
- Hungerbühler, D., 1997. Tertiary basins in the Andes of southern Ecuador (3°00'-4°20'): Sedimentary evolution, deformation and regional tectonic implications. PhD dissertation, Institute of Geology, ETH Zürich, Switzerland, 182 pp.
- Hungerbühler, D., Steinmann, M., Winkler, W., Seward, D., Eguez, A., Peterson, D. E., Helg, U., Hammer, C., 2002. Neogene stratigraphy and Andean geodynamics of southern Ecuador. *Earth-Sci. Rev.*, 57, 75-124.
- Hutley, L. B., Doley, D., Yates, D. J., Boonsaner, A., 1997. Water balance of an Australian subtropical rainforest at altitude: the ecological and physiological significance of intercepted cloud and fog. *Aust. J. Bot.*, 45, 311-329.
- Huwe, B., Zimmermann, B., Zeilinger, J., Quizhpe, M., Elsenbeer, H., 2008. Gradients and patterns of soil physical parameters at local, field and catchment scales, in: Beck, E., Bendix, J, Kottke, I., Makeschin, F., Mosandl, R. (Eds.), *Gradients in a tropical mountain ecosystem of Ecuador*. Ecological Studies, Springer Verlag, Berlin, Germany, pp. 391-402.
- IAMGOLD, 2006. Reporte de exploración. IAMGOLD Ecuador S.A.. IAMGOLD Ecuador S.A., Cuenca, Ecuador, Tech. Rep., 120 pp.
- INEC, 2011. Censo de Población y Vivienda. <http://www.inec.gov.ec/cpv/>
- Johnson, M, Lehmann, J., Guimarães, E., Novães, J., Riha, S., 2006. DOC and DIC in flowpaths of Amazonian headwater catchments with hydrologically contrasting soils. *Biogeochem.*, 81, 45-57.
- Kendall, C., McDonnell, J., 1998. *Isotope tracers in catchment hydrology*. Elsevier, Amsterdam, 839 pp.

- Kennerley, J. B., 1980. Outline of the geology of Ecuador. *Overseas Geol. and Min. Resour.*, 55, 17 pp.
- Kessler, J., Oosterbaan, R. J., 1974. Determining hydraulic conductivity of soils, in: de Ridder, N. A., Takes, Ch. A. P., van Someren, C. L., Bos, M. G., Messemaekers, R. H., de Graaf, C. D., Bokkers, A. H. F. (Eds.), *Drainage Principles and Applications 24*, International Institute for Land Reclamation & Improvement, Wageningen, Netherlands, 3 pp.
- Kirkby, M.J., 1978. *Hillslope hydrology*. Wiley, Chichester, 389 pp.
- Klemeš, V., 1986. Operational testing of hydrological simulation models. *Hydrol. Sci. J.*, 31, 13-24.
- Klemeš, V., 1983. Conceptualization and scale in hydrology, *J. Hydrol.*, 65(1), 1– 23.
- Kraft, P., Vaché, K. B., Breuer, L., Frede, H.-G., 2008. A solute and water flux library for catchment models. In: Sánchez-Marrè, M., et al. (Eds.). *Integrating sciences and information technology for environmental assessment and decision making*. 4th Biennial Meeting of iEMSS, pp 2053-2056.
- Lane, S.N., Reaney, S.M., Heathwaite, A.L., 2009. Representation of landscape hydrological connectivity using a topographically driven surface flow index. *Water Resour. Res.*, 45, W08423, doi:10.1029/2008WR007336.
- Leibundgut, Ch., 1987. *Hydroökologische Untersuchungen in einem alpinen Einzugsgebiet-Grindelwald*, Schlessbericht zum Schweizerischen MAB-Program Nr. 30, unpublished report, Institute of Geography, University of Berne, Germany.
- Ließ, M, Glaser, B, Huwe, B., 2009. Digital soil mapping in southern Ecuador. *Erdkunde*, 63(4), 309-319.
- Litherland, M, Aspen, J. A., Jemielita, R. A., 1994. The metamorphic belts of Ecuador. *Overseas Memoir British Geological Survey*, 11, 1-147.
- Luteyn, J. L., 1992. Páramos: why study them?, in: Balslev, H., Luteyn, J. L. (Eds.), *Páramo: An Andean ecosystem under human influence*. Academic Press, London, 14 pp.
- Lorieri, D., Elsenbeer, H., 1997. Aluminium, iron and manganese in near-surface waters of a tropical rainforest ecosystem. *Sci. Total Environ.*, 205(1), 13-23.
- Luteyn, J.L., 1992. Páramos: why study them?, in: Balslev, H., Luteyn, J.L. (Eds.). *Páramo: An Andean ecosystem under human influence*. Academic Press, London, 14 pp.
- Makeschin, F., Haubrich, F., Abiy, M., Burneo, J. I., Klinger, T., 2008. Pasture management and natural soil regeneration, in: Beck, E., Bendix, J, Kottke, I.,

- Makeschin, F., Mosandl, R. (Eds.), Gradients in a tropical mountain ecosystem of Ecuador. Ecological Studies, Springer Verlag, Berlin, Germany, pp. 431-441.
- Maloszewski, P., Rauert, W., Stichler, W., Herrmann, A., 1983. Application of flow models in a alpine catchment area using tritium and deuterium data. *J. Hydrol.*, 66, 319-330.
- Maloszewski, P., Zuber, A., 1993. Principles and practice of calibration and validation of mathematical models for interpretation of environmental tracer data in aquifers. *Adv. Water Resour.*, 16, 173-190.
- McDonnell, J.J., 1990. A rationale for old water discharge through macropores in a steep, humid catchment. *Water Resour. Res.*, 26, 2821-2832.
- McDonnell, J., Rowe, L.K., Stewart, M.K., 1999. A combined tracer-hydrometric approach to assess the effect on catchment scale on water flow path, source and age, in: Leibundgut, C., McDonnell, J., Schults, G. (Eds.). *Integrated Methods in Catchment Hydrology-Tracers, Remote Sensing and New Hydrometric Techniques*, IAHS Publ., 258: 265-273.
- McDowell, W., Asbury, C.E., 1994. Export of Carbon, Nitrogen, and Major Ions from 3 Tropical Montane Watersheds. *Limnol. Oceanogr.*, 39(1), 111-125.
- McGuire, K.J., DeWalle, D.R., Gburek, W.J., 2002. Evaluation of mean residence time in subsurface water using oxygen-18 fluctuations during drought conditions in the mid-Appalachians. *J. Hydrol.*, 261, 132-149.
- McGuire, K.J., McDonnell, J.J., Weiler, M., Kendall, C., McGlynn, B.L., Welker, J.M., Seibert, J., 2005. The role of topography on catchment-scale water residence time. *Water Resour. Res.*, 41, W05002, doi:10.1029/2004WR003657.
- McGuire, K.J., McDonnell, J.J., 2006. A review and evolution of catchment transit time modeling. *J. Hydrol.*, 330(3-4), 543-563.
- Medina, G., Vásconez, P. M., 2001. Los páramos en el Ecuador, in: Vásconez, P. M., Medina, G., Hofstede, R. (Eds.), *Los páramos del Ecuador*, Proyecto Páramo, Quito, Ecuador, 24 pp.
- Merz, R., Blöschl, G., 2004. Regionalisation of catchment model parameters. *J. Hydrol.*, 287, 95-123.
- Montanari, L., Sivapalan, M., Montanari, A., 2006. Investigation of dominant hydrological processes in a tropical catchment in a monsoonal climate via the downward approach. *Hydrol. Earth Syst. Sc.*, 10, 769-782.
- Morales, L., 2008. Evaluación de las propiedades físicas e hidráulicas del suelo bajo influencia de tres coberturas vegetales en Porcé II, Antioquia, Colombia. Undergraduate thesis, Universidad Nacional de Colombia, Sede Medellín, Colombia, 36 pp.

- Moriasi, D.N., Arnold, J.G., Van Liew, M.W., Binger, R.L., Harmel, R.D., Veith, T.L., 2007. Model evaluation guidelines for systematic quantification of accuracy in watershed simulations. *Transactions of the ASABE*, 50(3), 885-900.
- Mortatti, J., Moraes, J. M., Victoria, R. L., Martinelli, A., 1997. Hydrograph separation of the Amazon river, A methodological study. *Aquat. Geochem.*, 3, 117-128.
- Mosandl, R., Günter, S., Stimm, B., Weber, M., 2008. Ecuador suffers the highest deforestation rate in South America, in: Beck, E., Bendix, J., Kottke, I., Makeschin, F. Mosandl, R. (Eds.). *Gradients in a tropical mountain ecosystem of Ecuador*. Springer Verlag, Berlin, Heidelberg, Ecological Studies 198, 431-441.
- Motzer, T., 2003. Bestandesklima, Energiehaushalt und Evapotranspiration eines neotropischen Bergregenwaldes, Forstmeteorologische und ökophysiologische Untersuchungen in den Anden Süd-Ecuadors. Ph.D. dissertation, University of Mannheim, Mannheim, Germany, 145 pp.
- Myers, N., Mittermeier, R.A., Mittermeier, C.G., da Fonseca, G.A.B., Kent, J., 2000. Biodiversity hotspots for conservation priorities. *Nature*, 403, 853-858.
- Nandakumar, N., Mein, R.G., 1997. Uncertainty in rainfall-runoff model simulations and the implications for predicting the hydrologic effects of land-use change. *J. Hydrol.*, 192, 211-232.
- Nash, J.E., Sutcliffe, J.V., 1970. River flow forecasting through conceptual models. Part I: A discussion of principles. *J. Hydrol.*, 10, 282-90.
- Niemi, A.J., 1977. Residence time distribution of variable flow processes. *Int. J. Appl. Radiat.*, 28, 855-860.
- Neill, C., Elsenbeer, H., Krusche, A.V., Lehmann, J., Markewitz, D., Figueiredo, R.D., 2006. Hydrological and biogeochemical processes in a changing Amazon: results from small watershed studies and the large-scale biosphere-atmosphere experiments. *Hydrol. Process.*, 20(12), 2467-2476.
- Newbold, J.D., Sweeney, B.W., Jackson, J.K., Kaplan, L.A., 1995. Concentrations and Export of Solutes from 6 Mountain Streams in Northwestern Costa-Rica. *J. N. Am. Benthol. Soc.*, 14(1), 21-37.
- Parajka, J., Merz, R., Blöschl, G., 2005. A comparison of regionalisation methods for catchment model parameters. *Hydrol. Earth Syst. Sci.*, 9, 157-171.
- Payne, B.R., Schroeter, P., 1979. Importance of infiltration from Chimbo river in Ecuador to groundwater. In *Isotope Hydrology*, IAEA, Vienna I, 145-158.
- Pearce, A.J., 1990. Streamflow generation processes: an Austral view. *Water Resour. Res.*, 26, 3037-3047.
- Plesca, I., Timbe, E., Exbrayat, J.F., Windhorst, D., Kraft, P., Crespo, P., Vaché, K., Frede, H-G., Breuer, L., 2011. Model intercomparison to explore catchment

- functioning: Results from a remote montane tropical rainforest. *Ecol. Mod.*, in press, doi:10.1016/j.ecolmodel.2011.05.005
- Pinder, G. F., Jones, J. F., 1969. Determination of ground-water component of peak discharge from chemistry of total runoff. *Water Resour. Res.*, 5(2), 438-455.
- Pratt, W. T., Figueroa, J. F., Flores, B. G., 1997. Geology and mineralization of the area between 3 and 48S, Western Cordillera, Ecuador. British Geological Survey, Open File Report, WCr97r28.
- PROMAS/IAMGOLD, 2009. Elaboración de la línea base en hidrología de los páramos de Quimsacocha y su área de influencia. Universidad de Cuenca, Cuenca, Ecuador. Tech. Rep., 68 pp.
- Ramírez, D., Valladares, A. F., Blasco, A., Bellot, J., 2006. Assessing transpiration in the tussock grass *Stipa tenacissima* L.: The crucial role of the interplay between morphology and physiology. *Acta Oecologica*, 30(3), 386-398.
- Roa-García, M.C., Brown, S., Schreier, H., Lavkulich, L.M., 2011. The role of land use and soils in regulating water flow in small headwater catchments of the Andes. *Water Resour. Res.* 47, W05510, doi:10.1029/2010WR009582.
- Robson, A., Neal, C., 1990. Hydrograph separation using chemical techniques: An application to catchments in mid-Wales. *J. Hydrol.*, 116, 345-363.
- Rodgers, P., Soulsby, C., Waldron, S., Tetzlaff, D., 2005. Using stable isotope tracers to assess hydrological flow paths, residence times and landscape influences in a nested mesoscale catchment. *Hydrol. Earth Syst. Sc.*, 9, 139-155.
- Rollenbeck, R., Fabian, P., Bendix, J., 2005. Precipitation dynamics and chemical properties in tropical mountain forests of Ecuador. *Advances in Geosciences*, 6, 1-4.
- Rollenbeck, R., 2006. Variability of precipitation in the Reserva Biológica San Francisco / Southern Ecuador. *Lyonia*, 9, 43-51.
- Romkens, M. J. M., S. N. Prasad, Whishler, F.D., 1990. Surface sealing and infiltration. Process Studies, in: Anderson, M. G., Burt, I. P. (Eds.). *Hillslope Hydrology*, John Wiley and Sons, 127-172.
- Schellekens, J., Scatena, F.N., Bruijnzeel, L.A., van Dijk, A.I.J.M., Groen, M.M.A., van Hogezaand, R.J.P., 2004. Stormflow generation in a small rainforest catchment in the luquillo experimental forest, Puerto Rico. *Hydrol. Process.*, 18(3), 505-530.
- Sefton, C. E. M., Howarth, S. M., 1998. Relationships between dynamic response characteristics and physical descriptors of catchments in England and Wales. *J. Hydrol.*, 211, 1–16.
- Seibert, J., 1999. Regionalisation of parameters for a conceptual rainfallrunoff model. *Agric. For. Meteorol.*, 98, 179– 293.

- Seibert, J., McDonnell, J. J., 2002. On the dialog between experimentalist and modeler in catchment hydrology: Use of soft data for multicriteria model calibration, *Water Resour. Res.*, 38(11), 14, doi:1241 10.1029/2001wr000978.
- SENPLADES, 2007. Plan Nacional de desarrollo 2007-2010. 55 pp.
- Singh, V. P., Frevert, D., (Eds.) 2002. *Mathematical Models of Small Watershed Hydrology and Applications*. Water Resour. Publ., Highland Ranch, Colo. 950 pp.
- Sivapalan, M., Wagener, T., Uhlenbrook, S., Zehe, E., Laksmi, V., Liang, X., Tachikawa, Y., Kumars, P., 2006. Predictions in Ungauged Basins: Promises and Progress, *IAHS Publ.*, 303, 520 pp.
- Sklash, M.G., Farvolden, R.N., 1979. The role of groundwater in storm runoff. *J. Hydrol.*, 43, 45-65.
- Soulsby, C., Rodgers, P., Smart, R., Dawson, J., Dunn, S., 2003. A tracer based assessment of hydrological pathways at different scales in a mesoscale Scottish catchment. *Hydrol. Process.*, 17, 759-777.
- Soulsby, C., Tetzlaff, D., Rodgers, P., Dunn, S., Waldron, S., 2006. Runoff processes, stream water residence times and controlling landscape characteristics in a mesoscale catchment: An initial evaluation. *J. Hydrol.*, 325, 197-221.
- Soulsby, C., Tetzlaff, D., van den Bedem, N., Malcolm, I.A., Bacon, P.J., Youngson, A.F., 2007. Inferring groundwater influences on surface water in montane catchments from hydrochemical surveys of springs and streamwaters. *J. Hydrol.*, 333(2-4), 199-213.
- Staudinger, M., Stahl, K., Seibert, J., Clark, M.P., Tallaksen, L.M., 2011. Comparison of hydrological model structures based on recession and low flow simulations. *Hydrol. Earth Syst. Sci.*, 15, 3447-3459.
- Stephenson, G.R., Freeze, R.A., 1974. Mathematical simulations of subsurface flow contribution to snowmelt runoff, Reynolds Creek watershed, Idaho. *Water Resour. Res.*, 10(2), 284-294.
- Stewart, MK, McDonnell, JJ., 1991. Modeling baseflow water residence times from deuterium concentrations. *Water Resour. Res.*, 27, 2682-2693.
- Tobón, C., Bruijnzeel, L. A., Frumau, A., 2006. Physical and hydraulic properties of tropical montane cloud forest soils and their changes after conversion to pasture, in: *Proceedings of the second international symposium: Science for conserving and managing tropical montane cloud forest*, Waimea, Hawaii, July 27-August 1, 2004.
- Tsujimura, M., Onda, Y., Ito, J., 2001. Stream water chemistry in a steep headwater basin with high relief. *Hydrol. Process.*, 15(10), 1847-1858.

- Turner, J.V., Macpherson, D.K., Stokes, R.A., 1987. The mechanisms of catchment flow processes using natural variations in deuterium and oxygen-18. *J. Hydrol.*, 94, 143-162.
- Unnikrishna, P.V., McDonnell, J.J., Stewart, M.L., 1995. Soil water isotope residence time modeling, in: Trudgill, ST. (Eds.). *Solute modeling in catchment systems*, Wiley, Chichester, 237-260.
- US Bureau of Reclamation, 2001. *Water Measurement Manual*. US Department of the Interior, USA, Tech. Rep., 317 pp.
- Vaché, K. B., McDonnell, J. J., 2006. A process-based rejectionist framework for evaluating catchment runoff model structure, *Water Resour. Res.*, 42(2), 15, doi:W02409 10.1029/2005wr004247.
- van der Hammen, T., Hooghiemstra, H., 2000. Neogene and Quaternary history of vegetation, climate, and plant diversity in Amazonia. *Quat. Sci. Rev.*, 19, 725-742.
- Vázquez, R. F., Feyen, J., 2003. Effect of potential evapotranspiration estimates on effective parameters and performance of the MIKE SHE-code applied to a medium-size catchment. *J. Hydrol.*, 270(4), 309-327.
- Vázquez, R. F., Feyen, J., 2007. Assessment of the effects of DEM gridding on the predictions of basin runoff using MIKE SHE and a modelling resolution of 600 m. *J. Hydrol.*, 334, 73-87.
- Vignola, R., 2005. A literature review on forest and hydrological services: Perspectives for climate change adaptation, Publication of CATIE, retrieved on 15 May 2009 from <http://www.catie.ac.cr/>, 45 pp.
- Vuille, M., Bradley, R. S., Keimig, F., 2000. Climate variability in the Andes of Ecuador and its relation to tropical Pacific and Atlantic sea surface temperature anomalies. *J. Clim.*, 13(2), 2520-535.
- Wagner, K., 2002. Fractionation of oxygen and hydrogen isotopes in waters of microcatchments in an tropical mountain rain forest of Southern Ecuador. M.Sc thesis, Friedrich Alexander University of Erlanen, Nürnberg, Germany, 58 pp.
- Wels, C., Cornett, R.J., Lazarete, B.D., 1991. Hydrograph separation: A comparison of geochemical and isotopic tracers. *J. Hydrol.*, 122, 253-274.
- Werner, F., Homeier, J., Gradstein, R., 2005. Diversity of Vascular epiphytes on isolated remnant trees in the montane forest belt of Southern Ecuador. *Ecotropica*, 11, 21-40.
- Wilcke, W., Yasin, S., Abramowski, U., Valarezo, C., Zech, W., 2002. Nutrient storage and turnover in organic layers under tropical montane rain forest in Ecuador. *Eur. J. Soil Sci.*, 53, 15-27.

- Wilcke, W., Yasin, S., Schmitt, C., Valarezo, C., Zech, W., 2008. Soils along the altitudinal transect and in catchments, in: Beck, E., Bendix, J, Kottke, I., Makeschin, F., Mosandl, R. (Eds.), *Gradients in a tropical mountain ecosystem of Ecuador*. Ecological Studies, Springer Verlag, Berlin, Germany, pp. 75-86.
- Willems, P., 2000. Probabilistic immission modelling of receiving surface waters. PhD dissertation, Department of Civil Engineering, K.U.Leuven, Leuven, Belgium, 347 pp.
- Willems, P., 2009. A time series tool to support the multi-criteria performance evaluation of rainfall-runoff models. *Environ. Model. Softw.*, 24(3), 311-321.
- Wolock, D.M., Fan, J., Lawrence, G.B., 1997. Effects of basin size on low-flow stream chemistry and subsurface contact time in the Neversink River watershed, New York. *Hydrol. Process.*, 11, 45-57.
- Young, A. R., 2006. Stream flow simulation within UK ungauged catchments using a daily rainfall-runoff model, *J. Hydrol.*, 320, 155–172.
- Zimmermann, B., 2007. Spatial and temporal variability of the soil saturated hydraulic conductivity in gradients of disturbance. Ph.D. Dissertation, Potsdam University, Potsdam, Germany, 106 pp.

## ACKNOWLEDGMENTS

Looking back, I am surprised and at the same time very grateful for all I received throughout the doctoral period. This not only culminated in the writing up of a dissertation, but most importantly it shaped me as a person and led me to where I am standing today. Given the many persons and institutions that in one or other way helped me through, the acknowledgements will be general, and any possible omissions will not be by purpose.

While it appears most obvious that my research achievements have everything to do with guidance received over the last years, I can not help but pay tribute for all the instructions that I have received, from school days to today. After all, without the ability to read and write, to add, to reason logically, and to appreciate the diversity of the world, it would be most challenging to progress on to understanding and appreciating the multitude of problems mankind faces, and how engineering know-how is contributing to their solution by continually devising innovative solutions.

The research as presented in this dissertation would not have been possible without the funding received from DFG, the Deutsche Forschungsgemeinschaft, within the Research Unit 816: Biodiversity and Sustainable Management of a Megadiverse Mountain Ecosystem in South Ecuador; more in particular through subproject B3.2, BR223814-1. Additional funding in the last year was provided by the SENEKYT projects PIC-08-460 and PIC-11-715. In addition to the direct funding, thanks are due to all the institutions, organizations and companies that shared hydrometeorological data and helped me with the collection of data, such as PROMAS of the University of Cuenca, IAMGOLD S.A. (via the Quimsacocha Project), PROTOS (a Belgian NGO), and DIUC, the Central Research Office of the University of Cuenca via the project “Estudio bio-hidrológico de un ecosistema de páramo húmedo Andino.

I wish to thank especially Prof. Hans-George Frede and Dr. Lutz Breuer, both from the Institute for Landscape Ecology and Resources Management (ILR), Justus-Liebig University Giessen, who in addition of supervising this research provided a comfortable environment and facilities to conduct advanced research. I am particular grateful for the

many innovative suggestions, criticism, and comments from Dr. Lutz Breuer, which ultimately lead to the acceptance of the dissertation. Thanks also for the moments we spent together after office hours discussing how to improve the research attitude of Ecuadorian universities. Danke schön Lutz. Of course it is evident to thank the colleague doctoral students, administrative and technical staff of ILR for their support and assistance. You in particular made the days I spent in Giessen very fruitful and agreeable.

I am most grateful to Prof. Jan Feyen who has been a very supportive person throughout the doctoral project. He encouraged me many times in a very simple and efficient way. In particular I like to acknowledge the academic support I received in discussions and in particular in reviewing the papers that are the scientific product of this research and the first draft of the dissertation. Thanks also for your never ending support to the Grupo de Ciencias de la Tierra y del Ambiente (GTCA) of the University of Cuenca, and of course also for the social moments we shared together with colleagues after office hours in one of Cuenca's bars. Mil gracias, siempre lo voy a recordar.

My gratitude goes also to the multitude of professionals with whom I interacted in different capacities in the course of the doctoral project. In particular I am very grateful to Rolando Célleri who accompanied me in the process of the doctoral project since 2009. In addition, I like to acknowledge that thanks to him and many other colleagues we took the challenge creating a new research group in the University of Cuenca, being the breeding place for many projects in the field of climate and hydrology in support of undergraduate and graduate thesis projects. It is a challenge but a pleasure working day after day with all of you. Gracias a todos por su apoyo y por las tantas veces que con una cerveza o un trago la pasamos genial.

Muchas gracias a mi hermanita Amelie, la verdad es que la pasamos muy bien trabajando juntos. Siempre tuviste una sonrisa para todo y estuviste disponible para conversar cuando lo necesitaba. Gracias a Diego Mejía, sin tu ayuda nunca hubiera sido posible hacer todo el trabajo de campo. Gracias también por tu amistad.

Gracias a todos los que conforman la ECSF, en especial a Felix, Joerg, María, Rocío, Tati, Abraham, Pipo, Gabriel, Kenni, Pablo, Kalle, Bruno, Karin. Sin su apoyo los días en la estación hubieran sido imposibles, al final la pasamos muy bien verdad!.

Finalmente, agradecer a las personas mas importantes en mi vida, mi esposa, Irene, mis padres, mis hermanos, mis cuñadas, mi sobrina, mi sobrino. Ustedes siempre me apoyaron y creyeron en mi, nunca hubiera sido posible sin Ustedes. La verdad ni siquiera hay palabras para agradecerles todo su amor. Irene espero pasar el resto de mi vida compartiendo contigo. A toda mi familia, mis abuelos, tíos, tías, y todos mis primos. Simplemente gracias. Abuelito Manuel y Luis Felipe siempre les voy a recordar.

---

## ERKLÄRUNG

Ich erkläre: Ich habe die vorgelegte Dissertation selbständig und ohne unerlaubte fremde Hilfe und nur mit den Hilfen angefertigt, die ich in der Dissertation angegeben habe. Alle Textstellen, die wörtlich oder sinngemäß aus veröffentlichten Schriften entnommen sind, und alle Angaben, die auf mündlichen Auskünften beruhen, sind als solche kenntlich gemacht. Bei den von mir durchgeführten und in der Dissertation erwähnten Untersuchungen habe ich die Grundsätze guter wissenschaftlicher Praxis, wie sie in der „Satzung der Justus-Liebig-Universität Gießen zur Sicherung guter wissenschaftlicher Praxis“ niedergelegt sind, eingehalten.

---

Patricio Javier Crespo Sánchez

Gießen, Mai 2012